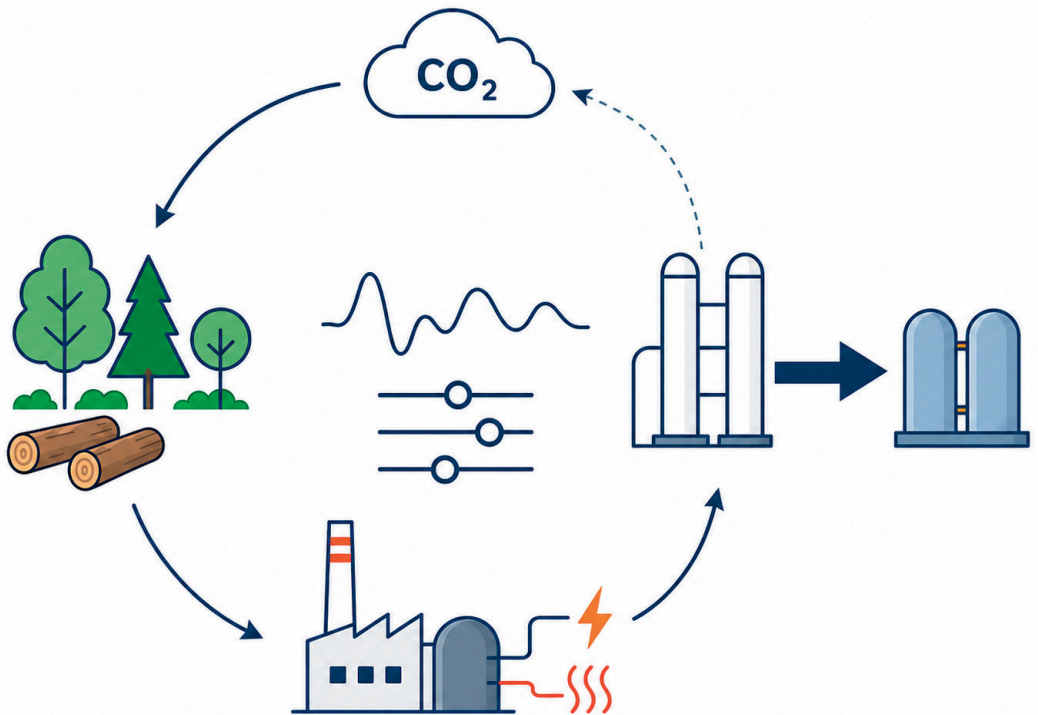


# Improving dynamic operation of CO<sub>2</sub> capture in biomass-fired CHP plants to boost negative emissions

Beibei Dong



Mälardalen University Press Dissertations

No. 465

**IMPROVING DYNAMIC OPERATION OF CO<sub>2</sub> CAPTURE IN  
BIOMASS-FIRED CHP PLANTS TO BOOST NEGATIVE EMISSIONS**

**Beibei Dong**

**2026**



Department of Engineering Sciences

Copyright © Beibei Dong, 2026  
ISBN 978-91-7485-756-6  
ISSN 1651-4238  
Printed by E-Print AB, Stockholm, Sweden

Mälardalen University Press Dissertations  
No. 465

IMPROVING DYNAMIC OPERATION OF CO<sub>2</sub> CAPTURE IN  
BIOMASS-FIRED CHP PLANTS TO BOOST NEGATIVE EMISSIONS

Beibei Dong

Akademisk avhandling

som för avläggande av teknologie doktorsexamen i energi- och miljöteknik  
vid Institutionen för teknikvetenskap kommer att offentligens försvaras  
måndagen den 8 juni 2026, 09.00 i Gamma, Mälardalens universitet, Västerås.

Fakultetsopponent: Professor Xi Jiang, Queen Mary University of London



Institutionen för teknikvetenskap

## Abstract

Integrating bioenergy with carbon capture and storage (BECCS) into biomass-fired combined heat and power (CHP) plants offers crucial potential for achieving negative emissions. To respond to fluctuating heat demand and volatile electricity markets, CHP plants must operate dynamically, and this results in largely fluctuating operation of CO<sub>2</sub> capture. This dissertation aims to improve the dynamic operation of CO<sub>2</sub> capture in biomass-fired CHP plants to boost negative emissions through dynamic modelling, advanced control and potential assessment under different operating modes.

To provide systematic guidance for selecting appropriate modelling approaches, both first principles and machine learning (ML) approaches are established and compared. Systematic comparison is first conducted across three first-principles models (ideal static models, dynamic models with control, and dynamic models without control) under three varying operating parameters (flue gas flow rate, CO<sub>2</sub> concentration, and available heat). Three ML models (Informer, long short-term memory, and back-propagation neural network) are further compared across four applications (system identification, monitoring, optimisation, and performance estimation). Results show that no single model consistently outperforms the others across all cases. While Informer achieves the highest accuracy in most applications and for most target variables, model selection should be tailored to the specific application. Model predictive control (MPC) is then developed and evaluated for managing operational variability of CHP plants. MPC demonstrates superior controller performance over conventional proportional integral (PI) control, achieving a 47–62% reduction in settling time and recovery time, and a 66–74% reduction in integrated absolute errors for CO<sub>2</sub> capture rate.

With modelling foundations, negative emission potential is evaluated at both plant and national scales under two operating modes (OMs), both of which prioritise heat supply. OM1 maximises CO<sub>2</sub> capture by sacrificing electricity output while maintaining heat supply, achieving 8.7 MtCO<sub>2</sub>/yr nationwide negative emissions at a levelized cost of CO<sub>2</sub> avoided of 36.9 \$/tCO<sub>2</sub>. OM2 maximises CO<sub>2</sub> capture while maintaining both heat and electricity supply, yielding 4.3 MtCO<sub>2</sub>/yr positive emissions at 52.0 \$/tCO<sub>2</sub> (but still reducing emissions by 6.3 MtCO<sub>2</sub>/yr compared with the reference plant without CO<sub>2</sub> capture). The biogenic fraction of fuel emerges as the critical parameter, requiring minimum fractions of 32.8% and 84.3% for the two OMs to meet Sweden's 3 MtCO<sub>2</sub>/yr target.

The contributions of this work include: (i) systematic guidance for dynamic model selection tailored to different CO<sub>2</sub> capture applications, (ii) quantitative evidence of MPC's superiority over PI control under realistic CHP dynamic scenarios, and (iii) a national-scale BECCS potential and cost assessment for Sweden under maintained heat supply constraints. Results demonstrate that Sweden's BECCS climate targets (3–10 MtCO<sub>2</sub>/yr by 2045) are technically achievable, as OM1 alone can deliver 8.7 MtCO<sub>2</sub>/yr negative emissions. The choice between operating modes represents a fundamental trade-off between maximising carbon removal and maintaining electricity supply. These results offer quantitative guidance for policymakers weighing carbon removal ambitions against energy system constraints.

*There is a crack in everything. That's how the light gets in.*



# Acknowledgements

This work would not have been possible without the support, guidance, and encouragement of many individuals, to whom I am sincerely grateful.

I gratefully acknowledge the Swedish Energy Agency (Energimyndigheten) for the financial support that made this research possible.

My deepest gratitude goes to my main supervisor, Prof. Hailong Li. What I have learned from you goes far beyond knowledge – you have always steered me toward identifying problems, thinking independently, and growing as a researcher. You lead by example, and I have learned enormously from watching how you approach research and mentorship. Your patience, encouragement and genuine investment in my development have profoundly shaped who I am today. I am equally grateful to my co-supervisors. Prof. Eva Thorin, your thoughtfulness and depth of insight have been a constant source of inspiration, and our conversations always left me with something new to think about. Your ability to see the bigger picture has helped me find clarity when I felt lost in the details. Dr. Jan Skvaril, thank you for the practical wisdom, invaluable experience, tools and skills you introduced me to and generous encouragement along the way. The skills and ways of thinking you shared with me will stay with me long beyond this thesis.

I would like to thank our industrial collaboration partners, Stockholm Exergi (especially Kåre Gustafsson), Mälarenergi, and Eskilstuna Strängnäs Energi och Miljö. Every meeting brought new perspectives and kept my research grounded in real-world challenges. Those conversations were invaluable. To Shuo Wang, from another university, thank you for being a wonderful collaborator and for the many stimulating discussions we have had during the collaboration.

My sincere thanks go to Associate Prof. Salman Raza Naqvi and Dr. Lara Carvalho for their thorough and thoughtful reviews of this thesis. Your feedback made this work substantially better.

To my colleagues and friends at FEC, thank you for the company, the conversations, the fika, and everything in between. A special mention to Heidi Ivan, Silvia Ma Lu and Reyhaneh Gorji: thank you for your patience and support whenever I needed help or someone to talk to. A particular thank you to Chenyu Su, whose friendship has been one of the unexpected joys of this chapter of my life. The memories we made together, in research and in life, are ones I will carry with me.

A heartfelt thank you to my landlord, Pelle Svensson, whose warmth and generosity made settling into life in Sweden far easier and more enjoyable.

Finally, to my family and friends, thank you for your unwavering belief in me. A special thank you to Huan Liu – your presence and support have been my anchor throughout this journey.

*Beibei Dong*

Västerås, Sweden, February 2026

# Summary

Integrating bioenergy with carbon capture and storage (BECCS) into biomass-fired combined heat and power (bio-CHP) plants offers crucial potential for achieving negative emissions. In Sweden, biomass and waste are widely used as fuel for CHP plants serving district heating networks. However, the dynamic operation of CHP plants introduces significant challenges for CO<sub>2</sub> capture, stemming from fluctuating heat demand and electricity price signals, volatile electricity markets, and variable biomass fuel properties.

Despite the growing interest in BECCS deployment in bio-CHP plants, critical knowledge gaps remain regarding the dynamic operation of CO<sub>2</sub> capture that hinder its effective implementation. First, how different modelling approaches perform across application scenarios for CO<sub>2</sub> capture in bio-CHP plants has not been systematically compared, leaving unclear guidance on model selection. There are also no control strategies capable of coordinating heat supply, electricity market participation, and CO<sub>2</sub> capture efficiency under fluctuating conditions. Furthermore, there is also a lack of methodologies for quantifying BECCS potential in existing CHP infrastructure under realistic constraints. To address these gaps, this dissertation evaluates dynamic modelling and advanced control approaches for CO<sub>2</sub> capture in bio-CHP plants and investigates their operation modes to enable effective BECCS deployment in bio-CHP plants, contributing to Sweden's climate neutrality goals by 2045.

To provide systematic guidance for selecting appropriate modelling approaches, both first principles and machine learning (ML) approaches were developed and benchmarked. This dissertation first systematically compared three first-principles-based approaches, including ideal static models (IST), dynamic models without control (Dw/oC), and dynamic models with control (DwC), representing the first such comparison for CO<sub>2</sub> capture in bio-CHP plants. Clear differences were identified, with captured CO<sub>2</sub> varying up to 22%. Application-specific guidance was established: Dw/oC for understanding system dynamics, DwC for control design and hourly optimisation, and IST for long-term potential estimation. Building upon this foundation, ML using Informer was introduced, representing the first application of Informer to CO<sub>2</sub> capture modelling. Informer predicted CO<sub>2</sub> capture rate and energy use with mean absolute percentage errors (MAPEs) of 6.2% and 2.7%, respectively. Extending the ML investigation to a broader comparison, three ML approaches (Informer, long short-term memory (LSTM) and

back-propagation neural network (BPNN)) were compared across four applications (system identification, monitoring, optimisation, and performance estimation). All ML models achieve satisfactory accuracy, with most MAPEs below 5%. Although Informer generally performs best, no single model consistently outperforms the others, confirming that selection should be tailored to the application. Collectively, these studies establish a comprehensive modelling approach with systematic guidance for selecting appropriate models under different operational needs.

With reliable models established, model predictive control (MPC) was developed and evaluated for managing operational fluctuations characteristic of bio-CHP plants, through setpoint tracking scenarios and disturbance rejection scenarios. MPC consistently demonstrated superior controller performance over conventional proportional integral (PI) control, achieving a 3–66% reduction in overshoot and maximum deviation, a 47–62% reduction in settling time and recovery time, and a 66–74% reduction in integrated absolute errors for CO<sub>2</sub> capture rate. Regarding process performance, the performance depends on the direction of system changes. The cumulative differences in CO<sub>2</sub> capture amount between MPC and PI range from 4.4% to 8.7%. These results demonstrate that MPC could coordinate dynamic CO<sub>2</sub> capture through improved control quality and smoother dynamic responses.

Finally, the negative emission potential was assessed from plant level to national scale. An example CHP plant was evaluated using two operating modes (OMs) reflecting Sweden's prioritised heat supply. OM1 maximises CO<sub>2</sub> capture by allowing electricity sacrifice, while OM2 maintains both heat and electricity supply. With an average biogenic fraction of 55%, operating in OM1 achieved 181 kilotonnes per year (kt/yr) negative emissions (81.8% capture rate), while operating in OM2 resulted in 121 kt/yr positive emissions (20.3% capture rate) but still reduced emissions by 85.8 kt/yr compared to the reference case without CO<sub>2</sub> capture. Scaling up to national level, Sweden's potential was evaluated under the same constraint of maintained heat supply – the first such national assessment for Swedish BECCS in CHP plants. Under the same biogenic fraction, operating in OM1 can achieve 8.7 megatonnes per year (Mt/yr) negative CO<sub>2</sub> emissions, meeting Sweden's expected BECCS target (3–10 MtCO<sub>2</sub>/yr). The levelised cost of CO<sub>2</sub> avoided was 36.9 U.S. dollars per tonne CO<sub>2</sub> (\$/tCO<sub>2</sub>) for OM1 and 52.0 \$/tCO<sub>2</sub> for OM2. Furthermore, the biogenic fraction critically influences results, with minimum fractions of 32.8% (OM1) and 84.3% (OM2) required to achieve 3 MtCO<sub>2</sub>/yr negative emissions. These findings demonstrate that Sweden's BECCS targets are technically and economically achievable, with operating mode choice fundamentally determining the negative emission boundary.

This dissertation contributes to BECCS research through the systematic comparison of three first-principles modelling approaches for CO<sub>2</sub> capture in bio-CHP plants, the application of ML (specifically Informer) to CO<sub>2</sub> capture modelling with systematic guidance for different applications, and the first national-scale BECCS assessment for Sweden under maintained heat supply constraints. The work progressively integrates dynamic modelling, control design, and performance assessment, offering systematic guidance to system designers and policymakers. Future work should focus on validating ML models with operational data, extending MPC to integrated CHP-capture optimisation, incorporating carbon pricing mechanisms, and broadening assessment to other Nordic and European countries to strengthen generalisability of BECCS deployment strategies.

## Swedish summary

Integrering av bioenergi med koldioxidavskiljning och lagring (BECCS) i biomassaeldade kraftvärmeverk (KVV) erbjuder avgörande potential för att uppnå negativa utsläpp. I Sverige används biomassa och avfall i stor utsträckning som bränsle i KVV som försörjer fjärrvärmenät. Den dynamiska driften av KVV introducerar dock betydande utmaningar för CO<sub>2</sub>-avskiljning, till följd av fluktuerande värmebehov och elprissignaler, volatila elmarknader samt bränslets varierande egenskaper.

Trots det växande intresset för BECCS-implementering i biomassaeldade KVV kvarstår kritiska kunskapsluckor avseende den dynamiska driften av CO<sub>2</sub>-avskiljning, vilket hindrar en effektiv implementering. För det första har olika modelleringsansatser för CO<sub>2</sub>-avskiljning i biomassaeldade KVV inte systematiskt jämförts i olika tillämpningsscenarier, vilket leder till en oklar vägledning för modellval. Det saknas även kontrollstrategier som kan koordinera värmeförsörjning, elmarknadsdeltagande och CO<sub>2</sub>-avskiljningseffektivitet under fluktuerande förhållanden. Vidare saknas metoder för att kvantifiera BECCS-potentialen i befintlig KVV-infrastruktur under realistiska begränsningar. För att åtgärda dessa luckor utvärderas denna avhandling dynamisk modellering och avancerade tillvägagångssätt att reglera CO<sub>2</sub>-avskiljning i biomassaeldade KVV, samt undersöker deras driftlägen för att möjliggöra en effektiv implementering av BECCS och bidra till Sveriges mål om klimatneutralitet år 2045.

För att ge systematisk vägledning vid val av lämpliga modelleringsansatser utvecklades och utvärderades både första-princip-baserade ansatser och maskininlärningsansatser (ML). I avhandlingen jämförs systematiskt tre första-princip-baserade ansatser: ideala statiska modeller (IST), dynamiska modeller utan reglering (Dw/oC) och dynamiska modeller med reglering (DwC) – vilket är den första jämförelsen av detta slag för CO<sub>2</sub>-avskiljning i biomassa-KVV. Tydliga skillnader identifierades, där mängden avskild CO<sub>2</sub> varierade med upp till 22%. Tillämpningsspecifik vägledning fastställdes: Dw/oC för förståelse av systemdynamik, DwC för design av styrning och timbaserad optimering, samt IST för uppskattning av den långsiktiga potentialen. Med utgångspunkt i denna grund introducerades ML med hjälp av Informer, vilket representerar den första tillämpningen av Informer-arkitekturen för CO<sub>2</sub>-avskiljningsmodellering. Informer predikerade CO<sub>2</sub>-avskiljningsgrad och energianvändning med ett genomsnittligt absolut procentuellt fel (MAPE) på 6,2% respektive 2,7%. I en utvidgad jämförelse utvärderades tre ML-ansatser – Informer, Long Short-Term Memory (LSTM) och Back-

propagation Neural Network (BPNN) – inom fyra tillämpningsområden: systemidentifiering, övervakning, optimering och prestandaskattning. Samtliga ML-modeller uppnår tillfredsställande noggrannhet med MAPE-värden som i de flesta fall understiger 5%. Även om Informer generellt presterar bäst, överträffar ingen enskild modell konsekvent de övriga, vilket bekräftar att modellvalet bör anpassas efter tillämpningen. Sammantaget etablerar dessa studier en övergripande modelleringsansats med systematisk vägledning för val av lämpliga modeller under olika driftbehov.

Med tillförlitliga modeller som grund utvecklades och utvärderades modellprediktiv reglering (MPC) för hantering av driftfluktuationer karakteristiska för biomassaeldade KVV, genom scenarier för börvärdessparning och störningsavvisning. MPC uppvisade konsekvent överlägsen reglerprestanda jämfört med konventionell proportionell-integral-reglering (PI), med 3–66% reduktion av överskjutning och maximal avvikelse, 47–62% reduktion av insvängningstid och återhämtningstid, samt 66–74% reduktion av integrerat absolut fel för CO<sub>2</sub>-avskiljningsgraden. Vad gäller processprestanda beror utfallet på riktningen för systemförändringar. De kumulativa skillnaderna i avskild CO<sub>2</sub>-mängd mellan MPC och PI varierar från 4,4% till 8,7%. Dessa resultat visar att MPC kan koordinera dynamisk CO<sub>2</sub>-avskiljning genom förbättrad reglerkvalitet och jämnare dynamiska förlopp.

Slutligen bedömdes potentialen för negativa utsläpp på skalnivåer från enskild anläggning till nationell nivå. Ett exempel-KVV utvärderades med hjälp av två driftlägen (DL) som speglar Sveriges prioritering av värmeförsörjning. DL1 maximerar CO<sub>2</sub>-avskiljning och tillåter minskning av elproduktionen, medan DL2 upprätthåller både värme- och elförsörjning. Med en genomsnittlig biogen fraktion på 55% uppnåddes vid drift i DL1 negativa utsläpp på 181 kilotonnes per year (kt/yr) (avskiljningsgrad 81,8%), medan drift i DL2 resulterade i positiva utsläpp på 121 kt/yr (avskiljningsgrad 20,3%), men ändå reducerade utsläppen med 85,8 kt/yr jämfört med referensfallet utan CO<sub>2</sub>-avskiljning. Vid uppskalning till nationell nivå utvärderades Sveriges potential under samma restriktion om bibehållen värmeförsörjning – den första studien med denna typ av bedömning på nationell nivå för svensk BECCS i KVV. Med samma biogena fraktion kan drift i DL1 uppnå negativa utsläpp på 8,7 megatonnes per year (Mt/yr), vilket täcker Sveriges förväntade BECCS-mål. Den beräknade kostnaden per undviktonne CO<sub>2</sub> uppgick till 36,9 U.S. dollars per tonne CO<sub>2</sub> (\$/tCO<sub>2</sub>) (DL1) respektive 52,0 \$/tCO<sub>2</sub> (DL2). Vidare har den biogena fraktionen en kritisk påverkan på resultaten: minimifraktioner på 32,8% (DL1) respektive 84,3% (DL2) krävs för att uppnå negativa utsläpp på 3 Mt/yr. Dessa resultat visar att Sveriges BECCS-mål är tekniskt och ekonomiskt möjliga att uppnå, och att valet av driftläge fundamentalt bestämmer gränsen för negativa utsläpp.

Denna avhandling bidrar till BECCS-forskningen genom den systematiska jämförelsen av tre första-princip-baserade modelleringsansatser för CO<sub>2</sub>-avskiljning i biomassaldade-KVV, tillämpningen av ML (specifikt Informer) för CO<sub>2</sub>-avskiljningsmodellering med systematisk vägledning för olika tillämpningar, samt den första nationella BECCS-bedömningen för Sverige under restriktionen om bibehållen värmeförsörjning. Arbetet integrerar progressiv dynamisk modellering, design av styrning och prestanda-bedömning, och erbjuder systematisk vägledning till systemkonstruktörer och beslutsfattare. Framtida arbete bör fokusera på validering av ML-modeller med driftsdata, utvidgning av MPC till integrerad optimering av KVV och CO<sub>2</sub> avskiljningen, inkludering av koldioxidprissättningsmekanismer samt utöka uppskattningen av potentialen för avskiljning till andra nordiska och europeiska länder för att stärka generaliserbarheten av strategier för implementering av BECCS.

# List of papers

## Publications included in the thesis

This thesis is based on the following papers, which are referred to in the text by their roman numerals.

- I. **Dong, B.**, Hu, C., Skvaril, J., Thorin, E., Li, H. (2023). Selecting the approach for dynamic modelling of CO<sub>2</sub> capture in biomass/waste fired CHP plants. *International Journal of Greenhouse Gas Control*, 130, 104008.
- II. **Dong, B.**, Chen, J., Shi, X., Li, H. (2023). AI-based Dynamic Modelling for CO<sub>2</sub> Capture. In *Energy Proceedings of the International Conference on Energy, Ecology and Environment (ICEEE)*, 37, August 14–18, 2023, London, UK.
- III. **Dong, B.**, Gustafsson, K., Shi, X., Hedén Sandberg, A., Skvaril, J., Thorin, E., Li, H. (2025). Using machine learning for modelling dynamic operation of CO<sub>2</sub> capture considering different application requirements. In *Energy Proceedings of the Applied Energy Symposium and Forum: Resilient Energy Systems*, 61, Sep. 23–25, 2025.
- IV. **Dong, B.**, Skvaril, J., Thorin, E., Li, H. (2025). Model predictive control for CO<sub>2</sub> capture from biomass-fired CHP plants: Performance evaluation during operational transitions. [Manuscript]
- V. Wang, S., **Dong, B.**, Gustafsson, K., Ma, C., Sun, Q., Li, H. (2023). Assessing the CO<sub>2</sub> capture potential for waste-fired CHP plants. *Journal of Cleaner Production*, 428, 139379.
- VI. **Dong, B.**, Wang, S., Thorin, E., Sun, Q., Li, H. (2024). Negative emission potential from biomass/waste combined heat and power plants integrated with CO<sub>2</sub> capture: An approach from the national perspective. *Journal of Cleaner Production*, 467, 142917.

Reprints were made with permission from the respective publishers.

## Publications not included in the thesis

- I. **Dong, B.**, Wang, S., Sun, Q., Skvaril, J., Thorin, E., Li, H. (2022). Aggregated Negative Emission from Biomass Fired CHP Plants in Sweden. In *Energy Proceedings of the 14<sup>th</sup> International Conference on Applied Energy, ICAE2022, 29*, August 8–11, 2022, Bochum, Germany.
- II. **Dong, B.**, Li, W., Li, H. (2022). Removing CH<sub>4</sub> from the Waste Gas of Biogas Upgrading. In *Energy Proceedings of the 14<sup>th</sup> International Conference on Applied Energy, ICAE2022, 29*, August 8–11, 2022, Bochum, Germany.
- III. **Dong, B.**, Wang, S., Sun, Q., Thorin, E., Li, H. (2024). Marginal cost of CO<sub>2</sub> capture. *The International Conference on Energy, Ecology and Environment (ICEEE)*, August 26–29, 2024, Rome, Italy.
- IV. Pan, S., Shi, X., **Dong, B.**, Skvaril, J., Zhang, H., Liang, Y., Li, H. (2024). Multivariate time series prediction for CO<sub>2</sub> concentration and flowrate of flue gas from biomass-fired power plants. *Fuel*, 359, 130344.
- V. Li, H., **Dong, B.**, Nookuea, W., Sun, Q., Thorin, E., Yu, Z. (2025). Selecting proper technologies for capturing CO<sub>2</sub> from bioenergy conversion. *Renewable and Sustainable Energy Reviews*, 218, 115747.
- VI. Wang, S., **Dong, B.**, Gustafsson, K., Thorin, E., Sun, Q., Li, H. (2026). Capturing CO<sub>2</sub> from waste-fired CHP plants at low marginal cost. *Applied Energy*, 410, 127558.

# Contents

Acknowledgements .....	i
Summary .....	iii
Swedish summary .....	vi
List of papers .....	ix
List of figures .....	xiii
List of tables .....	xv
Nomenclature .....	xvii
Preface .....	xxii
1 Introduction .....	1
1.1 Background .....	1
1.2 Objectives and research questions .....	3
1.3 Contributions .....	4
1.4 Dissertation outline .....	6
2 Literature study .....	9
2.1 Dynamic modelling of CO <sub>2</sub> capture process .....	9
2.1.1 Applications of dynamic modelling .....	9
2.1.2 First principles-based models of CO <sub>2</sub> capture .....	11
2.1.3 Machine learning-based models of CO <sub>2</sub> capture .....	12
2.2 Control of CO <sub>2</sub> capture .....	13
2.2.1 Proportional–integral–derivative (PID) controllers .....	14
2.2.2 Model predictive control (MPC) .....	15
2.3 Assessment of CO <sub>2</sub> capture in biomass CHP plants .....	16
2.3.1 Plant-level assessment .....	16
2.3.2 National-level assessment .....	17
3 Methodology .....	19
3.1 Overview .....	19
3.2 Dynamic process modelling and simulation .....	20
3.2.1 Development of first principles-based models .....	20
3.2.2 Development of machine learning-based surrogate models ...	25
3.3 Model predictive control design .....	26
3.3.1 System description and model identification .....	26
3.3.2 Model predictive control design .....	29
3.4 Potential assessment framework .....	32
3.4.1 Modelling an example CHP plant .....	32
3.4.2 National aggregation of all CHP plants .....	36

3.4.3 Case study – Sweden.....	39
4 Selecting dynamic modelling approaches for different applications of CO <sub>2</sub> capture .....	43
4.1 First principles-based modelling approaches for CO <sub>2</sub> capture.....	43
4.1.1 Case setup .....	43
4.1.2 Comparison of different modelling approaches .....	44
4.1.3 Selection of modelling approaches .....	46
4.2 Machine learning-based models of CO <sub>2</sub> capture .....	47
4.2.1 Application definition and case setup .....	47
4.2.2 Data generation .....	48
4.2.3 Performance of machine learning models .....	51
5 Performance evaluation of model predictive control .....	55
5.1 System identification results.....	55
5.2 MPC performance evaluation and comparison with PI control.....	55
5.2.1 Case 1: Setpoint tracking with varying capture rates .....	55
5.2.2 Case 2: FG flow rate disturbance rejection .....	58
5.2.3 Case 3: Disturbance rejection of FG flow rate and CO <sub>2</sub> concentration.....	61
5.2.4 Summary of MPC controller performance improvements .....	63
6 Potential assessment of CO <sub>2</sub> capture in Swedish CHP plants .....	65
6.1 Plant-level potential of CO <sub>2</sub> capture in the reference CHP plant....	65
6.1.1 CO <sub>2</sub> capture potential .....	65
6.1.2 CO <sub>2</sub> capture cost.....	66
6.2 Nationwide potential of CO <sub>2</sub> capture in all Swedish CHP plants ...	67
6.2.1 Model validation .....	67
6.2.2 CO <sub>2</sub> capture potential .....	68
6.2.3 CO <sub>2</sub> capture cost.....	69
7 Delimitations .....	73
8 Conclusions .....	75
9 Future work .....	77
Appendix .....	79
A: Validation of the steady-state model in IST .....	79
B: Validation of the dynamic model in Dw/oC and DwC .....	80
C: Validation of the waste-fired CHP plant model .....	82
D: Validation of machine learning models .....	83
D1: Heat demand model.....	83
D2: CHP model.....	84
References .....	85

# List of figures

Figure 3.1: Methodology schematic outline for addressing research questions. ....	19
Figure 3.2: Rate-based MEA simulation flowsheet in Aspen Plus. ....	20
Figure 3.3: MEA-based CO <sub>2</sub> capture without control strategy. ....	21
Figure 3.4: MEA-based CO <sub>2</sub> capture with control strategy. ....	22
Figure 3.5: Flue gas data from a w-CHP plant. ....	24
Figure 3.6: Flowsheet of the designed MEA-CA in Aspen Plus Dynamics. ....	27
Figure 3.7: Implemented random signals for system identification (a): Flue gas flow rate; (b): CO <sub>2</sub> content; (c): Lean solvent flow rate; (d): Reboiler duty. ....	28
Figure 3.8: Scheme of the bottom-up approach. ....	33
Figure 3.9: Schematic of integration of w-CHP and CO <sub>2</sub> capture and compression. ....	33
Figure 3.10: Calculation flowchart for two operating modes. ....	34
Figure 3.11: Calculation flowchart for other CHP plants. ....	39
Figure 3.12: Distribution and installed capacities of CHP plants in Sweden (Ahlmén & Hellsberg, 2020). ....	41
Figure 4.1: Relative differences in accumulated captured CO <sub>2</sub> under different operating parameters. ....	45
Figure 4.2: Relative differences in specific reboiler duty under different operating parameters. ....	46
Figure 4.3: Variation of flue gas in Case 1. ....	49
Figure 4.4: Variation of reboiler duty in Case 1. ....	49
Figure 4.5: Variation of lean solvent flow rate in Case 1. ....	50
Figure 4.6: Variation of CO <sub>2</sub> capture rate targets in Case 3. ....	50
Figure 4.7: Variations of flue gas and reboiler duty in Case 4. ....	51
Figure 5.1: Comparison between Aspen Plus Dynamics and identified models: CO <sub>2</sub> capture rate (deviates from 84%) and reboiler temperature (deviates from 116°C). ....	56
Figure 5.2: Comparison of MPC and PI controllers in Case 1. ....	57
Figure 5.3: Flue gas disturbance in Case 2. ....	58
Figure 5.4: Comparison of MPC and PI controllers in Case 2. ....	59
Figure 5.5: Flue gas disturbance in Case 3. ....	61
Figure 5.6: Comparison of MPC and PI controllers in Case 3. ....	62
Figure 6.1: Breakdown of LCCA of example plant. ....	67

Figure 6.2: The influence of biogenic fraction of the waste on net CO<sub>2</sub> emission. .... 69

Figure 6.3: LCCA and LCC from each CHP plant..... 70

Figure 6.4: Breakdown of national LCCA. .... 71

# List of tables

Table 2.1 Summary of machine learning models for dynamic CO <sub>2</sub> capture. .....	13
Table 3.1 Summary of model parameters and column settings (Li et al., 2015). .....	21
Table 3.2: Dynamic model parameters (Harun, 2012). .....	22
Table 3.3: Manipulated and controlled variables and targets (Harun et al., 2012; Nittaya et al., 2014).....	23
Table 3.4: The scaled-up capture system and other input parameters.....	24
Table 3.5: Streams under the designed operating point (Dong et al., 2023; Zanco et al., 2021; Zhou et al., 2022). .....	27
Table 3.6: Process constraints considered in the MPC formulation.....	30
Table 3.7: The factors used in the assessment of CAPEX and OPEX (Christensen & Dysert, 2011; Gerdes et al., 2011; Li et al., 2015). 37	
Table 3.8: Main operating parameters of the example CHP plant with CO <sub>2</sub> capture and compression. ....	40
Table 3.9: Economic evaluation assumptions of CO <sub>2</sub> capture and compression (Li et al., 2015). .....	41
Table 4.1: An overview of the defined cases. ....	44
Table 4.2: Inputs and outputs of different cases.....	48
Table 4.3: Prediction accuracy for Case 1.....	51
Table 4.4: Prediction accuracy for Case 2.....	52
Table 4.5: Prediction accuracy for Case 3.....	52
Table 4.6: Prediction accuracy for Case 4.....	53
Table 5.1: Comparison of controller performance metrics in Case 1.....	57
Table 5.2: Comparison of process performance metrics in Case 1. ....	58
Table 5.3: Comparison of controller performance metrics in Case 2.....	60
Table 5.4: Comparison of process performance metrics in Case 2. ....	60
Table 5.5: Comparison of controller performance metrics in Case 3.....	62
Table 5.6: Comparison of process performance metrics in Case 3. ....	63
Table 5.7: Summary of MPC controller performance improvement over PI. .....	64
Table 6.1: CO <sub>2</sub> capture potential and the influence on example CHP. ....	65
Table 6.2: Costs related to CO <sub>2</sub> capture in the example CHP plant. ....	66
Table 6.3: Nationwide potential of CO <sub>2</sub> capture in all CHP plants in Sweden. .....	68
Table 6.4: Costs related to CO <sub>2</sub> capture in all CHP plants in Sweden. ....	70



# Nomenclature

## *Abbreviations*

ABS	absorber
APE	absolute percentage error
APEA	Aspen Process Economic Analyzer
AR6	Sixth Assessment Report
ARX	autoregressive exogenous input
BANN	bootstrap-aggregated neural network
BEC	bare erected cost
BECCS	bioenergy with carbon capture and storage
bio-CHP	biomass-fired combined heat and power
BPNN	back-propagation neural network
CA	chemical absorption
CAPEX	total capital expenditure
CCS	carbon capture and storage
CDR	carbon dioxide removal
CHP	combined heat and power
CO <sub>2</sub>	carbon dioxide
CO <sub>2</sub> vol%	CO <sub>2</sub> concentration
CVs	controlled variables
DBN	deep belief network
DH	district heating
DwC	dynamic models with control
Dw/oC	dynamic models without control
EC	engineering and contractor
EMPC	economic MPC
EPC	engineering procurement and construction
EU ETS	European Union Emissions Trading System
FG	flue gas
FIC	flow rate indicating controller
GHG	greenhouse gas
HPC	hot potassium carbonate
IAE	integrated absolute error
IMTP	Intalox Metal Tower Packing
INN	integral neural network
IPCC	Intergovernmental Panel on Climate Change
ISE	integral squared error
IST	ideal static models

ITAE	integrated time and absolute error
KPIs	key performance indicators
LCC	life-cycle cost
LCCA	levelised cost of CO <sub>2</sub> avoided
L/G ratio	liquid-to-gas ratio
LIC	level indicating controller
LSTM	long short-term memory
MAE	mean absolute error
MAPE	mean absolute percentage error
MD	maximum deviation
MEA	monoethanolamine
MEA-CA	MEA-based chemical absorption
MIMO	multiple-input multiple-output
ML	machine learning
ML_CHP	machine learning-based modelling for CHP
ML_demand	machine learning-based modelling for heat demand
MPC	model predictive control
MSE	mean squared error
MVs	manipulated variables
NARX-NN	nonlinear autoregressive NN with exogenous input
NETs	negative emission technologies
NLARX	nonlinear autoregressive model with exogenous input
NN	neural network
OC	owner's cost
O&M	operating and maintenance
OM	operating mode
OPEX	annual operating and maintenance cost
OS	overshoot
PC	process contingency
PCC	post combustion capture
PI	proportional–integral
PID	proportional–integral–derivative
PIINN	physics-informed integral neural network
PJC	project contingency
PPA	power purchase agreement
RGA	relative gain array
RQs	research questions
RT	rise time
RTd	recovery time
SDGs	Sustainable Development Goals
SISO	single-input single-output
SMHI	Swedish Meteorological and Hydrological Institute

ST	settling time
STR	stripper
TDC	total direct cost
TIC	temperature-indicating controller
TIC_cost	total indirect cost
TOU	time of use
TPC	total plant cost
TS	time step
w-CHP	waste-fired combined heat and power

### **Symbols**

$Heat_{reboiler}$	reboiler duty
$A$	Matrix coefficient of state-space model
$A_{CO_2}$	amount of avoided CO <sub>2</sub>
$a_{i,k}$	autoregressive coefficients for output $y_i$
$B_d$	Matrix coefficient of state-space model
$b_{ij,k}$	input coefficients from input $u_j$ to output $y_i$
$B_u$	Matrix coefficient of state-space model
$C$	Matrix coefficient of state-space model
$C_{CO_2}$	amount of captured CO <sub>2</sub>
$C_{CO_2,acc}$	accumulated amount of captured CO <sub>2</sub> over 4 hours
$CO_{2,pro}$	amount of CO <sub>2</sub> in the product stream
$D_d$	Matrix coefficient of state-space model
$d_k$	measured disturbance variables
$e_i$	modelling error
$El$	amount of net electricity generation
$F$	amount of consumed fuel
$G_{CO_2}$	amount of generated CO <sub>2</sub>
$J$	cost function
$M_{chemical}$	consumed amount of chemicals
$m_{CO_2}$	hourly optimised amount of captured CO <sub>2</sub>
$n_a$	autoregressive order
$n_b$	exogenous input order
$N_c$	control horizon
$n_{k,j}$	time delay from input $u_j$ to the outputs
$NetE$	net CO <sub>2</sub> emission
$N_p$	prediction horizon
$OPEX_{variable}$	variable O&M cost
$Q$	output tracking weight matrix
$Q_{reb}$	available heat for reboiler/reboiler heat duty
$Q_{DH}$	hourly heat demand
$R$	input rate penalty matrix

$r$	discount rate
$r_{k+i}$	desired setpoint trajectory
$R_{CO_2}$	CO <sub>2</sub> capture rate
$S_{amb}$	hourly wind speed
$SRD_{ave}$	average specific reboiler duty
$T$	plant economic life/integral time/time step
$T_{amb}$	hourly ambient temperature
$t_f$	final time of the evaluation period
$u_1$	FG flow rate
$u_2$	FG CO <sub>2</sub> concentration
$u_3$	lean solvent flow rate
$u_4$	reboiler heat duty
$u_k$	manipulated variables
$u_{k+i}$	manipulated inputs
$UP_{chemical}$	unit price of chemicals
$UE_{electricity}$	unit price of electricity
$wl\%$	weight per cent
$x_k$	state vector
$y_1$	CO <sub>2</sub> capture rate
$y_2$	reboiler temperature
$y_k$	controlled variables
$y_{k+i}$	predicted controlled variables
$y_i$	$i^{th}$ actual value
$\hat{y}_i$	$i^{th}$ predicted value
$y_{sp}$	setpoint of the controlled variables
$\alpha_{fos}$	fossil fraction of the fuel
$\Delta$	changes
$\Delta u_{k+i}$	change rate of manipulated inputs

### **Subscripts**

$Ex$	example CHP plant
$I$	$i^{th}$ CHP plant
$In$	installed capacity
$Integ$	integrated system with CO <sub>2</sub> capture
$J$	$j^{th}$ hour
$K$	$k^{th}$ chemicals
$k+i$	time step $k+i$
$Max$	maximum constraints
$Min$	minimum constraints
$N$	total number of CHP plants
$nation$	aggregated national results
$P$	total number of chemicals

*Ref* reference plant without CO<sub>2</sub> capture  
*Y* yearly results

***Units of measurement***

t tonne (1,000 kilograms)  
kt kiloton (1,000 metric tonnes)  
Mt megaton (1,000,000 metric tonnes)  
\$ U.S. dollars

# Preface

This doctoral thesis was conducted at the Department of Engineering Sciences at Mälardalen University, in partial fulfilment of the requirements for the degree of Doctor of Philosophy in Energy and Environmental Engineering. The work was carried out under the supervision of Professor Hailong Li and co-supervised by Professor Eva Thorin and Dr. Jan Skvaril. The research began in November 2021 and has since evolved through several studies focusing on dynamic modelling, advanced control, and negative emission potential assessment of bioenergy with carbon capture and storage (BECCS) in biomass-fired combined heat and power (CHP) plants.

This thesis presents the main results of the doctoral work and provides an integrated synthesis of the included scientific publications. It is intended to be read in combination with the appended publications, as it serves as motivation for, and summary of, the work presented in the original publications. The enclosed chapters offer insights into the modelling approaches, control strategies, and negative emission potential of BECCS in biomass-fired CHP plants, while addressing the broader implications for Sweden's transition towards climate neutrality by 2045.

# 1 Introduction

*This chapter defines the research questions and outlines the structure of the dissertation.*

## 1.1 Background

To reduce the risks and impacts of global warming, including poverty, extreme heat, sea level rise, habitat loss, and drought (NRDC, 2021; United Nations Environment Programme, 2024), the Paris Agreement has been adopted with a long-term temperature goal to keep the rise in global surface temperature to well below 2°C, preferably to 1.5°C, above pre-industrial levels (IPCC, 2018; UNFCCC, 2016). To pursue the 1.5°C target, the Intergovernmental Panel on Climate Change (IPCC) Sixth Assessment Report (AR6) confirms that global greenhouse gas (GHG) emissions need to be reduced by 43% by 2030 relative to 2019 and reach net-zero CO<sub>2</sub> emissions around 2050 (Lee & Romero, 2023). However, achieving these targets presents unprecedented challenges. The year 2024 was confirmed as the warmest year on record globally, with multiple independent datasets indicating it exceeded 1.5°C above the pre-industrial baseline (Copernicus Climate Change Service, 2025; World Meteorological Organization, 2025). Moreover, the 2015–2024 decade represents the warmest 10-year period on record (United Nations Environment Programme, 2024). To achieve the Paris Agreement target, all climate mitigation scenarios indicate requiring the deployment of carbon dioxide removal (CDR) at substantial scale by using negative emissions technologies (NETs) (European Academies’ Science Advisory Council, 2018; Lee & Romero, 2023; Rau & Greene, 2015). CDR would be used to compensate for residual emissions from sources where mitigation measures are difficult to implement to achieve net negative emissions to return global warming to 1.5°C following a peak (Lee & Romero, 2023). Such efforts are also aligned with the United Nations Sustainable Development Goals (SDGs), particularly SDG 13 (Climate Action) and SDG 7 (Affordable and Clean Energy), which call for urgent action on climate change and the transition to sustainable energy systems.

Among the various NETs, bioenergy with carbon capture and storage (BECCS) has emerged as one of the most viable and cost-effective options for achieving negative emissions (Carbon Brief, 2019; Joint Task Force on Biomass and CCS, 2018; Wang et al., 2024). BECCS involves capturing and permanently storing CO<sub>2</sub> from processes in which biomass is converted into fuels or directly burned to generate energy (IEA, 2024). Because plants absorb CO<sub>2</sub> from the atmosphere during growth through photosynthesis, capturing and storing this biogenic CO<sub>2</sub> effectively removes CO<sub>2</sub> from the atmosphere, resulting in negative emissions (Drax Group, 2021). According to IPCC AR6, BECCS plays a crucial role in climate mitigation scenarios designed to meet Paris Agreement targets (Lee & Romero, 2023). The International Energy Agency projects that BECCS deployment could reach 10 gigatonnes of CO<sub>2</sub> removal per year by 2050 (Joint Task Force on Biomass and CCS, 2018).

Among various applications of BECCS, integrating CO<sub>2</sub> capture with biomass and waste-fired combined heat and power (CHP) plants presents unique opportunities for commercial operation of BECCS (Shahbaz et al., 2021). In northern Europe, biomass and waste are widely used as fuel for CHP plants serving district heating (DH) networks (Anca-Couce et al., 2021). Taking Sweden as an example, biomass and waste-fired CHP (bio/w-CHP) plants account for the second largest contribution of CO<sub>2</sub> emission sources in the energy sector (Johnsson & Kjärstad, 2019). Integrating BECCS with bio/w-CHP plants is therefore a promising solution to reduce CO<sub>2</sub> emissions and contribute to the Swedish climate goal of net-zero emissions by 2045 (Shahbaz et al., 2021).

The integration of BECCS with CHP plants is transitioning from pilot to full-scale implementation. For example, Stockholm Exergi, as a pioneer, built a pilot carbon capture plant using hot potassium carbonate (HPC) in 2019. In March 2025, the company made a final investment decision to implement the world's first large-scale BECCS project at its Värtan bio-CHP plant in Stockholm, which is scheduled to begin operations in 2028 (Bioenergy International, 2025). The project has also received substantial support, including a EUR 180 million EU Innovation Fund grant and SEK 20 billion in funding from the Swedish Energy Agency (Bioenergy International, 2025). This development demonstrates both the technical feasibility and the increasing policy support for large-scale BECCS deployment in CHP applications. Reliable quantification of achievable negative emissions and associated costs under realistic operational constraints therefore remains essential for guiding policy decisions and investment planning.

CHP plants supply heat to DH networks. Their operations dynamically vary on an hourly basis due to fluctuating heat demand and electricity market conditions (Beiron, Göransson, et al., 2022). The increasing penetration

of intermittent renewable electricity generation further intensifies such variability, as the operation of CHP plants varies more frequently to balance the grid (Beiron, Normann, et al., 2022). In addition, the use of versatile biomass and waste as fuel leads to variations in flue gas (FG) properties depending on fuel composition.

The operational characteristics of CHP plants create significant operational challenges for the integrated CO<sub>2</sub> capture process. The dynamic operation leads to fluctuations in FG flow rate and composition. It is well-recognised that the dynamic variation of FG can obviously affect the performance of downstream CO<sub>2</sub> capture processes, particularly for monoethanolamine (MEA)-based chemical absorption (MEA-CA), the most commercially mature post-combustion CO<sub>2</sub> capture technology (Li, Dong, et al., 2019; Tan et al., 2016). Furthermore, the steam extracted from CHP plants to MEA-CA for driving solvent regeneration also varies widely with electricity and heat demand, which directly affects the CO<sub>2</sub> amount generated in the stripper. CO<sub>2</sub> capture processes must therefore be capable of adapting to these dynamic operational fluctuations while maintaining high energy efficiency (Akram et al., 2016). This not only requires a thorough understanding of the dynamic behaviour of CO<sub>2</sub> capture but also demands advanced control strategies capable of coordinating competing operational objectives under continuously changing conditions.

## 1.2 Objectives and research questions

The overarching objective of this dissertation is to improve the dynamic operation of CO<sub>2</sub> capture in bio-CHP plants, with the aim of maximising CO<sub>2</sub> capture and thereby maximising net negative emissions.

Despite the recognised potential of BECCS in CHP applications, several critical knowledge gaps hinder its implementation. The modelling requirements and approaches may differ significantly across various application scenarios, from process design and optimisation to control system development, yet guidance on appropriate model selection and formulation for different purposes remains scarce. Furthermore, control strategies capable of coordinating heat supply obligations, electricity market participation, and CO<sub>2</sub> capture efficiency in the context of fluctuating bio-CHP operation remain underexplored. Moreover, robust methodologies for quantifying the technical and economic potential of BECCS in existing CHP infrastructure under varying markets and operational conditions need further development. To address these gaps, the following research questions (RQs) have been formulated:

- RQ1** How should the dynamic modelling approaches be selected for different applications of CO<sub>2</sub> capture in biomass-fired CHP plants?
- RQ2** How does model predictive control perform for CO<sub>2</sub> capture under the dynamic operating conditions of biomass-fired CHP plants?
- RQ3** What are the potentials for negative emissions and associated costs when implementing BECCS in biomass-fired CHP plants, from plant level to national scale?

### 1.3 Contributions

This thesis is composed of six papers with the following contributions and links to the research questions:

**Paper I** This paper systematically compares three first principles-based dynamic modelling approaches for CO<sub>2</sub> capture in bio/w-CHP plants: ideal static models (IST), dynamic models without control (Dw/oC), and dynamic models with control (DwC), which represent the same MEA-CA process modelled at increasing levels of complexity. The performance of approaches is assessed under the variations of key parameters. The key contribution is the provision of recommendations for approach selection tailored to different applications. Specifically, Dw/oC is recommended for safety boundary analysis, DwC is recommended for control system design and hourly dynamic optimisation, and IST is recommended for estimating the long-term CO<sub>2</sub> capture potential. This study contributes to **RQ1** by providing systematic guidance for selecting appropriate first principles-based modelling approaches based on application requirements.

**Paper II** Building upon **Paper I**, this paper introduces a machine learning (ML)-based modelling approach using Informer to predict dynamic responses of CO<sub>2</sub> capture. The key contribution is verification of the feasibility of the ML approach for dynamically modelling CO<sub>2</sub> capture. It was found that Informer could predict CO<sub>2</sub> capture rate and energy use with mean absolute percentage errors (MAPEs) of 6.2% and 2.7%, respectively. This work advances **RQ1** by providing a computationally efficient alternative to first principles-based models.

**Paper III** Extending the ML modelling work in **Paper II**, this paper compares three distinct ML approaches (Informer, long short-term

memory network (LSTM), and back-propagation neural network (BPNN)) across four distinct application cases: system identification for control development, system monitoring and diagnosis, operational optimisation, and system performance estimation. The primary contribution is the provision of systematic guidance on ML model development and selection (including how to choose inputs and outputs) for different CO<sub>2</sub> capture dynamic modelling purposes. It was found that ML models can achieve high accuracy for all cases (MAPEs less than 5%), but no single model outperforms the others across all cases. This work comprehensively addresses **RQ1** by evaluating the capability of using ML approaches to develop dynamic models for different purposes.

**Paper IV** Based on simulations, this paper develops and evaluates model predictive control (MPC) strategies for scenarios of setpoint tracking of CO<sub>2</sub> capture rate and disturbance rejection to FG and compares MPC with conventional proportional–integral (PI) control. The key contribution is the demonstration of MPC’s superiority over PI control in managing typical dynamic scenarios of CO<sub>2</sub> capture in CHP plants. Specifically, MPC achieves a 3–66% reduction in overshoot, a 47–62% reduction in settling time, and a 66–74% reduction in control errors. This study addresses **RQ2** by providing quantitative evidence of MPC’s value in achieving flexible and efficient CO<sub>2</sub> capture operation.

**Paper V** This paper establishes a comprehensive assessment framework for evaluating CO<sub>2</sub> capture potential at the plant level. The first principles-based dynamic models from **Paper I** and ML models from **Paper III** are employed. The key contributions are an investigation into the coordination of dynamic operation of CO<sub>2</sub> capture in bio-CHP plants and the identification of CO<sub>2</sub> capture potential boundaries. Two operating modes are investigated considering the characteristics of Swedish CHP plants. This study contributes to **RQ3** by determining the coordinated operating strategies and CO<sub>2</sub> capture potential at the plant level.

**Paper VI** Extending the assessment in **Paper V** to national scale, this paper evaluates Sweden’s negative emission potential from bio/w-CHP plants. The primary contribution is the quantification of achievable negative emission potential range and economic viability and the evaluation of contributions to Swedish climate goals. Under the operating mode where heat supply remains unchanged, electricity supply

can be sacrificed, and optimal operation can achieve 8.7 MtCO<sub>2</sub>/yr negative emission at a cost of 36.9 \$/tCO<sub>2</sub>. This is sufficient to meet the expected target set by Sweden on negative emissions from the adoption of BECCS. Other contributions include an investigation into the influence of biogenic fractions of fuel on negative emissions and the identification of minimum biogenic fractions needed to meet Swedish climate targets under different operating modes. This work comprehensively addresses **RQ3** by providing policy-relevant insights into BECCS deployment on the national scale.

## 1.4 Dissertation outline

This dissertation is based on the appended papers and is structured as follows:

### **Chapter 1** *Introduction*

Introduces the research context and problem framing and describes the motivation for dynamic modelling and control of CO<sub>2</sub> capture in bio-CHP plants. The chapter defines the research questions and outlines how the appended papers relate to them.

### **Chapter 2** *Literature study*

Presents a comprehensive review of dynamic modelling of CO<sub>2</sub> capture processes, control strategies, and assessment studies for CO<sub>2</sub> capture in bio-CHP plants. The chapter provides the conceptual foundation used to formulate the research questions.

### **Chapter 3** *Methodology*

Details the dynamic process modelling and simulation approaches, model predictive control design, and the potential assessment framework developed and applied in the dissertation.

### **Chapter 4** *Selecting dynamic modelling approaches for different applications of CO<sub>2</sub> capture*

Presents the results on the selection of first principles-based and machine learning-based modelling approaches, providing systematic guidance for choosing appropriate models under different operational applications of CO<sub>2</sub> capture.

### **Chapter 5** *Performance evaluation of model predictive control*

Presents the results on MPC performance in managing typical dynamic scenarios of CO<sub>2</sub> capture in CHP plants, covering setpoint tracking and disturbance rejection cases, and compares MPC against conventional PI control.

**Chapter 6** *Potential assessment of CO<sub>2</sub> capture in Swedish CHP plants*

Presents the results on CO<sub>2</sub> capture potential and associated costs, at both the individual plant level and the national level across Swedish CHP plants.

**Chapter 7** *Delimitations*

Outlines the scope boundaries of the dissertation with respect to dynamic modelling, control design, and potential assessment, clarifying assumptions and limitations when interpreting the results.

**Chapter 8** *Conclusions*

Summarises the main findings of the dissertation, particularly with respect to CO<sub>2</sub> capture modelling, control, and capture potential assessment.

**Chapter 9** *Future work*

Proposes future directions grounded in the findings from all appended papers.

The six papers on which this thesis is based are appended after the main chapters as Papers I–VI.



## 2 Literature study

*This chapter reviews dynamic modelling approaches, control strategies, and BECCS assessment studies, organised into Sections 2.1–2.3.*

### 2.1 Dynamic modelling of CO<sub>2</sub> capture process

Dynamic modelling is essential for understanding the transient behaviour of CO<sub>2</sub> capture processes and enabling their effective integration with bio/w-CHP plants. This section reviews the current state of dynamic modelling approaches for CO<sub>2</sub> capture process. Section 2.1.1 first identifies the key applications that require dynamic models and establishes the motivation for dynamic modelling. Subsequently, Section 2.1.2 reviews first principles-based models, while Section 2.1.3 examines ML-based approaches. Most of the works focus on the MEA-CA capture technology, as it is a commercialised CO<sub>2</sub> capture technology and has been widely applied in the industry (Li et al., 2023). This comprehensive review highlights existing modelling capabilities and identifies research gaps that the present work aims to address.

#### 2.1.1 Applications of dynamic modelling

Various applications of CO<sub>2</sub> capture systems require dynamic models to address challenges that steady-state models cannot adequately handle (Chikukwa et al., 2012; Wu et al., 2020). This subsection reviews the key applications for which dynamic modelling is essential.

Dynamic models are needed for system identification and control development. System identification models could enable prediction of transient responses to disturbances and manipulated variables (MVs), which is essential for control design. Wu et al. (2020) emphasised that the development of effective control systems relies heavily on understanding the dynamic behaviour of CO<sub>2</sub> capture systems, which dynamic models can represent through system identification. Some dynamic models have been developed for MEA-CA system identification to support the design of different control systems. For example, dynamic models have been developed for designing proportional–integral–derivative (PID) controllers (Nittaya et al., 2014) and

MPC controllers (Cormos et al., 2015; Gaspar et al., 2015; Liang et al., 2018), with the objective of tracking desired CO<sub>2</sub> capture rates.

Dynamic models are also needed for system monitoring and diagnosis. During the capture process operation, it is vital for operators to detect faults, such as sensor drift, actuator malfunctions and process anomalies, and to assess controller effectiveness and maintain reliable operation. To achieve this, dynamic models can be developed as soft sensors to generate the reference MVs and compare them with actual control actions. To ensure reliable operation, the control system is normally designed to maintain a consistent CO<sub>2</sub> capture rate (Magnanelli et al., 2021). Some dynamic models have been developed for MEA-CA to study the regulation of lean solvent flow rate and reboiler duty to ensure a constant CO<sub>2</sub> capture rate (Gaspar et al., 2015).

Dynamic models are required for operational optimisation, and interest in optimising dynamic performance is growing as CO<sub>2</sub> capture is increasingly integrated with CHP plants. To support optimisation, CO<sub>2</sub> capture systems need to respond to fluctuating heat demand, electricity prices and regulatory requirements for CO<sub>2</sub> emissions over time (Bui et al., 2014). Dynamic models are therefore needed to account for temporal constraints and time-varying operating conditions (Bui et al., 2014). Some dynamic models have been developed for operational optimisation with various objectives (Cohen et al., 2012; Tang & Wu, 2023; Wang et al., 2023). For example, Cohen et al. (2012) developed dynamic models to optimise solvent flow rates and reboiler duties in response to time-varying electricity prices. Wang et al. (2023) employed dynamic models to optimise capture operation considering available waste heat fluctuations in CHP plants.

Dynamic models are needed for performance estimation under actual operating profiles since they can provide more accurate performance metrics than steady-state models, offering useful insights and valuable support to decision-makers and policymakers. Bui et al. (2014) noted that annual or seasonal performance cannot be accurately estimated without accounting for dynamic operation. Some dynamic models have been developed to examine the CO<sub>2</sub> capture feasibility and capability in w-CHP or bio-CHP plants (Magnanelli et al., 2021; Zhang et al., 2022). For example, Magnanelli et al. (2021) investigated seasonal capture scenarios in waste-to-energy plants using dynamic models with real operational data, revealing clear deviations from steady-state predictions.

Dynamic models of MEA-CA systems can be broadly categorised into first principles-based models and ML-based models (Wu et al., 2020). First principles-based models, built on mass transfer, heat transfer and chemical kinetics, are high-fidelity but computationally intensive and require substantial domain expertise (F. Li et al., 2015). ML models, built on data and ML approaches, offer a promising alternative, especially for real-time

applications, due to their lower computational cost (F. Li et al., 2015). However, systematic guidance on selecting appropriate dynamic modelling approaches for different applications in bio-CHP plants remains lacking, which is addressed in the following sections.

### 2.1.2 First principles-based models of CO<sub>2</sub> capture

Rigorous first principles-based modelling is generally developed prior to ML modelling for dynamic CO<sub>2</sub> capture systems. Dynamic modelling of the CO<sub>2</sub> capture by MEA-CA can be done in different ways. Three approaches commonly used in literature are included here.

A steady-state model can be used to approximate dynamic simulations, an approach known as “ideal static model (IST)”. It is assumed that in each time step the process is in steady state, but for different time steps, the input parameters can vary. For example, Martinez Castilla et al. (2019) developed an IST to study the influence of the variation of available heat for CO<sub>2</sub> capture. Results showed that, with the time step of 1 hour, the amount of captured CO<sub>2</sub> was 41.1 kt over a two-week period, when the available heat varied hourly in the range of 80–150 MW, and the FG flow rate was kept constant (140 kg/s).

Without controllers being implemented, dynamic models (Dw/oC) can be used to study the natural response of CO<sub>2</sub> capture in the face of disturbance. For example, Åkesson et al. (2012) developed a rate-based dynamic model of MEA-CA using Modelica to study the effect of FG flow rate fluctuation, which was reduced by 30%. The CO<sub>2</sub> removal rate in the absorber was shown to increase rapidly, while more than 1 hour was required for the top temperature of the stripper to reach a new steady state. Bui et al. (2018) developed a dynamic model to gain insight into the interaction between key process parameters under realistic and flexible operation. The results showed that increasing the MEA solution’s liquid-to-FG (L/G) ratio can result in higher CO<sub>2</sub> capture rates, while turning off the heat supply to the reboiler leads to a gradual decline in reboiler temperature.

Dynamic models with controllers implemented (DwC) can be used to handle the disturbance of input variations. For example, Lin et al. (2011) developed a dynamic model with PI controllers in Aspen Dynamics. For the increase of FG flow rate (a step change of 10%) or CO<sub>2</sub> concentration (a step change of 16%), increasing the recycle solvent flow rate and reboiler duty was needed to maintain a 90% removal target. Magnanelli et al. (2021) developed a dynamic model in MATLAB to study capturing CO<sub>2</sub> seasonally only when there is excess heat. The fluctuations of both FG and available heat were thus included. The recycle solvent flow rate was adjusted to achieve the designed L/G ratio of 3 kg/kg.

There are some comparisons of different dynamic modelling approaches. For example, Montañés et al. (2017) compared the IST with the DwC with different control structures in Modelica for MEA-CA. Results showed that the difference in the amount of captured CO<sub>2</sub> was approximately 2% over a period of 8 hours, when the FG flow rate was ramped up from 70 to 100% in 3 minutes. Martínez Castilla et al. (2019) estimated the amount of CO<sub>2</sub> capture from an industrial steel mill CHP plant. Four models were compared, including a “steady-state model” with a constant heat load, as well as IST, Dw/oC and DwC with the actual heat load. Results showed that the amounts over a two-week period were 40.9 kt, 41.1 kt, 41.9 kt and 42.4 kt for the four models, respectively.

Although there are a few comparisons of different first principles-based modelling approaches in the literature studies, there hasn’t been any guidance on the selection of modelling approaches. This is largely because existing studies are conducted under heterogeneous conditions, with different operating parameter ranges, evaluation metrics, and plant contexts (predominantly coal-fired rather than bio/w-CHP plants), making cross-study synthesis into actionable selection criteria difficult. Specifically, most studies focus on the step change or ramp change of the parameters, which does not reflect actual variations from bio/w-CHP plants. Moreover, only the variation of the FG flow rate or the available heat was considered. There is a lack of comprehensive studies considering all possible key influencing parameters from bio/w-CHP plants. Furthermore, the time step is another key parameter for dynamic simulations that can clearly affect the model accuracy. However, little attention has been paid to studying its influence.

### 2.1.3 Machine learning-based models of CO<sub>2</sub> capture

There are some studies that have explored the use of ML models in dynamic CO<sub>2</sub> capture systems by MEA-CA (Abdul Manaf et al., 2016; Li et al., 2016; Li et al., 2015; Li et al., 2018; Sha et al., 2025), including system identification of control design and accurate assessment of CO<sub>2</sub> capture performance. Table 2.1 summarises the ML models developed in the literature, including their application, model inputs and outputs, and reported accuracy.

For the development of ML models, the selection of input features and the determination of outputs are crucial (Wu et al., 2020). Improperly selected input features can lead to poor model accuracy, and the improper outputs will make the model unrealistic and unable to be used since ML models can only provide results for explicitly specified outputs.

The literature highlights a range of dynamic model applications, each requiring different inputs and outputs. While ML models have been applied to some applications (Abdul Manaf et al., 2016; Li et al., 2016; Li et al., 2015; Li et al., 2018; Sha et al., 2025), including system identification of control

design and performance assessment, others remain unexplored, such as system monitoring and diagnosis and operational optimisation, as identified in Section 2.1.1. In addition, there has been no holistic study on what should be considered as inputs and outputs for different applications.

Table 2.1 Summary of machine learning models for dynamic CO<sub>2</sub> capture.

Application	Model	Inputs	Outputs	Accuracy	Ref.
System identification	Nonlinear autoregressive model with exogenous input (NLARX)		<ul style="list-style-type: none"> <li>• CO<sub>2</sub>vol% at top absorber</li> <li>• CO<sub>2</sub>vol% at top desorber</li> <li>• Desorber top flow rate</li> </ul>	<u>APE</u> <sup>#</sup> CO <sub>2</sub> capture rate: 0.034 Energy penalty: 0.012–0.064	(Abdul Manaf et al., 2016)
	Nonlinear autoregressive neural network with exogenous input (NARX-NN)	<ul style="list-style-type: none"> <li>• FG flow rate</li> <li>• FG CO<sub>2</sub>vol%*</li> <li>• Lean solvent flow rate</li> <li>• Reboiler duty</li> </ul>	<ul style="list-style-type: none"> <li>• CO<sub>2</sub> capture rate</li> </ul>	<u>MAPE</u> <sup>#</sup> 13.2–20.9% and 0.1–98.3%	(Sha et al., 2025)
	Integral neural network (INN)		<ul style="list-style-type: none"> <li>• Reboiler temperature</li> </ul>	<u>MAPE</u> 1.4–32.1% and 0.1–0.7%	
	Physics-informed integral neural network (PIINN)			<u>MAPE</u> 1.1–3.7% and 0.02–0.3%	
Performance assessment	Bootstrap-aggregated neural network (BA-NN)	<ul style="list-style-type: none"> <li>• FG flow rate</li> <li>• FG CO<sub>2</sub>vol%</li> <li>• FG pressure</li> </ul>		<u>MSE</u> <sup>#</sup> 0.01–0.0771 kg/s and 0.08–0.2%	(Li et al., 2015)
	Bootstrap-aggregated extreme learning machine (BA-ELM)	<ul style="list-style-type: none"> <li>• FG temperature</li> <li>• Lean solvent flow rate</li> <li>• Lean solvent MEAwt%</li> </ul>	<ul style="list-style-type: none"> <li>• CO<sub>2</sub> capture amount</li> <li>• CO<sub>2</sub> capture rate</li> </ul>	<u>MSE</u> 0.0441 kg/s and 0.00043%	(Li et al., 2016)
	Deep belief network (DBN)	<ul style="list-style-type: none"> <li>• Lean solvent temperature</li> </ul>		<u>RMSE</u> <sup>#</sup> 0.000246 kg/s and 0.0321%	(Li et al., 2018)

\* FG: flue gas; CO<sub>2</sub>vol%: CO<sub>2</sub> concentration. <sup>#</sup> APE: absolute percentage error; MAPE: mean absolute percentage error; MSE: mean squared error; RMSE: root mean squared error.

## 2.2 Control of CO<sub>2</sub> capture

The dynamic operation of bio-CHP plants leads to significant fluctuations in FG flow rate, composition, and available heat for solvent regeneration, all of which directly affect the performance of downstream CO<sub>2</sub> capture processes (Li, Dong, et al., 2019; Tan et al., 2016). For MEA-CA, FG flow rate

strongly influences the CO<sub>2</sub> removal rate in the absorber, CO<sub>2</sub> concentration affects the regeneration heat duty, and available heat directly affects the generated CO<sub>2</sub> in the stripper (Enaasen et al., 2014). In addition, CHP plants can also benefit from flexible operation in modern electricity markets, which can further lead to frequent operational adjustments. CO<sub>2</sub> capture processes must be capable of adapting to these varying operational demands via changing CO<sub>2</sub> capture amounts in response to different operational and economic objectives under disturbances from load variations and fuel quality fluctuations. Achieving such operational flexibility critically relies on robust control that can handle a range of variations.

Handling various operational variations requires two fundamental control capabilities: setpoint tracking and disturbance rejection. Setpoint tracking (such as of CO<sub>2</sub> capture rate) refers to the ability of the controller to make the actual CO<sub>2</sub> capture rate follow changing setpoint values (Devarakonda et al., 2025; Rohini et al., 2022). Disturbance rejection refers to the ability of the controller to maintain desirable system behaviour by reducing the impacts of disturbance (Devarakonda et al., 2025; Rohini et al., 2022). These capabilities are particularly critical during operational variations of bio-CHP plants. For flexible operation, the CO<sub>2</sub> capture rate setpoint should be adjusted in response to changing operational and economic conditions, such as DH system balancing needs, electricity price variations, and carbon market requirements. For example, the capture rate setpoint may need to be reduced from 80% to 70% during peak electricity demand periods or increased from 70% to 90% during periods of high demand for carbon removal. In addition to setpoint tracking, disturbance rejection is equally critical. Even when maintaining a constant CO<sub>2</sub> capture rate setpoint, the controller must be able to handle disturbances from FG variations. Biomass CHP plants experience frequent FG flow rate changes and CO<sub>2</sub> concentration variations. These disturbances directly affect the CO<sub>2</sub> capture rate and would cause unwanted deviations from the target without proper control compensation.

Many efforts have been made in control design to achieve desired targets during these operational transitions, including both conventional control strategies, such as PID controllers, and advanced control strategies, such as MPC (Wu et al., 2020).

### 2.2.1 Proportional–integral–derivative (PID) controllers

As the most conventional and reliable control approach, decentralised feedback control using PID controllers has been widely applied to maintain desired capture rate and ensure process stability (Nittaya et al., 2014). For example, Montañés et al. (2017) developed PID controllers to maintain a removal target of 85% and reboiler temperature of 120.9°C when FG flow rate was ramped up from 13.5 kg/s to 19.3 kg/s based on the dynamic model in

Modelica. The results showed that the required settling time (ST) was 71 min for CO<sub>2</sub> absorbed, 113 min for CO<sub>2</sub> desorbed, and 201 min for lean CO<sub>2</sub> loading.

For PID controllers, conservative tuning leads to slower responses to avoid oscillations, while aggressive tuning results in oscillatory behaviour. Since PID can only react after deviations occur and operates based on a single-input single-output (SISO) loop, it is difficult to achieve both fast and smooth transitions simultaneously. These limitations in managing transitions have motivated the investigation of advanced control strategies with predictive capability and multivariable coordination.

### 2.2.2 Model predictive control (MPC)

MPC has been widely investigated as a promising control strategy for handling various operational variations. Previous studies have demonstrated that MPC offers distinct advantages over conventional PI/PID control through three key capabilities: anticipating process dynamics through its prediction horizon, explicitly handling multivariable interactions in the control framework, and optimising performance during state changes (Qin & Badgwell, 2003). These characteristics make MPC suitable for MEA-based CO<sub>2</sub> capture, where the slow dynamics can be anticipated through MPC's predictive capability, and the multivariable system can be handled explicitly within MPC's framework. Many studies have focused on designing and evaluating MPC for CO<sub>2</sub> capture operations, primarily for setpoint tracking and disturbance rejection tasks.

For setpoint tracking, some studies have demonstrated MPC's superior performance in following time-varying CO<sub>2</sub> capture rate targets (Sahraei & Ricardez-Sandoval, 2014; Wu et al., 2018; Q. Li et al., 2021). For example, Sahraei and Ricardez-Sandoval (2014) tested MPC's setpoint tracking performance when the setpoints ramped from 96.6% to 80% in 1.5 h using the dynamic model in ASPEN HYSYS. The results showed that the ISEs for the CO<sub>2</sub> capture rate were 8187.6 %\*s for MPC and 14218.7 %\*s for PI. In addition, the MPC-based control scheme was able to perform 45 min faster setpoint changes than the PI-based scheme, with STs of 1.5 h and 2.2 h, respectively. Q. Li et al. (2021) also tested setpoint tracking when the setpoints stepped from 70% to 80%, using the dynamic model in Aspen Plus Dynamics. It was found that the integrated time and absolute error (ITAE) of MPC ( $6.0134 \times 10^5$ ) was greatly reduced compared with that of PID ( $1.2052 \times 10^6$ ).

For disturbance rejection, some studies have qualitatively evaluated MPC's performance under FG variations (Mehleri et al., 2015; Mejdell et al., 2022; Wu et al., 2018). For example, Mehleri et al. (2015) tested MPC's disturbance rejection performance to a step increment of 20% in the FG flow

rate. The results showed that implementing MPC enables fast recovery of CO<sub>2</sub> capture rate to its setpoint with only small deviations. Mejdell et al. (2022) tested MPC's simultaneous disturbance rejection performance and found that the FG flow rate changed from 160 to 200 m<sup>3</sup>/h and the CO<sub>2</sub>vol% changed from 11% to 14.5%. The results showed that the capture rate was kept at the setpoint value of 90% most of the time after initial transitions.

While literature studies demonstrate that MPC achieves superior performance during operational variations compared to conventional PI/PID control, three critical knowledge gaps remain. First, existing studies predominantly focus on controller performance metrics, such as rise time, ST, and ITAE (Q. Li et al., 2021; Mehleri et al., 2015; Mejdell et al., 2022; Sahraei & Ricardez-Sandoval, 2014; Wu et al., 2018), while the evaluation of process-level performance, such as cumulative CO<sub>2</sub> capture amount and energy use, has received limited attention. Without quantifying process-level outcomes, it remains unclear whether improved controller performance (e.g., faster settling) translates into meaningful operational benefits (e.g., higher CO<sub>2</sub> capture amount), and if so, to what extent. Second, while existing studies have evaluated MPC's rejection performance under different disturbances, systematic quantitative assessment remains limited (Mehleri et al., 2015; Mejdell et al., 2022; Wu et al., 2018), especially under simultaneously coupled disturbances (FG flow rate and CO<sub>2</sub>vol%), which are characteristic of bio-CHP operation due to load variations and fuel quality fluctuations. Third, most existing studies focus on coal- or gas-fired power plants and evaluate MPC under disturbances or setpoint changes of 10–20% in a single direction (Q. Li et al., 2021; Mehleri et al., 2015; Mejdell et al., 2022; Sahraei & Ricardez-Sandoval, 2014; Wu et al., 2018). However, bio-CHP plants experience larger operational variations (potentially >30%) with bidirectional changes due to the high variability of biomass fuel properties and the dynamic nature of liberalised energy markets. Such bidirectional variations with larger magnitudes create more challenging control conditions yet remain inadequately investigated in literature.

## 2.3 Assessment of CO<sub>2</sub> capture in biomass CHP plants

### 2.3.1 Plant-level assessment

Most previous studies have estimated the potential amount of CO<sub>2</sub> capture and the associated costs of integrating CO<sub>2</sub> capture with CHP plants on the plant level (Ignell & Johansson, 2021; Martinez Castilla et al., 2019; Öberg, 2017; Pröll & Zerobin, 2019). For example, Ignell and Johansson (2021)

evaluated the capture potential from a 220 MW w-CHP plant by using a steady-state simulation of MEA-CA. Results showed that the amount of captured CO<sub>2</sub> was 500 kt/yr when it was assumed that the fuel consumption remained unchanged. Due to the energy penalty of CO<sub>2</sub> capture, the generated heat and electricity were reduced by 80 GWh/yr and 50 GWh/yr, respectively. It was also estimated that the annual capital cost was 7 million euros per year (M€/yr), and the operating and maintenance (O&M) cost was 13 M€/yr, which led to an average CO<sub>2</sub> avoided cost of 42 €/tCO<sub>2</sub>. Öberg analysed the cost of partial CO<sub>2</sub> capture from a w-CHP plant, which had a thermal capacity of 46.2 MW (Öberg, 2017). Results showed that capturing 40% of CO<sub>2</sub> (about 43.2 ktCO<sub>2</sub>/yr) resulted in an investment of 26.3 M€ and an O&M cost of 1.4 M€/yr. The average CO<sub>2</sub> avoided cost was 118 €/tCO<sub>2</sub>.

However, existing plant-level assessments largely rely on steady-state simulations. Our previous work has shown that variations in operating conditions, such as the heat demand, can result in substantial changes in the amount of captured CO<sub>2</sub> and energy penalty (Dong et al., 2023). Conducting dynamic simulations of CO<sub>2</sub> capture is therefore crucial to obtaining accurate results on CO<sub>2</sub> capture.

In some countries and regions, such as the Scandinavian countries, CHP plants are in operation throughout the year and the core business of CHP is to supply heat for the DH network; meeting heat demand is therefore usually prioritised (Thorin et al., 2015). This implies that if the integration of CO<sub>2</sub> capture reduces heat generation, other supplementary units will be needed to compensate for such reductions. Although CHP plants are usually equipped with supplementary units, their operations typically consume more expensive fuels, such as bio-oil or even fossil fuel, which will largely increase the operating costs of CHP plants and even lead to increased emissions. It is therefore important to account for the constraint of maintaining heat supply unchanged to obtain a realistic negative emission potential. However, this constraint has not been explicitly incorporated in most assessments, potentially leading to overestimation of the achievable CO<sub>2</sub> capture potential.

### 2.3.2 National-level assessment

For policymakers, it is essential to understand the potential contribution and the associated costs on the national level in order to make strategic plans to promote the integration of BECCS in CHP plants.

A few studies have conducted assessments on the national level. Beiron et al. (2021) estimated the capture potential for the integration of CO<sub>2</sub> capture in all Swedish bio-CHP and w-CHP plants. Two scenarios were considered: Scenario 1 was to maximise the electricity generation, and Scenario 2 was to maximise the heat generation. It was found that about 18.1

MtCO<sub>2</sub>/yr could be captured in S1, which was more than could be captured in S2 (15.0 MtCO<sub>2</sub>/yr). Results also showed that the delivered heat was reduced by 7.1 TWh/yr when maximising the electricity generation, while the delivered electricity was reduced by 12.3 TWh/yr when maximising the heat generation. Beiron, Norrmann et al. (2022) also conducted a techno-economic assessment of capturing CO<sub>2</sub> from all Swedish bio-CHP and w-CHP plants. Results showed that if 90% CO<sub>2</sub> is captured, which was about 19.3 MtCO<sub>2</sub>/yr, the electricity and heat generation will be reduced by around 20% and 40%–60%, respectively. The estimated specific cost of CO<sub>2</sub> capture and transportation via truck to intermediate storage hubs was in the range of 45–125 €/tCO<sub>2</sub> for most CHP plants, depending on the plant size and utilisation.

The results of Beiron et al.'s studies clearly demonstrated that integrating CO<sub>2</sub> capture with CHP plants will reduce heat generation and/or electricity generation. Therefore, similar to the limitations identified at the plant level, existing national-scale assessments have not fully accounted for the heat supply constraint and likewise rely on steady-state simulations. The present work builds on and extends Beiron et al.'s studies by explicitly incorporating the heat supply constraint and employing dynamic simulations to improve the accuracy of national-scale negative emission assessment.

# 3 Methodology

This chapter details the methodological approach underpinning Papers I–VI, covering dynamic modelling (Section 3.2), MPC evaluation (Section 3.3), and potential assessment (Section 3.4).

## 3.1 Overview

The methodology developed in this dissertation enables dynamic modelling, control design, and negative emission assessment of CO<sub>2</sub> capture operation in bio/w-CHP plants. Figure 3.1 illustrates the overall structure of this methodology and how the methods connect across the three research questions.

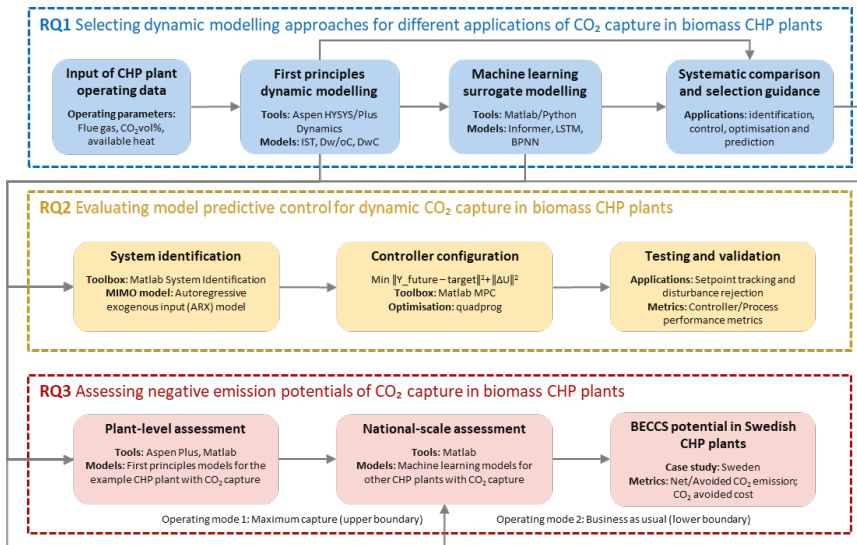


Figure 3.1: Methodology schematic outline for addressing research questions.

To address **RQ1**, two modelling approaches were employed: first principles modelling and ML surrogate modelling. Three first-principles models were developed in Aspen HYSYS/Plus Dynamics: IST, Dw/oC, and DwC. Based on the dynamic simulation data generated from first principles models,



Table 3.1 Summary of model parameters and column settings (Li et al., 2015).

Model and column properties	Absorber	Desorber
Number of stages	20	20
Packing material	IMTP#38MM <sup>a</sup>	IMTP#38MM
Total packed height	7.136 m (4x1.784 m)	7.168 m (2x3.584 m)
Column diameter	350 mm	250 mm
Flow model	Mixed model	Mixed model
Interfacial area factor	1.8	1.8
Initial liquid holdup	0.03 L	0.03 L
Film resistance	Discrxn <sup>b</sup> for liquid; Film for vapour	Discrxn for liquid; Film for vapour
Discretisation points for liquid film	5	5
Mass transfer correlation	Bravo et al. (1985)	Bravo et al. (1985)
Heat transfer correlation	Chilton-Colburn	Chilton-Colburn
Interfacial area method	Bravo et al. (1985)	Bravo et al. (1985)
Liquid holdup correlation method	Bravo et al. (1993)	Bravo et al. (1993)

<sup>a</sup> IMTP#38MM: Intalox Metal Tower Packing 38 mm. <sup>b</sup> Discrxn: discretised reaction.

**Dynamic model without control (Dw/oC).** For Dw/oC, a dynamic model is developed in Aspen HYSYS V12.1 based on a pressure-flow solver, where pressure loss is correlated to stream flow rates. The flow diagram is shown in Figure 3.3.

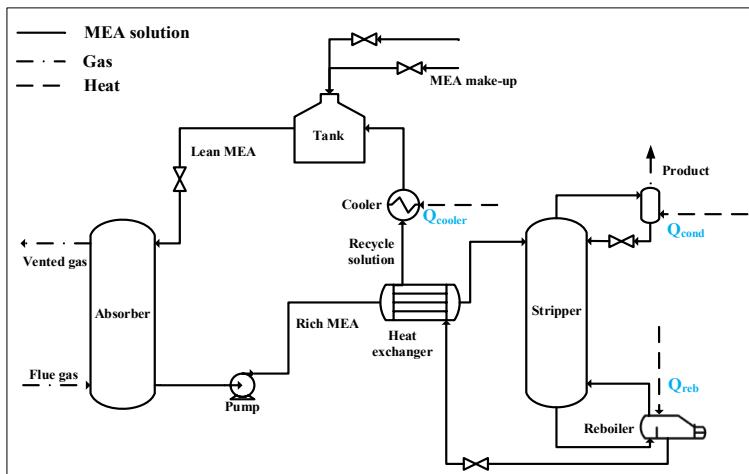


Figure 3.3: MEA-based CO<sub>2</sub> capture without control strategy.

The primary input parameters are summarised in Table 3.2 (refer also to Appendix A2 (Figure A2 and Table A4) in Paper I). A time step of 5 seconds is used. The dynamic model is validated against the results from Harun et al. (2012), with details provided in Appendix B.

Table 3.2: Dynamic model parameters (Harun, 2012).

Parameter	Value
<b>Absorber</b>	
Packing height and column diameter (m)	6.1/0.43
Packing type	IMTP#38MM
Stage number	10
<b>Stripper</b>	
Packing height and column diameter (m)	6.1/0.43
Packing type	IMTP#38MM
Stage number	10
<b>Flue gas (FG), solution and reboiler duty</b>	
CO <sub>2</sub> volume concentration in FG (vol%)	17.5
Solution flow rate (kg/s)	31.4
Reboiler duty (kW)	155

**Dynamic model with control (DwC).** DwC uses the same dynamic model as Dw/oC and additionally integrates PI controllers to achieve the set targets, as shown in Figure 3.4 (refer also to Appendix A3 (Figure A5) in Paper I). The time step is also 5 seconds.

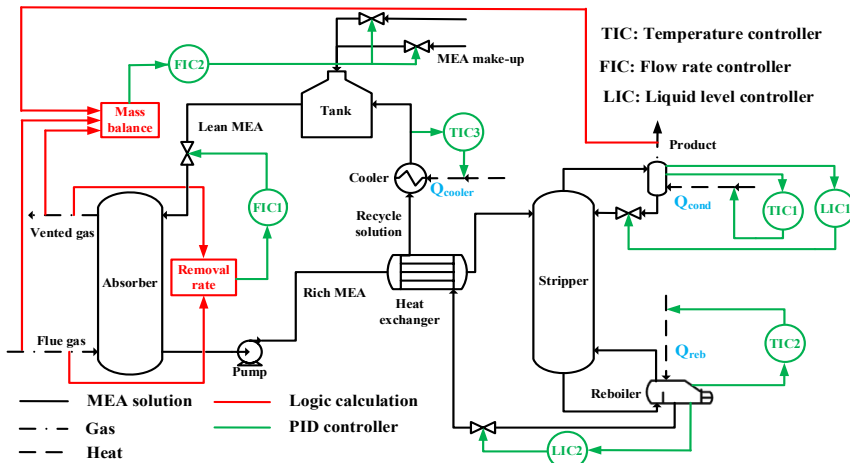


Figure 3.4: MEA-based CO<sub>2</sub> capture with control strategy.

The controlled and manipulated variables and their targets are summarised in Table 3.3 (refer also to Appendix A3 (Table A7) in Paper I). The controller configuration depends on the availability of heat ( $Q_{reb}$ ). The CO<sub>2</sub> removal rate is controlled by manipulating the lean MEA solution flow rate using FIC1 (flow rate indicating controller), where CO<sub>2</sub> removal rate is calculated based on the CO<sub>2</sub> amount in the FG and in the vented gas from the top of the absorber. The reboiler temperature is controlled by manipulating the reboiler heat duty using TIC2 (temperature indicating controller) (Lin et al., 2011). When the available heat is used as the input parameter, TIC2 is deactivated and the lean loading is controlled by manipulating the lean MEA solution flow rate using FIC1. Regardless of heat availability, the liquid level indicating controllers (LIC) remain active, maintaining liquid levels at their setpoints by adjusting the outlet solution flow rates.

Table 3.3: Manipulated and controlled variables and targets (Harun et al., 2012; Nittaya et al., 2014).

Controller	Manipulated variables	Controlled variables	Target
FIC1*	Lean solution flow rate	Removal rate (when available heat can meet need of reboiler)	90%
		Lean loading (when available heat is input)	0.287 mol/mol
FIC2	Make-up of MEA and H <sub>2</sub> O	Mass balance	MEA 30 wt%
TIC1*	Cooling supply to condenser	Condenser temperature	350 K
TIC2	Heat supply to reboiler	Reboiler temperature	386 K
TIC3	Cooling supply to cooler	Lean solution temperature	314 K
LIC1*	Reflux flow rate	Liquid level of condenser	50%
LIC2	Recycle solution flow rate	Liquid level of reboiler	50%

\*FIC: flow rate indicating controller, TIC: temperature indicating controller, LIC: level indicating controller.

### 3.2.1.2 Model scale-up

To be able to compare different approaches under identical input conditions, a real w-CHP plant is selected as the case study. The thermal capacity of the plant is 167 MW<sub>th</sub>, and the fuel mainly consists of household waste, industrial waste, and recycled wood. The FG data collected from the plant over the period of 1 January 2017 to 31 December 2017 are used as input parameters for simulations and are illustrated in Figure 3.5 (refer also to Section 2.2.1 (Figure 1) in Paper I). The time resolution is 30 minutes. In general,

the variation of FG flow rate and CO<sub>2</sub>vol% are in the range of 180.57–375.21 kNm<sup>3</sup>/h and 7.70–15.72 vol%, respectively.

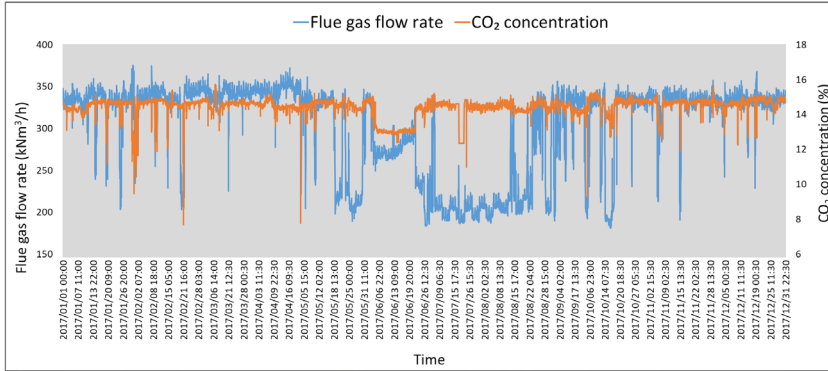


Figure 3.5: Flue gas data from a w-CHP plant.

Based on the method proposed by Otitoju et al. (2020), the dimensions of the absorber and stripper are estimated, including the diameter and height of the packed columns, with details provided in Appendix A3 in Paper I. For other vessels, including the reboiler and the buffer tank between the absorber and stripper, their volumes are determined based on a residence time of 10 minutes for the incoming liquid and a liquid level of 50%. The scaled-up system parameters and other required input parameters, including the lean MEA solution and FG, are summarised in Table 3.4 (refer also to Appendices A1–A3 (Table A3, A6 and A8) in Paper I).

Table 3.4: The scaled-up capture system and other input parameters.

Components		Value	Input streams	Value	
<b>Ab-sorber</b>	Packing type	IMTP#38MM	<b>Flue gas</b>	Temperature (K)	319.7
	Height/diameter (m)	17.4/8.7		O <sub>2</sub> (vol%)	2.7
	Pressure (kPa)	101.3		H <sub>2</sub> O (vol%)	4.8
<b>Strip-per</b>	Packing type	IMTP#38MM	<b>Lean MEA solution</b>	MEA concentra-tion (wt%)	30
	Height/diameter (m)	10.9/4.3		Lean loading	0.287
	Reboiler volume (m <sup>3</sup> )	352		Temperature (K)	314
	Volume of tank between absorber and stripper (m <sup>3</sup> )	330		Flow rate (kg/h)	Model-depend ent*
	Condenser/reboiler tem-perature (K)	350/386			
	Condenser pressure (kPa)	159			

\*IST: manipulated by design specifications; Dw/oC: kept constant. DwC: manipulated by controllers.

### 3.2.1.3 Key performance indicators (KPIs)

The accumulated amount of captured CO<sub>2</sub> and the average specific reboiler duty are employed as KPIs to compare the overall performance of different approaches. The amount of captured CO<sub>2</sub> is calculated by integrating the dynamic results over a period of 4 hours, as shown in Equation 3-1. The average specific reboiler duty is calculated by taking the average over the period of 4 hours of reboiler duty per unit of captured CO<sub>2</sub>, as shown in Equation 3-2.

$$C_{CO_2,acc} = \int_0^t CO_{2,pro}(t)dt \quad (3-1)$$

$$SRD_{ave} = \frac{\int_0^t Q_{reb}(t)dt}{\int_0^t CO_{2,pro}(t)dt} \quad (3-2)$$

$C_{CO_2,acc}$  is the accumulated amount of captured CO<sub>2</sub> over the time of 4 hours, tonne/4 h;  $CO_{2,pro}(t)$  is the amount of CO<sub>2</sub> in the product stream at the time  $t$ , tonne/h;  $SRD_{ave}$  is the average specific reboiler duty per unit of captured CO<sub>2</sub> over the time of 4 hours, MJ/kg, and  $Q_{reb}(t)$  is the reboiler duty at the time  $t$ , GJ/h.

## 3.2.2 Development of machine learning-based surrogate models

Three ML approaches were selected.

**Informer** is a deep neural network architecture designed for sequence modelling, which captures dependencies between input elements by assigning importance weights. It introduces a probabilistic sparse self-attention mechanism to reduce computational costs by focusing on the most informative queries (Zhou et al., 2021).

**Long short-term memory network (LSTM)** was proposed to address the issue of recurrent neural networks, namely vanishing gradient and thus poor ability to learn long-term dependencies (Shahbaz et al., 2021). It introduces memory cell units, which facilitate the retention of relevant information across long sequences and consist of three gates: input gate, forgetting gate, and output gate. This architecture enables LSTM to capture both short-term and long-term dependencies, possibly making it an effective tool for dynamic systems with delayed responses.

**Back-propagation neural network (BPNN)** is a multilayer feed-forward network, with simpler architecture than Informer and LSTM. In a neural network, each layer is composed of neurons that are interconnected. The

layers work together to process data through a series of transformations. The learning process involves signal-forward propagation and error-back propagation. The core is designed to constantly adjust the weights and biases of the neurons in each layer to minimise the error. Although BPNN is not inherently designed for sequence modelling, time-series data can be transformed into a static tabular format compatible by employing a sliding window technique (D. Li et al., 2021). BPNN has high nonlinear mapping and good generalisation ability using the global approximation method (Pan et al., 2024).

To compare the performance of ML models, the MAPE and mean absolute error (MAE) were employed as performance metrics, defined in Equations 3-3 and 3-4, respectively.

$$MAPE = \frac{1}{n} \sum_{i=1}^n \left| \frac{y_i - \hat{y}_i}{y_i} \right| \times 100\% \quad (3-3)$$

$$MAE = \frac{1}{n} \sum_{i=1}^n |y_i - \hat{y}_i| \quad (3-4)$$

where  $n$  is the sample size;  $y_i$  is the  $i^{th}$  actual value; and  $\hat{y}_i$  is the  $i^{th}$  predicted value.

The datasets generated by the physical models, including input and output variables, were divided into training data (70%), validation data (10%), and testing data (20%). This split follows common practice in ML model development. The performance metrics were calculated based on testing data.

### 3.3 Model predictive control design

MPC relies on an explicit process model to predict system dynamics and optimise control decisions (Darby & Nikolaou, 2012). The methodology therefore consists of two main components: model identification and controller design.

#### 3.3.1 System description and model identification

##### 3.3.1.1 Dynamic model

The MEA-CA was simulated in Aspen Plus Dynamics V.14 with input conditions listed in Table 3.5. As rate-based RadFrac models are not supported (Q. Li et al., 2021), the equilibrium-based approach was adopted with Murphree stage efficiencies of 0.25 and 1.0 for the absorber and stripper, respectively (Øi, 2007). Figure 3.6 shows the converted dynamic model.

Table 3.5: Streams under the designed operating point (Dong et al., 2023; Zanco et al., 2021; Zhou et al., 2022).

Mass streams			
Flue gas		Lean MEA solvent	
Temperature (K)	319.7	Temperature (K)	314
Flow rate (kg/s)	86.44	Flow rate (kg/s)	269.04
Pressure (kPa)	101.3	Pressure (kPa)	101.3
CO <sub>2</sub> (vol%)	13.48	MEA concentration (wt%)	30
N <sub>2</sub> /O <sub>2</sub> /H <sub>2</sub> O (vol%)	79.02/2.7/4.8	Lean loading (molCO <sub>2</sub> /molMEA)	0.287
Heat streams			
Reboiler duty (MW)	61.22	Condenser duty (MW)	0.89

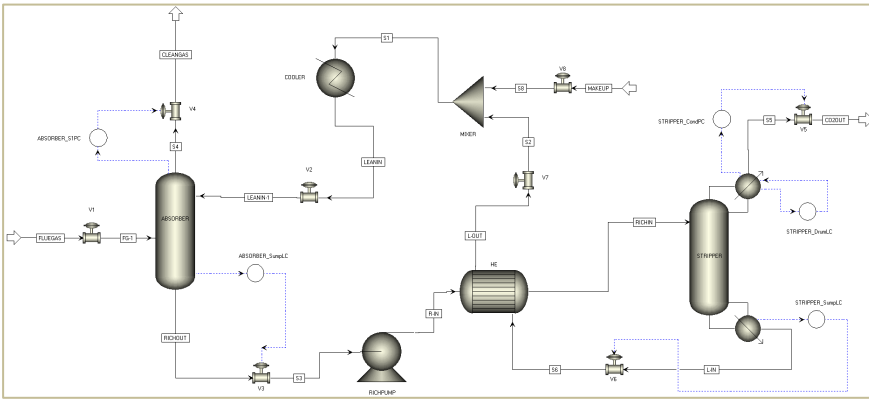


Figure 3.6: Flowsheet of the designed MEA-CA in Aspen Plus Dynamics.

### 3.3.1.2 Data generation and system identification

To implement MPC, a computationally efficient dynamic model is required for real-time optimisation and prediction (Darby & Nikolaou, 2012) by using System Identification Toolbox in MATLAB (Lennart, 1999).

The MEA-CA process has multiple inputs and outputs. Two disturbance variables were included: FG flow rate ( $u_1$ ) and FG CO<sub>2</sub> concentration ( $u_2$ ). Two MVs were selected: lean solvent flow rate ( $u_3$ ) and reboiler heat duty ( $u_4$ ). Two CVs were selected: CO<sub>2</sub> capture rate ( $y_1$ ) and reboiler temperature ( $y_2$ ). This configuration results in a 4-input, 2-output MIMO system. Input–output data were generated using the Aspen Plus Dynamics model from Section 2.1.2. Random multi-level signals were applied to all four inputs, as shown in Figure 3.7. The input ranges were determined based on the real bio-CHP plant specifications. Data were sampled at 18-second intervals. The simulation duration was set to 6 hours to ensure sufficient data for

reliable system identification, allowing multiple transient responses to be captured. This generated a dataset of 1200 input–output samples suitable for system identification.

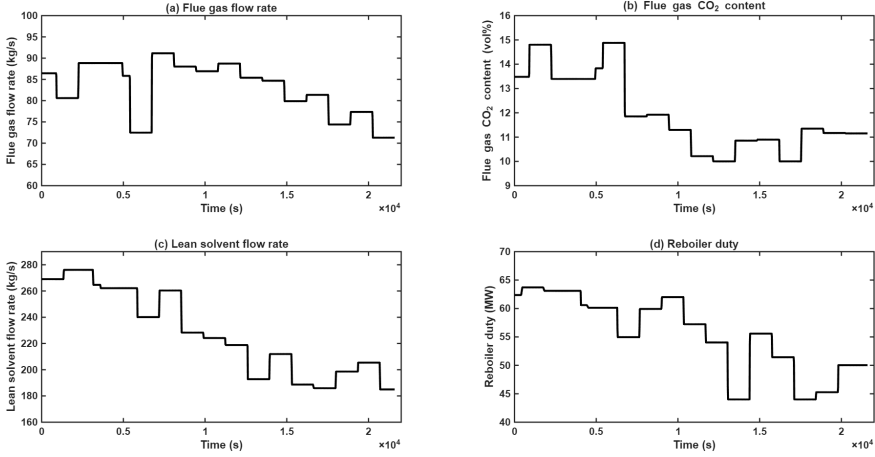


Figure 3.7: Implemented random signals for system identification (a): Flue gas flow rate; (b): CO<sub>2</sub> content; (c): Lean solvent flow rate; (d): Reboiler duty.

Different identification approaches were evaluated to determine the most suitable model structure. These included state-space models, transfer function models, and autoregressive exogenous input (ARX) models (Lennart, 1999). The ARX model structure was selected based on its superior prediction accuracy and computational efficiency (Perez & Yang, 2022). ARX models can be expressed as polynomial functions of past outputs and current/past inputs (Lennart, 1999). A standard parametric form of an ARX discrete time model is described by Equations 3-5 and 3-6. The identified ARX models were then converted into state-space form for integration with the MPC framework described in Section 2.2 (Wu, 2022).

$$y_1(t) = \sum_{k=1}^{n_a} a_{1,k} \times y_1(t - k) + \sum_{k=1}^{n_a} a_{12,k} \times y_2(t - k) + \sum_{j=1}^4 \sum_{k=0}^{n_b-1} b_{1j,k} \times u_j(t - n_{kj} - k) + e_1(t) \quad (3-5)$$

$$y_2(t) = \sum_{k=1}^{n_a} a_{2,k} \times y_2(t - k) + \sum_{k=1}^{n_a} a_{21,k} \times y_1(t - k) + \sum_{j=1}^4 \sum_{k=0}^{n_b-1} b_{2j,k} \times u_j(t - n_{kj} - k) + e_2(t) \quad (3-6)$$

where  $n_a$  is the autoregressive order (number of past output lags),  $a_{i,k}$  are autoregressive coefficients for output  $y_i$ ,  $a_{ij,k}$  are cross-coupling coefficients from output  $y_j$  to output  $y_i$ ,  $n_b$  is the exogenous input order (number of past input lags),  $b_{ij,k}$  are input coefficients from input  $u_j$  to output  $y_i$ ,

$n_{k,j}$  represents the time delay from input  $u_j$  to the outputs,  $e_i(t)$  is modeling error (white noise), and  $t$  is the time step. The model structure explicitly captures the coupling between the CO<sub>2</sub> capture rate and the reboiler temperature through the cross-coupling terms.

### 3.3.2 Model predictive control design

#### 3.3.2.1 MPC formulation and implementation

To achieve flexible operation of the CO<sub>2</sub> capture process, a standard linear MPC framework was employed (Camacho & Bordons, 2007). The MPC formulation follows the conventional approach widely adopted in CO<sub>2</sub> capture control studies (Q. Li et al., 2021; Wu et al., 2018), which optimises control actions while explicitly handling operational constraints and multi-variable interactions. The implementation was tailored to the MEA-CA system, with specific tuning parameters selected to ensure satisfactory control performance for the operational scenarios investigated in this study.

At each sampling instant, the MPC solves an optimisation problem that minimises both the deviation of CVs from their reference trajectories and the aggressiveness of control actions over a future time horizon. After determining the optimal control input sequence, only the first element of the optimal control sequence will be applied to the operation of CO<sub>2</sub> capture, and the optimisation is repeated at the next sampling instant with updated measurements. Consistent with the formulation used in previous CO<sub>2</sub> capture MPC studies (Q. Li et al., 2021; Wu et al., 2018), the cost function for a linear constrained MPC algorithm is defined from Equations 3-7 to 3-10:

$$J = \sum_{i=1}^{N_p} (y_{k+i} - r_{k+i})^T Q (y_{k+i} - r_{k+i}) + \sum_{i=1}^{N_c} \Delta u_{k+i}^T R \Delta u_{k+i} \quad (3-7)$$

$$(\Delta u_{k+i})_{min} \leq \Delta u_{k+i} \leq (\Delta u_{k+i})_{max} \quad (3-8)$$

$$(u_{k+i})_{min} \leq u_{k+i} \leq (u_{k+i})_{max} \quad (3-9)$$

$$(y_{k+i})_{min} \leq y_{k+i} \leq (y_{k+i})_{max} \quad (3-10)$$

where  $J$  is the cost function,  $N_p$  is the prediction horizon,  $N_c$  is the control horizon,  $y_{k+i}$  are the predicted CVs,  $r_{k+i}$  is the desired setpoint trajectory,  $Q$  is the output tracking weight matrix,  $R$  is the input rate penalty matrix,  $\Delta u_{k+i}$  is the change rate of manipulated inputs, and  $u_{k+i}$  is the manipulated inputs. The subscript  $k + i$  denotes prediction at time step  $k + i$ ; *min* and *max* are the minimum and maximum constraints.

To solve the optimisation problem described above, a prediction model is required to represent the dynamics of the CO<sub>2</sub> capture process. The identified ARX model from Section 2.1.3 serves as the prediction model, enabling the MPC to forecast the future behaviour of CVs based on current

system state and proposed control actions. To facilitate MPC implementation, the ARX model was converted to the state-space form following standard procedures (Q. Li et al., 2021; Olesen et al., 2013), which simplifies the multi-step prediction and constraint handling. The discrete time state-space model takes the form as Equations 3-11 and 3-12:

$$x_{k+1} = Ax_k + B_u u_k + B_d d_k \quad (3-11)$$

$$y_k = Cx_k + D_d d_k \quad (3-12)$$

where  $x_k$  is the state vector,  $u_k = [u_{k,1}, u_{k,2}]^T$  are the MVs (lean solvent flow rate and reboiler heat duty),  $d_k = [d_{k,1}, d_{k,2}]^T$  are the measured disturbance variables (FG flow rate and CO<sub>2</sub> concentration),  $y_k = [y_{k,1}, y_{k,2}]^T$  are the CVs (CO<sub>2</sub> capture rate and reboiler temperature), and the matrices  $A$ ,  $B_u$ ,  $B_d$ ,  $C$  and  $D_d$  are obtained from the ARX-to-state-space conversion (Olesen et al., 2013).

The optimisation was reformulated as a standard quadratic programming problem and solved at each sampling instant using MATLAB's quadprog solver. The tuning of weighting matrices and horizons in Equation 3-7 was performed to obtain satisfactory control performance for the CO<sub>2</sub> capture system. In this work, the weights for  $y_1$ ,  $y_2$ ,  $\Delta u_1$  and  $\Delta u_2$  are 1, 10, 1 and 1, respectively, with higher weight on reboiler temperature to ensure thermal stability and prevent equipment damage. The sampling interval in the Aspen Dynamics® model is set to be 0.005 h to ensure both the convergence and computational feasibility. The prediction and control horizons of MPC are set at 0.05 h and 0.005 h (corresponding to 10 and 1 intervals), respectively. The process input and output constraints (Table 3.6) were obtained based on the real FG from a bio-CHP plant to maintain operational safety and stability.

Table 3.6: Process constraints considered in the MPC formulation.

<b>Variables</b>	<b>Minimum</b>	<b>Maximum</b>
<b>Manipulated variables</b>		
Lean solvent flow rate (kg/s)	102	326
Reboiler heat duty (MW)	34	71
<b>Manipulated variables change rate</b>		
Change rate of lean solvent flow rate (kg/s per sampling interval)	-25.37	14.83
Change rate of reboiler heat duty (MW per sampling interval)	-7.62	9.89
<b>Controlled variables</b>		
CO <sub>2</sub> capture rate (%)	50	100
Reboiler temperature (°C)	112	120

### 3.3.2.2 Flexible operation cases of CO<sub>2</sub> capture from bio-CHP plants

To systematically evaluate MPC performance under realistic operational challenges of bio-CHP plants, three representative cases are defined, covering setpoint tracking and disturbance rejection capabilities.

**Case 1: Setpoint tracking with varying capture rate.** This case evaluates the controller's ability to make the actual CO<sub>2</sub> capture rate follow changing CO<sub>2</sub> capture rate setpoints. The CO<sub>2</sub> capture rate setpoint varies bidirectionally between 60% and 100%.

**Case 2: FG flow rate disturbance rejection.** This case evaluates the controller's disturbance rejection capability when the CO<sub>2</sub> capture rate setpoint is held constant. The FG flow rate varies between 60% and 100% of its nominal value, simulating boiler load changes. The controller must adjust lean solvent flow rate and reboiler duty to compensate for these FG flow rate variations and maintain the capture rate at its setpoint.

**Case 3: Simultaneous disturbance rejection of FG flow rate and CO<sub>2</sub> concentration.** This case considers simultaneous variations in both FG flow rate (60–100% of nominal) and CO<sub>2</sub> concentration (60–100% of nominal). Such coupled disturbances represent realistic operating conditions in which boiler load changes occur together with fuel quality variations.

These three cases provide comprehensive evaluation: Case 1 tests the ability to follow changing setpoints (command tracking for flexibility), and Cases 2 and 3 test the ability to maintain constant setpoints against disturbances (disturbance rejection for stable operation).

### 3.3.2.3 Performance evaluation metrics

To comprehensively evaluate controller performance across the three operational cases, two categories of metrics are employed: controller performance metrics that assess dynamic response characteristics, and process performance metrics that quantify overall operational outcomes.

**Controller performance metrics.** Different operational cases require distinct evaluation approaches. For setpoint tracking evaluation, four key metrics are employed. Rise time (RT) is defined as the time required for the CV to reach 90% of the new setpoint value from its initial value. Overshoot (OS) represents the maximum percentage deviation beyond the target setpoint during the transient response. Settling time (ST) measures the duration for the CV to reach and remain within  $\pm 2\%$  of the desired setpoint. Integrated absolute error (IAE) provides a comprehensive measure of tracking

performance by calculating the absolute tracking error accumulated over the entire operation period, based on the differences between the desired set-points and the actual outputs, defined as Equation 3-13:

$$IAE = \sum_{t=0}^{t_f} |y_{sp}(t) - y(t)| \quad (3-13)$$

where  $y_{sp}(t)$  is the setpoint,  $y(t)$  is the actual output at any given time, and  $t_f$  is the final time of the evaluation period.

For disturbance rejection evaluation, three metrics are employed. Recovery time (RTd) is defined as the time required for the CV to return and settle within  $\pm 2\%$  of its setpoint after a disturbance occurs. Maximum deviation (MD) represents the maximum absolute deviation of the CV from its setpoint during the disturbance response period. IAE accumulates the absolute deviation from the setpoint over the entire operation period.

**Process performance metrics.** Beyond controller performance, the overall operational effectiveness is evaluated using process-level metrics. The total CO<sub>2</sub> capture amount represents the cumulative amount of CO<sub>2</sub> captured over the operation period. Average specific reboiler duty quantifies the thermal energy use per unit of CO<sub>2</sub> captured, indicating energy efficiency. To avoid the dilution effect of long steady-state periods where both controllers perform similarly, the process performance metrics are evaluated within transient time windows rather than over the entire operation period. The time windows are selected to encompass each transient event from initiation to stabilisation, as specified for each case in Section 3.

## 3.4 Potential assessment framework

A bottom-up approach is established to analyse the negative emission potential for integrating CO<sub>2</sub> capture in CHP plants and the related costs on the national level, with its scheme shown in Figure 3.8 (refer also to Figure 1 in Paper VI).

### 3.4.1 Modelling an example CHP plant

#### 3.4.1.1 Configuration of the example plant

The schematic of the w-CHP plant integrated with CO<sub>2</sub> capture is illustrated in Figure 3.9 (refer also to Figure 2 in Paper VI). It comprises a boiler, a Rankine cycle, a MEA-CA CO<sub>2</sub> capture unit, and a CO<sub>2</sub> compression unit.

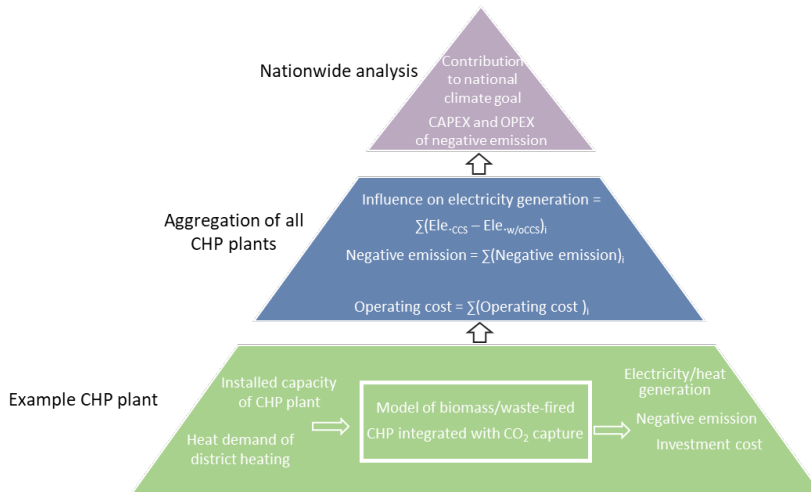


Figure 3.8: Scheme of the bottom-up approach.

### 3.4.1.2 System modelling

To simulate the CHP plant shown in Figure 3.9, an Aspen Plus model is developed for the Rankine cycle, including both electricity and heat generation. A dynamic model for CO<sub>2</sub> capture is developed in Aspen HYSYS Dynamics, which can adequately consider the influence of varied energy demands on the performance of CO<sub>2</sub> capture. These two models are coupled in simulation.

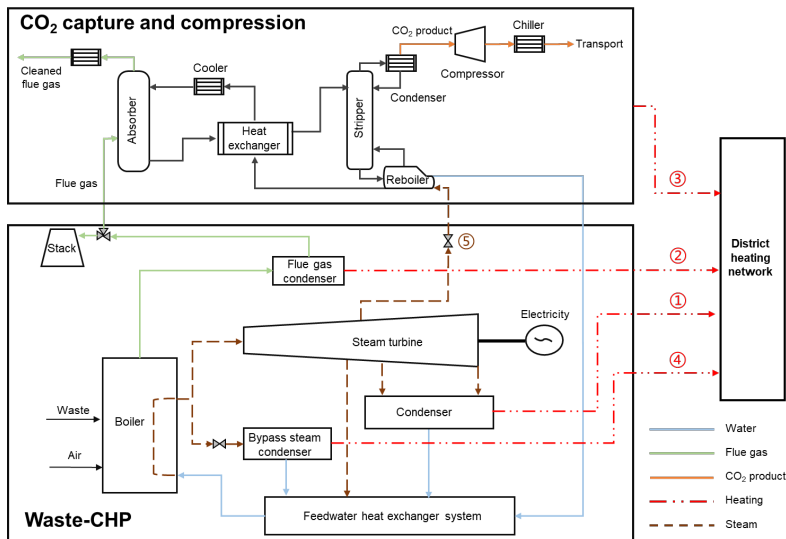


Figure 3.9: Schematic of integration of w-CHP and CO<sub>2</sub> capture and compression.

### 3.4.1.3 Operating modes of the plant

Two operating modes have been identified for CO<sub>2</sub> capture, which correspond to the lower and upper limits for the potential amounts of captured CO<sub>2</sub>.

**Operating mode 1 (OM1):** is designed to maximise the amount of captured CO<sub>2</sub> (CO<sub>2</sub>max\_upper) under the prerequisite that the heat generation (the heat supplied to the DH network) remains unchanged. The electricity generation can be sacrificed to enable capturing more CO<sub>2</sub>.

**Operating mode 2 (OM2):** is designed to maximise the amount of captured CO<sub>2</sub> (CO<sub>2</sub>max\_lower) under the prerequisite that both the heat generation and the net generated electricity remain unchanged.

Figure 3.10 (refer also to Figure 3 in Paper VI) shows the flowchart for simulating OM1 and OM2. The operation of the CHP plant without CO<sub>2</sub> capture is first simulated according to the heat demand to obtain electricity generation. There are constraints on the operation of the boiler, the steam turbine, and the CO<sub>2</sub> capture unit. When they are below their minimum loads, they will be shut down.

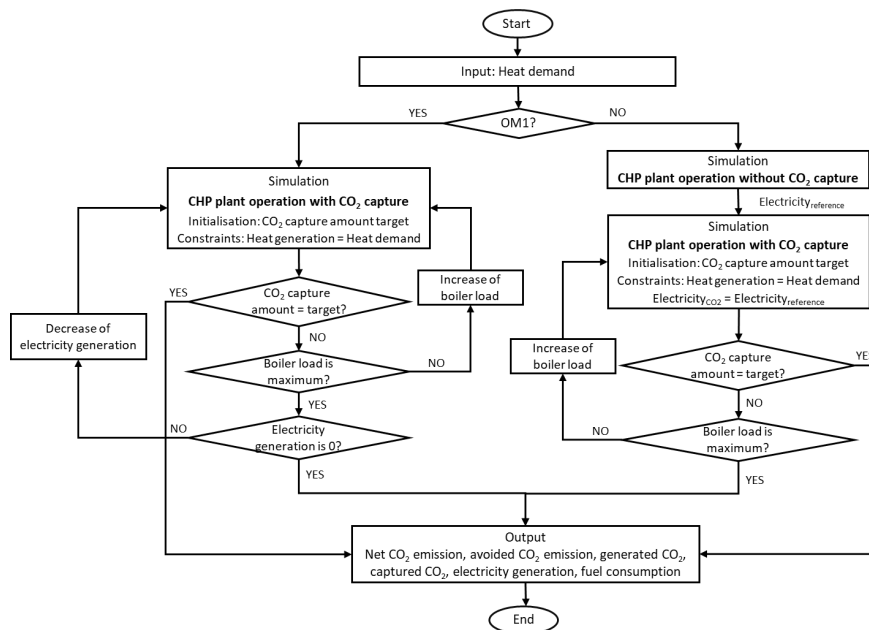


Figure 3.10: Calculation flowchart for two operating modes.

When CO<sub>2</sub> capture is integrated, compared to the CHP plant without CO<sub>2</sub> capture, total heat generation is assumed to remain unchanged in both OMs.

However, the distribution of heat from different sources may vary, for example, from the condensers of extracted steam and FG. Since this study mainly focuses on the capture potential, the detailed operating results of the CHP plants are not presented. More details about the heat generation can be found in Wang et al. (2023).

#### 3.4.1.4 Key performance indicators (KPIs)

The yearly captured CO<sub>2</sub> is a KPI and is calculated by aggregating the hourly results obtained by doing hourly simulations, as shown in Equation 3-14. In addition, the capture rate ( $R_{CO_2}$ ), the change in fuel consumption ( $\Delta F$ ), and the change in net electricity generation ( $\Delta El$ ) are also employed as KPIs, and are defined from Equation 3-15 to Equation 3-17, respectively.

$$C_{CO_2} = \sum_1^{8760} Opt(m_{CO_2,j}) \quad (3-14)$$

$$R_{CO_2} = C_{CO_2} / (G_{CO_2})_{integ} * 100\% \quad (3-15)$$

$$\Delta F = F_{integ} - F_{ref} \quad (3-16)$$

$$\Delta El = El_{ref} - El_{integ} \quad (3-17)$$

where  $m_{CO_2,j}$  is the optimised amount of captured CO<sub>2</sub> at the  $j^{th}$  hour,  $C_{CO_2}$  is the amount of captured CO<sub>2</sub> annually,  $G_{CO_2}$  is the amount of generated CO<sub>2</sub> annually,  $F$  and  $El$  are the amounts of consumed fuel and net electricity generation, respectively, and the subscripts *integ* and *ref* indicate the integrated system with CO<sub>2</sub> capture and compression and the w-CHP reference plant without CO<sub>2</sub> capture and compression, respectively.

As waste contains both a fossil share and a biogenic share, the generated CO<sub>2</sub> is also correspondingly divided into fossil CO<sub>2</sub> originated from the fossil share, and biogenic CO<sub>2</sub> originated from the biogenic share. Capturing fossil CO<sub>2</sub> can only achieve a maximum of zero emission, while capturing biogenic CO<sub>2</sub> can achieve negative emission. To take this into account, another KPI, net CO<sub>2</sub> emission (*NetE*), is introduced, as shown in Equation 3-18. When it is positive, it implies that the captured CO<sub>2</sub> is less than the generated fossil CO<sub>2</sub>, while if it is negative, it implies that the captured CO<sub>2</sub> is more than the generated fossil CO<sub>2</sub>.

$$NetE = (G_{CO_2})_{integ} * \alpha_{fos} - C_{CO_2} \quad (3-18)$$

where  $\alpha_{fos}$  is the fossil fraction of the used fuel.

In addition, as more fuel can be utilised when CO<sub>2</sub> capture is included, the avoided CO<sub>2</sub> emission ( $A_{CO_2}$ ) is also employed to estimate the contribution of BECCS more accurately, as defined by Equation 3-19.

$$A_{CO_2} = (G_{CO_2})_{ref} * \alpha_{fos} - NetE \quad (3-19)$$

To evaluate the economic performance for the integration of CO<sub>2</sub> capture, the life-cycle cost (*LCC*), which gives the total cost of CO<sub>2</sub> capture over its life cycle, and the levelised cost of CO<sub>2</sub> avoided (*LCCA*) are employed as KPIs, which can be calculated by Equations 3-20 and 3-21.

$$LCC = CAPEX + \sum_{i=1}^t [OPEX / (1 + r)^i] \quad (3-20)$$

$$LCCA = \left( CAPEX * \frac{r(1+r)^t}{(1+r)^t - 1} + OPEX \right) / A_{CO_2} \quad (3-21)$$

where *CAPEX* is the total capital expenditure, *OPEX* is the annual O&M expenditure, *t* is the economic life of the plant, and *r* is the discount rate. No salvage value is considered at the end of the plant's life.

Table 3.7 (refer also to Table 1 in Paper VI) shows the estimation of CAPEX and OPEX. For CAPEX, the Aspen Process Economic Analyzer (APEA) is first used to estimate the total direct cost (TDC) associated with constructing the CO<sub>2</sub> capture and compression plant. Other costs associated with the supportive materials and labour, facilities, engineering, contractors, and contingencies for plant construction and CAPEX are estimated based on TDC using multiplicative factors, which are taken from the U.S. Department of Energy report (Christensen & Dysert, 2011; Gerdes et al., 2011). OPEX consists of both fixed OPEX and variable OPEX (Li et al., 2015). The variable OPEX (*OPEX<sub>variable</sub>*) can be calculated by Equation 3-22.

$$OPEX_{variable} = \sum_{k=1}^p (UP_{chemical,k} * M_{chemical,k}) + UEl_{electricity} * \Delta El \quad (3-22)$$

where *p* is the total number of chemicals that are used in the CO<sub>2</sub> capture process, *k* indicates the *k<sup>th</sup>* chemicals (MEA solvent, cooling water, and corrosion inhibitor), *UP<sub>chemical</sub>* and *UEl<sub>electricity</sub>* are the unit price of chemicals and electricity, respectively, and *M<sub>chemical</sub>* is the amount of consumed chemicals.

## 3.4.2 National aggregation of all CHP plants

### 3.4.2.1 Assumptions

As all bio-CHP and w-CHP plants have different installed capacities but similar system configurations and operating strategies, the results of the example plant can be adapted to other plants. However, simulations based on physical models are highly time-consuming. For the assessment on the national level, ML models are developed to replace the physical models when simulating all CHP plants. To simplify the calculation, the following assumptions are made regarding CHP plants:

- All CHP plants use the same waste fuel as the example plant.
- All CHP plants have the same minimum boiler load ratio as the

example plant.

- All CHP plants have the same maintenance schedule as the example plant.
- All CHP plants use the same CCS technology as the example plant.

Table 3.7: The factors used in the assessment of CAPEX and OPEX (Christensen & Dysert, 2011; Gerdes et al., 2011; Li et al., 2015).

Item	Assumption	Inclusion
<b>CAPEX</b>		
Total direct cost (TDC)	Calculated by APEA	Direct costs for equipment, materials, and labour for construction.
Total indirect cost (TIC_cost)	20% of TDC	Non-manufacturing fixed-capital investment for construction overhead, such as land, administrative and other offices, warehouses, shipping, etc.
Bare erected cost (BEC)	TDC+TIC_cost	Total investment for process equipment, on-site facilities, infrastructure that supports the project, and the direct and indirect labour required for its construction.
Engineering and contractor (EC)	27% of BEC	Costs related to designing the project (engineering) and building it (construction).
Engineering procurement and construction (EPC)	127% of BEC	Costs paid to the contractor responsible for the project's engineering, procurement, and construction.
Process contingency (PC)	25% of BEC	Allowance for unforeseen risks or changes specifically related to the engineering and design processes.
Project contingency (PJC)	20% of EPC + 5% of BEC	The contingency reserve set to cover unforeseen costs and risks during the project, including the design and construction phases.
Total plant cost (TPC)	120% of EPC + 30% of BEC	Fixed-capital investment needed to supply required manufacturing and plant facilities.
Owner's cost (OC)	15% of TPC	Working capital necessary for the operation of the plant before sales revenue becomes available, such as financing costs.
CAPEX	115% of TPC	Total capital investment to complete a project.
<b>OPEX</b>		
Fixed OPEX	3% of CAPEX	Total maintenance and labour costs.
Variable OPEX	-	Costs of the chemicals and electricity used.
OPEX	3% of CAPEX + Variable O&M cost	Total operational and maintenance costs during the operational phase of a project.

### 3.4.2.2 Modelling other CHP plants

Figure 3.11 (refer also to Figure 4 in Paper VI) shows the calculation process of other CHP plants. The operation of CHP plants, such as the generated electricity, the consumption of fuel, and the generated CO<sub>2</sub>, is mainly dependent on the heat demand, which is further dependent on the meteorological parameters, such as the ambient temperature and the wind speed. Accordingly, the results of the example plant are first used to train an ML model (ML\_CHP), which can determine the amount of generated CO<sub>2</sub>, the net electricity generation, and the amount of captured CO<sub>2</sub> according to the heat demand. This ML\_CHP will be also used for other CHP plants. Due to the lack of actual hourly heat demands of other DH networks, it is further assumed that the variation in heat demands in different regions of the country has the same pattern as that of the example plant, and that heat demands are mainly dependent on the local meteorological parameters, i.e., the local ambient temperature and wind speed (Wang et al., 2022). Based on this assumption, another ML model (ML\_demand) is developed using the data from the example plant. This model is then used to estimate the hourly heat demands for other locations.

### 3.4.2.3 Result aggregation

Once the results are obtained for each CHP plant, the negative emission potential and the associated cost on the national level can be calculated by aggregating them, as shown in Equations 3-23 to 3-30.

$$(C_{CO2})_{nation} = \sum_{i=1}^n (C_{CO2})_i \quad (3-23)$$

$$(R_{CO2})_{nation} = (C_{CO2})_{nation} / (G_{CO2})_{integ,nation} * 100\% \quad (3-24)$$

$$(\Delta F)_{nation} = \sum_{i=1}^n (\Delta F)_i \quad (3-25)$$

$$(\Delta El)_{nation} = \sum_{i=1}^n (\Delta El)_i \quad (3-26)$$

$$(NetE)_{nation} = \sum_{i=1}^n (NetE)_i \quad (3-27)$$

$$(A_{CO2})_{nation} = \sum_{i=1}^n (A_{CO2})_i \quad (3-28)$$

$$(LCC)_{nation} = \sum_{i=1}^n (LCC)_i \quad (3-29)$$

$$(LCCA)_{nation} = \left[ (CAPEX)_{nation} * \frac{r(1+r)^t}{(1+r)^t - 1} + (OPEX)_{nation} \right] / (A_{CO2})_{nation} \quad (3-30)$$

where  $n$  is the total number of CHP plants in the country, and the subscripts  $i$  and  $nation$  indicate the  $i^{th}$  CHP plant and the aggregated performance for all CHP plants.

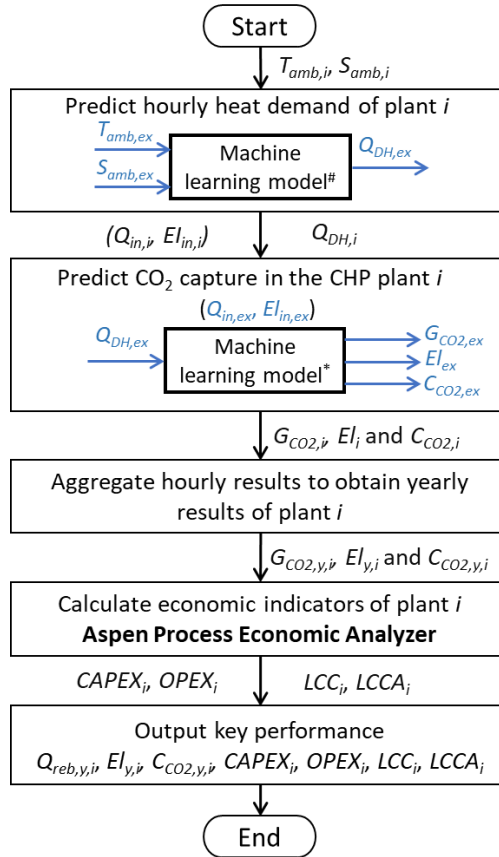


Figure 3.11: Calculation flowchart for other CHP plants.

# The ML model is designed to predict hourly heat demand by using hourly ambient temperature and wind speed as the input. \* The ML model is designed to predict hourly generated CO<sub>2</sub>, net electricity generation, and captured CO<sub>2</sub> by using hourly heat demand as input. Where  $T_{amb}$  is the hourly ambient temperature,  $S_{amb}$  is the hourly wind speed,  $Q_{DH}$  is the hourly heat demand,  $El$  is the hourly net electricity generation,  $Q_{in}$  and  $El_{in}$  are the installed capacities of heat and electricity,  $G_{CO_2}$  is the hourly generated CO<sub>2</sub>,  $C_{CO_2}$  is the hourly captured CO<sub>2</sub>,  $CAPEX$  is the total capital expenditure,  $OPEX$  is the annual O&M expenditure,  $LCC$  is the life-cycle cost and  $LCCA$  is the levelised cost of CO<sub>2</sub> avoided. The subscript  $y$  represents the aggregated yearly value. The subscripts  $ex$  and  $i$  represent the values of the example CHP plant and CHP plant  $i$ .

### 3.4.3 Case study – Sweden

To demonstrate the effectiveness of the proposed method, Sweden is employed as a case study.

### 3.4.3.1 Example plant

The w-CHP plant located in Västerås is chosen as the example plant. The main operating parameters of the example plant with CO<sub>2</sub> capture and compression are listed in Table 3.8 (refer also to Table 2 in Paper VI).

Table 3.8: Main operating parameters of the example CHP plant with CO<sub>2</sub> capture and compression.

Parameters	Value
<b>W-CHP plant (Li, Wang, et al., 2019; Wang et al., 2023)</b>	
Fuel flow rate (kg/s)	16.6
Fuel heating value (lower heating value) (MJ/kg)	12
Maximum electricity generation of the steam turbine, gross (MW)	50
Turbine condenser capacity (MW)	110
Flue gas (FG) condenser capacity (MW)	30
Bypass steam condenser capacity in heat-only mode (MW)	160
Live steam temperature (°C)	470
Live steam pressure (MPa)	7.4
Biogenic fraction (%)	55
Heat demand (GWh/yr)	835.72
Unused boiler capacity (%)	6.1
FG composition (vol%)	
CO <sub>2</sub>	12.7
O <sub>2</sub>	3.8
N <sub>2</sub>	73.7
H <sub>2</sub> O	9.8
<b>CO<sub>2</sub> capture (Dong et al., 2023; Harun et al., 2012), compression and liquefaction (Linnenberg et al., 2012; Zhao et al., 2017)</b>	
MEA concentration in lean solvent (wt%)	30
Type of packing in the absorber and stripper	IMTP#38MM
CO <sub>2</sub> lean loading (mol CO <sub>2</sub> /mol MEA)	0.29
Reboiler temperature (°C)	113
Flooding factor of the absorber (%)	70
Flooding factor of the stripper (%)	70
CO <sub>2</sub> capture target (%)	90
Outlet pressure of CO <sub>2</sub> compressor (MPa)	1.6
Outlet temperature of CO <sub>2</sub> compressor (°C)	40
Temperature for transport (°C)	-26
Energy efficiency ratio of the chiller	2.1

In order to calculate LCC and LCCA for the integration of CO<sub>2</sub> capture, the assumptions for economic analysis of CO<sub>2</sub> capture and compression are summarised in Table 3.9 (refer also to Table 3 in Paper VI).

The equipment sizes of the capture unit are determined according to the maximum FG flow rate, which is 100 kg/s for the example plant. For a capture rate of 90%, the diameters/heights of the columns are estimated to be 7.5 m/17.1 m and 5.3 m/7.1 m for the absorber and stripper, respectively (Otitoju et al., 2020).

Table 3.9: Economic evaluation assumptions of CO<sub>2</sub> capture and compression (Li et al., 2015).

Item	Value
Present value	2022 USD
Project life	25 years
Discount rate	8%
MEA price	2.09 \$/kg
MEA consumption	1.5 kg/tCO <sub>2</sub>
Corrosion inhibitor price	6.61 \$/t
Corrosion inhibitor consumption	0.055 kg/tCO <sub>2</sub>
Cooling water price	0.35 \$/m <sup>3</sup>
Cooling water make-up	2.4 m <sup>3</sup> /tCO <sub>2</sub>
Electricity price	42.63 \$/MWh (Beiron, Normann, et al., 2022)

### 3.4.3.2 Overview of CHP plants in Sweden

There are about 110 bio/w-CHP plants in Sweden, as shown in Figure 3.12 (refer also to Figure 5 and Figure 6 in Paper VI). Figure 3.12 also shows an overview of their installed capacities for heat and electricity (Ahlmén & Hellsberg, 2020). The ambient temperature and wind speed profiles of all CHP plants can be obtained from the Swedish Meteorological and Hydrological Institute (SMHI) (2019).

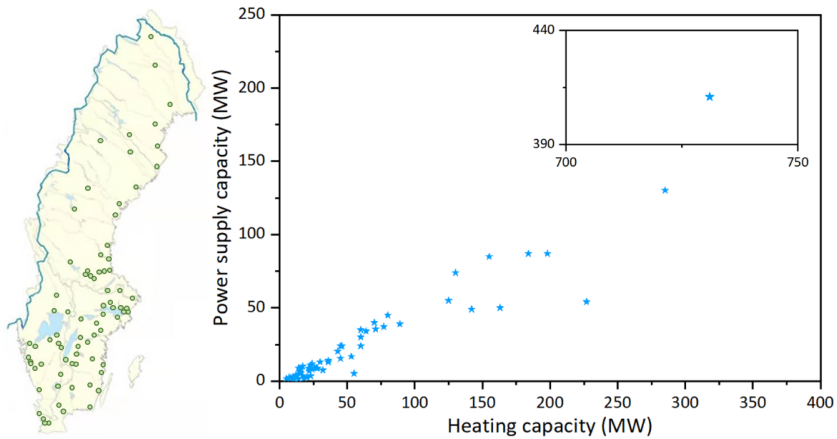


Figure 3.12: Distribution and installed capacities of CHP plants in Sweden (Ahlmén & Hellsberg, 2020).



## 4 Selecting dynamic modelling approaches for different applications of CO<sub>2</sub> capture

*This chapter addresses RQ1, covering first principles-based approaches (Section 4.1) and ML-based approaches (Section 4.2).*

### 4.1 First principles-based modelling approaches for CO<sub>2</sub> capture

This section presents the comparison and selection of first principles-based dynamic modelling approaches for CO<sub>2</sub> capture.

#### 4.1.1 Case setup

To evaluate the model performance under representative operating variations, five cases are defined by considering different key influencing parameters, including FG flow rate, FG CO<sub>2</sub>vol% and the available heat for CO<sub>2</sub> capture, as summarised in Table 4.1.

For all approaches, the lean MEA solution flow rate and reboiler duty are two important parameters. Their treatment differs depending on both the modelling approach and the case conditions.

For Case 1 to Case 3, if the available heat can always meet the reboiler's requirement, IST and DwC adjust the lean MEA solution flow rate and reboiler duty dynamically to achieve the set target of CO<sub>2</sub> capture rate (90%), in response to variations in FG flow rate and CO<sub>2</sub>vol%. In contrast, using Dw/oC, the lean MEA solution flow rate and reboiler duty remain constant, and are determined based on the average FG CO<sub>2</sub> content and a fixed capture rate (90%).

For Cases 4 and 5, when the available heat is specified as an input, for IST, the captured CO<sub>2</sub> is calculated based on the available heat and specific heat needed by capturing 1 kg CO<sub>2</sub>. For DwC, the controller will regulate the lean MEA solution flow rate to achieve the set target of lean loading (0.287 mol/mol), according to FG flow rate, CO<sub>2</sub>vol% and the available heat. For Dw/oC, the lean MEA solution flow rate remains constant, which

is determined based on the average available heat and fixed lean loading (0.287 mol/mol).

Table 4.1: An overview of the defined cases.

Case	Operating parameters	Sub-cases	Flue gas (FG) flow rate (kNm <sup>3</sup> /h)	CO <sub>2</sub> concentration (vol%)	Available heat (MW)
Case 1	FG flow rate <sup>a</sup>	Case 1-1 (↓)	340.77→264.73 (91%→70%)*	14.4 (average)	Sufficient for 90% CO <sub>2</sub> capture rate
		Case 1-2 (↑)	201.68→337.02 (53%→90%)		
Case 2	FG CO <sub>2</sub> vol% <sup>b</sup>	Case 2-1 (↓)	301.49 (average)	Sinusoidal variation: 15.7→9.7 (100%→61%)	Sufficient for 90% CO <sub>2</sub> capture rate
		Case 2-2 (↑)		Sinusoidal variation: 9.7→15.7 (61%→100%)	
Case 3	FG flow rate <sup>a</sup> + CO <sub>2</sub> vol% <sup>b</sup>	Case 3-1 (Flow rate↓ CO <sub>2</sub> vol%↑)	375.21→326.14 (100%→86%)	Sinusoidal variation: 12.0→13.6 (76%→87%)	Sufficient for 90% CO <sub>2</sub> capture rate
		Case 3-2 (Flow rate↑ CO <sub>2</sub> vol%↓)	327.94→351.00 (87%→94%)	Sinusoidal variation: 13.4→12.4 (85%→79%)	
Case 4	Available heat for CO <sub>2</sub> capture <sup>b</sup>	Case 4-1 (↓)	301.49 (average)	14.4 (average)	Sinusoidal variation: 96→49
		Case 4-2 (↑)			Sinusoidal variation: 49→96
Case 5	FG flow rate <sup>a</sup> + CO <sub>2</sub> vol% <sup>b</sup> + available heat <sup>b</sup>	Case 5-1	375.21→326.14 (100%→86%)	12.0→13.6 (76%→87%)	Sinusoidal variation: 90→104→90
		Case 5-2	327.94→351.00 (87%→94%)	13.4→12.4 (85%→79%)	

a = real data from the CHP plant. b = synthetic data. \* The value in brackets refers to the percentage compared to maximum value of real data.

#### 4.1.2 Comparison of different modelling approaches

The relative differences in accumulated captured CO<sub>2</sub> and average specific reboiler duty among approaches are shown in Figure 4.1 and Figure 4.2, respectively, which are calculated based on the result of IST for Dw/oC and DwC. Overall, Dw/oC results in larger differences with the other two approaches, and the magnitude of differences increases with the magnitude of input variations.

For the variation of FG flow rate and CO<sub>2</sub>vol% (Case 1 and Case 2), DwC shows an asymmetric pattern: it captures less CO<sub>2</sub> than IST under increasing variations but more under decreasing variations. This is attributed to the time delay inherent in controller response: when FG increases, the controller is slow to increase the lean solvent flow rate and reboiler duty for maintaining a constant capture rate, resulting in temporarily lower capture; the opposite occurs for decreasing variations.

For the variation of available heat (Case 4), the relationship between DwC and IST reverses compared to FG variation. DwC captures more CO<sub>2</sub> than IST under increasing variations but less under decreasing variations. This is also attributed to the controller's time delay: when available heat increases, the controller is slow to decrease the lean solvent flow rate for maintaining a constant lean loading, resulting in temporarily higher capture; the opposite occurs for decreasing variations.

Regarding the average specific reboiler duty, DwC consistently achieves lower values than IST across all cases. For Dw/oC, no consistent trend is observed, as the fixed operating parameters interact differently with each type of input variation.

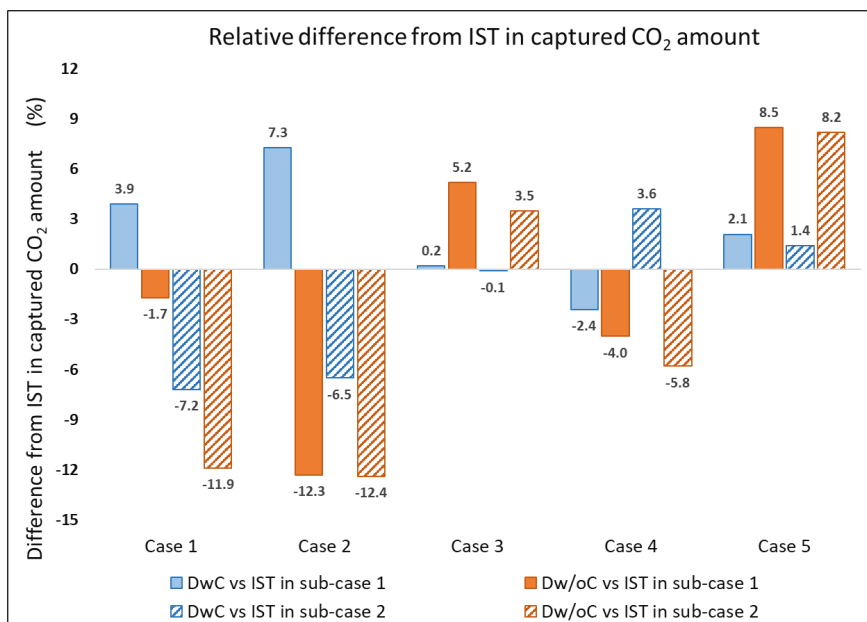


Figure 4.1: Relative differences in accumulated captured CO<sub>2</sub> under different operating parameters.

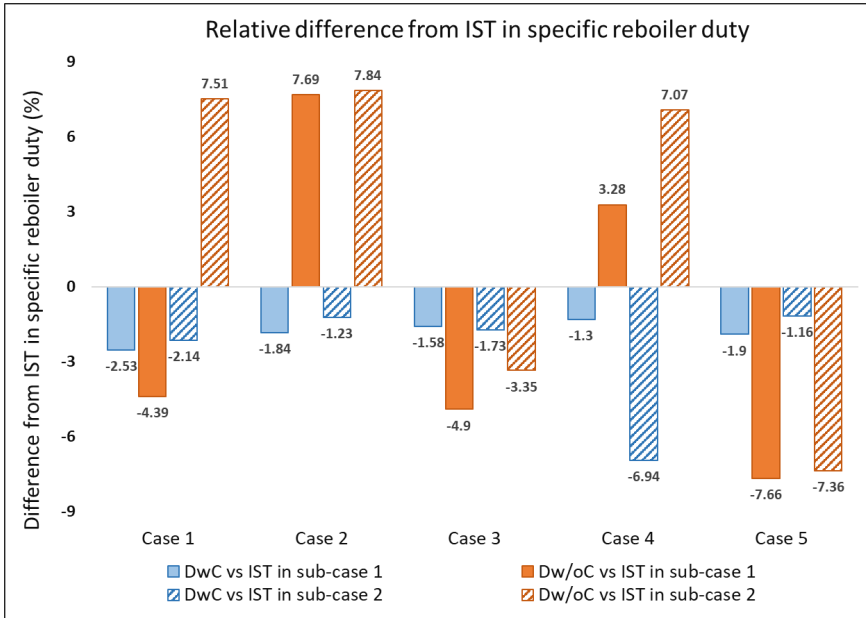


Figure 4.2: Relative differences in specific reboiler duty under different operating parameters.

### 4.1.3 Selection of modelling approaches

The selection of modelling approaches is mainly dependent on the specific application requirements. Based on the comparison results, guidance is provided across three stages: system design, plant operation, and operational optimisation.

During the system design stage, two applications are identified. For the equipment design of CO<sub>2</sub> capture, it is essential to check the boundary of safety operation by performing step response analysis and stability analysis. Then Dw/oC should be selected. For the control system design of CO<sub>2</sub> capture, the controller needs to be tested to see if it can handle the disturbance and maintain system stability. Then DwC should be selected.

During the plant operation stage, two applications are identified. For determining the amount of captured CO<sub>2</sub>, both DwC and IST may be employed depending on the given inputs and requirements. For short-term operations, DwC is recommended as it considers the impact of non-equilibrium and the deviation can be up to 7.3%. Nevertheless, for long-term operations where both increasing and decreasing variations are included, the difference between DwC and IST may become small because the positive and negative deviations may cancel each other. Considering the more time needed by both the model development and simulation execution of DwC, IST is preferable, and a time step of 30 minutes is recommended. Taking one day of real FG

data from the same w-CHP plant as an example, the difference in daily accumulated CO<sub>2</sub> between DwC and IST amounts to only 0.32%, despite clear hourly differences being observed, as demonstrated in Paper I. For dynamic operations of the CHP plant, the amount of steam (heat) that needs to be extracted from the steam turbine cycle should be determined in real time. For such a case, it is also possible to employ either DwC or IST. Even though the difference is usually less than 5%, DwC is recommended. This is because IST estimates heat based on the assumption that the specific reboiler duty is only dependent on CO<sub>2</sub>vol%, while DwC estimates the heat according to the target temperature set to the reboiler. For solvent regeneration, the temperature must reach a certain level.

During the operational optimisation stage, it is also possible to employ either DwC or IST. Optimisation is normally conducted based on electricity price and CO<sub>2</sub> price, and the model selection depends on the price mechanism adopted. When hourly prices from real electricity and carbon markets are used, DwC should be selected. This is because the operation of CO<sub>2</sub> capture cannot reach equilibrium with hourly changes. However, if alternative pricing mechanisms are adopted, such as time of use (TOU) or power purchase agreement (PPA), IST could show advantages over DwC since the prices do not vary hourly, and a larger time step, such as one hour, can be chosen.

## 4.2 Machine learning-based models of CO<sub>2</sub> capture

This section presents the development and performance evaluation of ML-based surrogate models for CO<sub>2</sub> capture across four defined application cases.

### 4.2.1 Application definition and case setup

Based on the literature review, there are various applications for dynamic CO<sub>2</sub> capture models, such as control design and operational optimisation, which can be categorised into four key cases, as shown in Table 4.2. According to the literature studies discussed in Section 2.1.3, ML models have been applied to system identification (Case 1) (Abdul Manaf et al., 2016; Sha et al., 2025) and system performance estimation (Case 4) (Li et al., 2016; F. Li et al., 2015; Li et al., 2018), but there is a gap in ML applications for system monitoring and diagnosis (Case 2) and operational optimisation (Case 3). After defining the application cases of dynamic CO<sub>2</sub> capture models, expected outputs (Integrated Environmental Control Model Team,

2019; Wu et al., 2019) and key input features for ML modelling must be selected, as summarised in Table 4.2.

Table 4.2: Inputs and outputs of different cases.

Cases	Key inputs	Expected outputs
Case 1 System identification for control development	<ul style="list-style-type: none"> <li>• Flue gas (FG) flow rate</li> <li>• FG CO<sub>2</sub>vol%</li> <li>• Lean flow rate</li> <li>• Reboiler duty</li> </ul>	<ul style="list-style-type: none"> <li>• CO<sub>2</sub> capture rate</li> <li>• Reboiler temperature</li> </ul>
Case 2 System monitoring and diagnosis	<ul style="list-style-type: none"> <li>• FG flow rate</li> <li>• FG CO<sub>2</sub>vol%</li> <li>• Constant CO<sub>2</sub> capture rate targets</li> </ul>	<ul style="list-style-type: none"> <li>• Reboiler duty</li> <li>• Lean flow rate</li> <li>• Electricity use</li> <li>• Cooling water flow rate</li> <li>• Real-time CO<sub>2</sub> capture rate</li> </ul>
Case 3 Operational optimisation	<ul style="list-style-type: none"> <li>• FG flow rate</li> <li>• FG CO<sub>2</sub>vol%</li> <li>• Varied CO<sub>2</sub> capture rate targets</li> </ul>	<ul style="list-style-type: none"> <li>• Reboiler duty</li> <li>• Lean flow rate</li> <li>• Energy penalty</li> </ul>
Case 4 System performance estimation	<ul style="list-style-type: none"> <li>• FG flow rate</li> <li>• FG CO<sub>2</sub>vol%</li> <li>• Available reboiler duty</li> </ul>	<ul style="list-style-type: none"> <li>• CO<sub>2</sub> capture amount</li> <li>• CO<sub>2</sub> capture rate</li> <li>• Energy penalty</li> </ul>

#### 4.2.2 Data generation

To generate data for ML model training and validation, dynamic simulations of MEA-CA were conducted using a physical model developed in Aspen HYSYS Dynamics V12.1. Detailed model development and validation can be found in a previous study (Dong et al., 2023). Different simulations were conducted for the four different cases identified in Section 2. For Case 1, the simulation was conducted for the open-loop process without any controllers. For Case 2, Case 3 and Case 4, the simulation was conducted for the closed-loop process with controllers, in which input–output behaviours show both the system dynamics and how the controller reacts.

The primary inputs included both dynamic and constant parameters. There were some constant input parameters that were the same for all four cases. These included FG temperature (47°C), initial pressure (143 kPa), and the initial conditions of the lean solvent (41°C, 107 kPa, 30 wt.% MEA and 0.287 lean loading).

For dynamic inputs, in Case 1, FG flow rate and CO<sub>2</sub>vol% data were obtained from a real w-CHP plant, which covered three days in 2019, as shown in Figure 4.3 (refer also to Figure 1 in Paper III). The FG flow rate and CO<sub>2</sub>vol% varied in ranges of 150–360 tonnes per hour (t/h) and 9.6–15.8 vol%, respectively. The time resolution was 1 minute. Based on the actual

FG flow rate and CO<sub>2</sub>vol%, a reboiler duty range can be obtained by using a range of possible capture rates (45–90%) and an average energy penalty (4.5 MJ/kg), based on which the dynamic input signal for reboiler duty (Figure 4.4; refer also to Figure 2 in Paper III) was generated. The dynamic input signal for lean solvent flow rate (Figure 4.5; refer also to Figure 3 in Paper III) was generated based on the actual FG flow rate and a physically realistic L/G ratio range of 1.5–3.5 kg/kg (mass basis) in MEA-CA systems (Zhang et al., 2017). This range maintains safe and stable hydraulic operation, ensuring adequate CO<sub>2</sub> capture efficiency while avoiding flooding risks (Zhang et al., 2017).

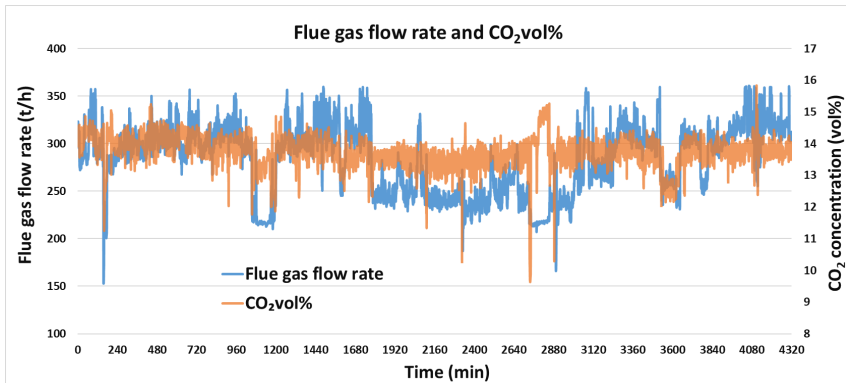


Figure 4.3: Variation of flue gas in Case 1.

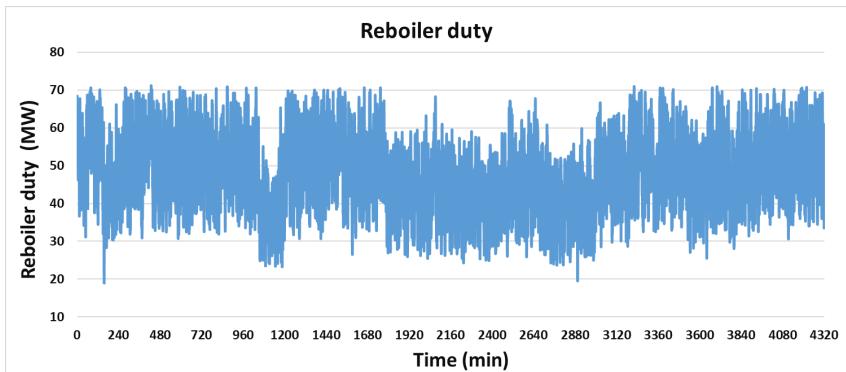


Figure 4.4: Variation of reboiler duty in Case 1.

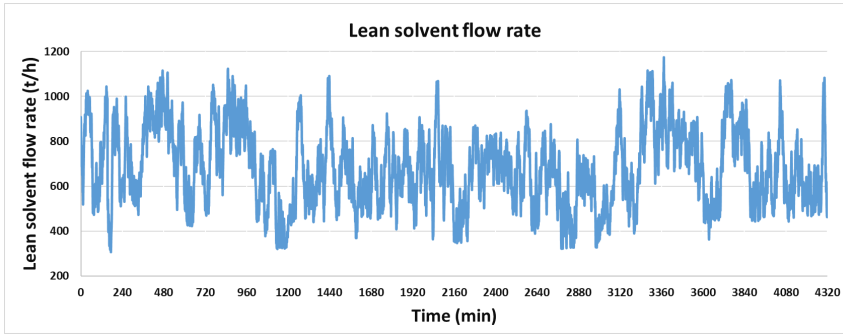


Figure 4.5: Variation of lean solvent flow rate in Case 1.

In Case 2 and Case 3, FG flow rate and  $\text{CO}_2$  vol% were the same as in Case 1. The constant  $\text{CO}_2$  capture rate targets were 70%, 80% and 90% in Case 2, and the varied  $\text{CO}_2$  capture rate signal was generated randomly in the range of 45%–90% (Figure 4.6; refer also to Figure 4 in Paper III) in Case 3, since it was assumed that the  $\text{CO}_2$  capture system was not operating when the  $\text{CO}_2$  capture rate was less than 45%. To achieve those  $\text{CO}_2$  capture rate targets, the lean solvent flow rate and reboiler duty were manipulated by adding PID controllers.

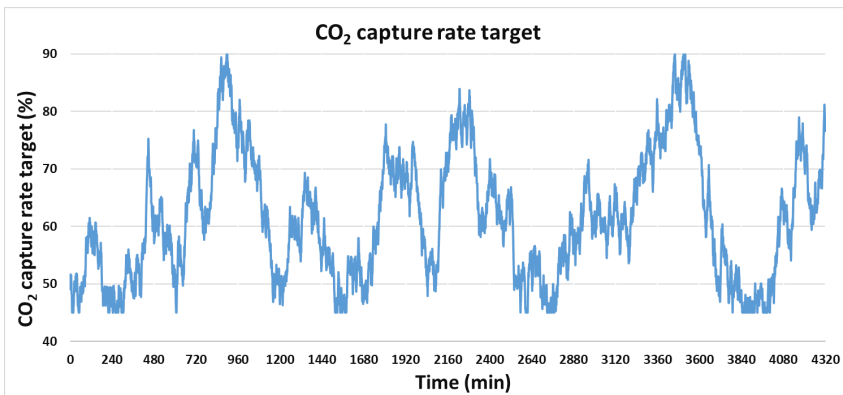


Figure 4.6: Variation of  $\text{CO}_2$  capture rate targets in Case 3.

In Case 4, FG (flow rate and  $\text{CO}_2$  vol%) and reboiler duty were determined by optimising the operation of the CHP plant integrated with  $\text{CO}_2$  capture. Based on the two operating strategies in Wang et al. (2023), the corresponding FG and reboiler duty were shown in Figure 4.7 (refer also to Figure 5 in Paper III) based on optimisation in 3600 minutes. To alleviate the fluctuation of  $\text{CO}_2$  absorption efficiency, the lean solvent flow rate was manipulated by PID controllers to maintain the desired reboiler temperature and thus the desired  $\text{CO}_2$  lean loading.

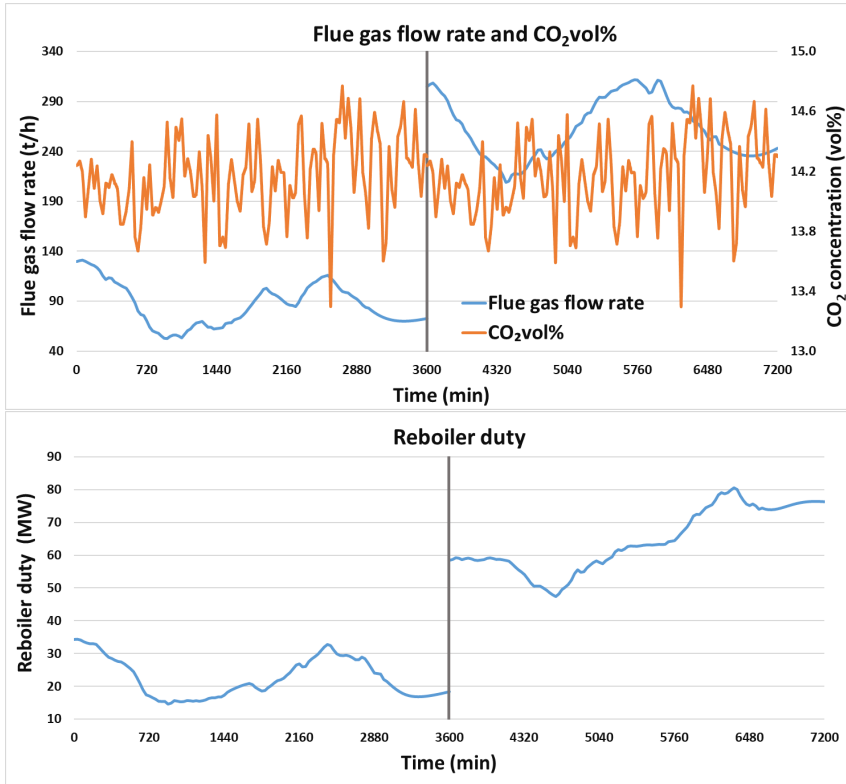


Figure 4.7: Variations of flue gas and reboiler duty in Case 4.

### 4.2.3 Performance of machine learning models

#### 4.2.3.1 Case 1: system identification for control development

Table 4.3 (refer also to Table 2 in Paper III) presents the performance metrics of the three ML models for Case 1. Overall, all models achieve acceptable performance. In comparison, Informer shows the best performance, BPNN is superior to LSTM when it comes to CO<sub>2</sub> capture rate, and LSTM is superior to BPNN for the reboiler temperature.

Table 4.3: Prediction accuracy for Case 1.

ML models	CO <sub>2</sub> capture rate		Reboiler temperature
	MAPE (%)	MAE	MAE (°C)
<b>Informer</b>	<b>3.68</b>	<b>0.025</b>	<b>0.06</b>
LSTM	7.42	0.053	0.09
BPNN	5.53	0.038	1.05

#### 4.2.3.2 Case 2: system monitoring and diagnosis

Table 4.4 (refer also to Table 3 in Paper III) presents the performance metrics of the three ML models for Case 2. Overall, all models achieve satisfactory performance, with MAPE values below 5%. In comparison, Informer consistently shows the best performance across all five outputs. The comparison between LSTM and BPNN varies with the outputs. LSTM can show slightly better performance (such as power use), or worse performance (such as lean solvent) than BPNN. In addition, the prediction errors of LSTM/BPNN are more than twice as high as Informer’s for most of the predicted outputs.

Table 4.4: Prediction accuracy for Case 2.

ML models	Reboiler duty		Lean solvent			
	MAPE (%)	MAE (MW)	MAPE (%)	MAE (t/h)		
<b>Informer</b>	<b>0.89</b>	<b>0.43</b>	<b>1.33</b>	<b>12.6</b>		
LSTM	2.98	1.60	3.84	36.6		
BPNN	2.82	1.54	2.89	28.2		

ML models	Power use		Cooling water		CO <sub>2</sub> capture rate	
	MAPE (%)	MAE (kW)	MAPE (%)	MAE (t/h)	MAPE (%)	MAE
<b>Informer</b>	<b>1.08</b>	<b>0.26</b>	<b>1.09</b>	<b>34</b>	<b>2.97</b>	<b>0.024</b>
LSTM	2.39	0.58	1.67	53	4.63	0.038
BPNN	2.50	0.67	2.97	101	3.03	0.024

#### 4.2.3.3 Case 3: operational optimisation

Table 4.5 (refer also to Table 4 in Paper III) presents the performance metrics of the three ML models for Case 3. Overall, all models achieve acceptable performance, with most MAPE values below 5%, except when modeling the regulation of lean solvent flow rate using LSTM. In comparison, as with Case 2, Informer consistently shows the best performance across all three outputs, particularly excelling in predicting reboiler duty and energy penalty. BPNN shows overall better performance than LSTM.

Table 4.5: Prediction accuracy for Case 3.

ML models	Reboiler duty		Lean solvent		Energy penalty	
	MAPE (%)	MAE (MW)	MAPE (%)	MAE (t/h)	MAPE (%)	MAE (MJ/kg)
<b>Informer</b>	<b>0.90</b>	<b>0.40</b>	<b>3.53</b>	<b>24.9</b>	<b>0.64</b>	<b>0.03</b>
LSTM	3.82	1.54	5.78	41.7	4.64	0.21
BPNN	3.84	1.57	3.57	25.6	2.22	0.10

#### 4.2.3.4 Case 4: system performance estimation

Table 4.6 (refer also to Table 5 in Paper III) presents the performance metrics of the three ML models for Case 4. Overall, all models demonstrate satisfactory performance, with MAPE values below 5% for all outputs. Unlike the previous cases, no single model performs best across all outputs. Instead, the performance varies depending on the target outputs. Informer yields the most accurate predictions for CO<sub>2</sub> capture rate, LSTM slightly outperforms the others for the energy penalty, and BPNN shows the lowest error for CO<sub>2</sub> capture amount.

Table 4.6: Prediction accuracy for Case 4.

ML models	CO <sub>2</sub> capture amount		Energy penalty		CO <sub>2</sub> capture rate	
	MAPE (%)	MAE (t/h)	MAPE (%)	MAE (MJ/kg)	MAPE (%)	MAE
<b>Informer</b>	3.26	1.15	1.52	0.08	<b>0.52</b>	<b>0.005</b>
<b>LSTM</b>	4.27	1.37	<b>1.02</b>	<b>0.05</b>	1.75	0.017
<b>BPNN</b>	<b>2.57</b>	<b>0.72</b>	3.79	0.19	2.42	0.023



# 5 Performance evaluation of model predictive control

*This chapter addresses RQ2, organised into system identification (Section 5.1) and MPC performance evaluation across three control scenarios (Section 5.2).*

## 5.1 System identification results

Following the methodology in Section 2.1.3, a coupled MIMO ARX model was identified with polynomial orders  $n_a = 4$  and  $n_b = 4$ . Figure 5.1 shows the comparison between the model's predictions and the Aspen Plus Dynamics model on the validation dataset, which was given in terms of deviations of CVs from the initial values at the design point (84% capture rate and 116°C reboiler temperature). The identified model demonstrates excellent agreement with the Aspen Plus Dynamics model, achieving validation fit percentages of 91.19% for CO<sub>2</sub> capture rate and 95.73% for reboiler temperature. The strong validation performance demonstrates that the linear ARX structure adequately captures the dominant dynamics of the CO<sub>2</sub> capture process, providing a reliable foundation for the MPC design and performance evaluation described in the following sections.

## 5.2 MPC performance evaluation and comparison with PI control

### 5.2.1 Case 1: Setpoint tracking with varying capture rates

Case 1 evaluates setpoint tracking performance when the CO<sub>2</sub> capture rate setpoint changes from its initial value of 84% to 62% at  $t=1500$  s (step decrease), and then to 97% at  $t=9000$  s (step increase), while the reboiler temperature setpoint remains constant at 116°C throughout the operation. The FG flow rate is held constant at 82.9 kg/s and CO<sub>2</sub> concentration is held constant at 11.9 vol%.

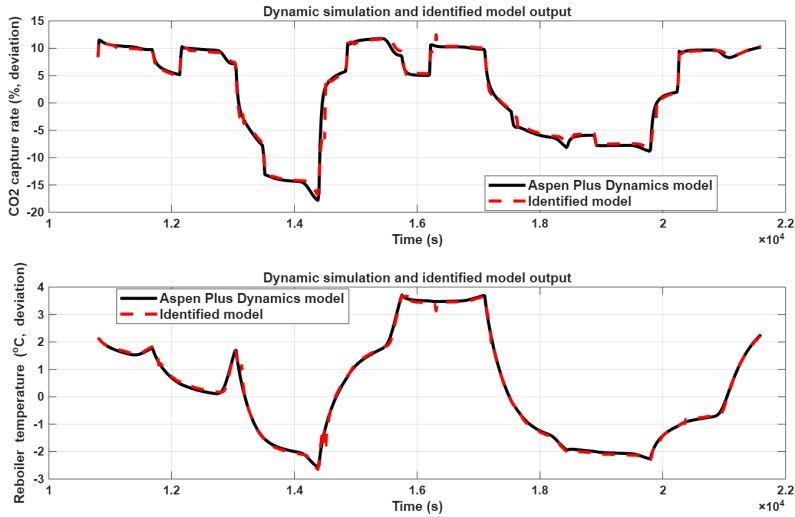


Figure 5.1: Comparison between Aspen Plus Dynamics and identified models: CO<sub>2</sub> capture rate (deviates from 84%) and reboiler temperature (deviates from 116°C).

The simulation results in Figure 5.2 show that MPC reaches the CO<sub>2</sub> capture rate setpoint more quickly with a smaller overshoot than PI. To decrease/increase the CO<sub>2</sub> capture rate, the MVs (lean solvent flow rate and reboiler heat duty) are also decreased/increased, which is in line with the actual process. A notable pattern emerges: MPC consistently initiates control actions earlier than PI. In addition, PI control produces more aggressive and oscillatory adjustments, which could increase mechanical wear. Even though both controllers adjust the MVs in similar directions, MPC and PI produce drastically different reboiler temperature outcomes. This is because the timing, magnitude, and coordination of the adjustments are critical in this coupled multivariable system, where lean solvent flow rate and reboiler duty affect temperature through opposite mechanisms. Furthermore, compared to MPC, PI control shows more noticeable temperature swings that take longer to settle. The difference between MPC and PI is more pronounced in controlling reboiler temperature than in controlling CO<sub>2</sub> capture rate.

These qualitative observations are quantified in the performance metrics. Table 5.1 presents the quantitative controller performance metrics for Case 1. It shows that, compared to PI, MPC consistently achieves superior control performance with higher robustness for both CVs. Taking the step increase period as an example, for CO<sub>2</sub> capture rate, the most significant improvement appears in IAE, with MPC achieving a 67% reduction. Consistent with Figure 5.2, the MPC achieves a 47% faster response with a rise time of 720 s, a 62% faster settling with a ST of 2358 s, and a 19% less overshoot,

compared with the PI. For the constant reboiler temperature setpoint, MPC produces around 55% lower maximum deviation ( $1.7^{\circ}\text{C}$ ) than PI ( $3.7^{\circ}\text{C}$ ). MPC returns to the setpoint faster than PI, with a 64% shorter recovery time. In addition, MPC achieves 82% IAE reduction. These improvements stem from MPC's predictive optimisation framework, which anticipates system behaviour over a several-step horizon and proactively coordinates both lean solvent flow rate and reboiler duty. In contrast, PI control employs independent SISO loops that react only to current tracking errors, leading to delayed corrections and poor coordination between the two MVs.

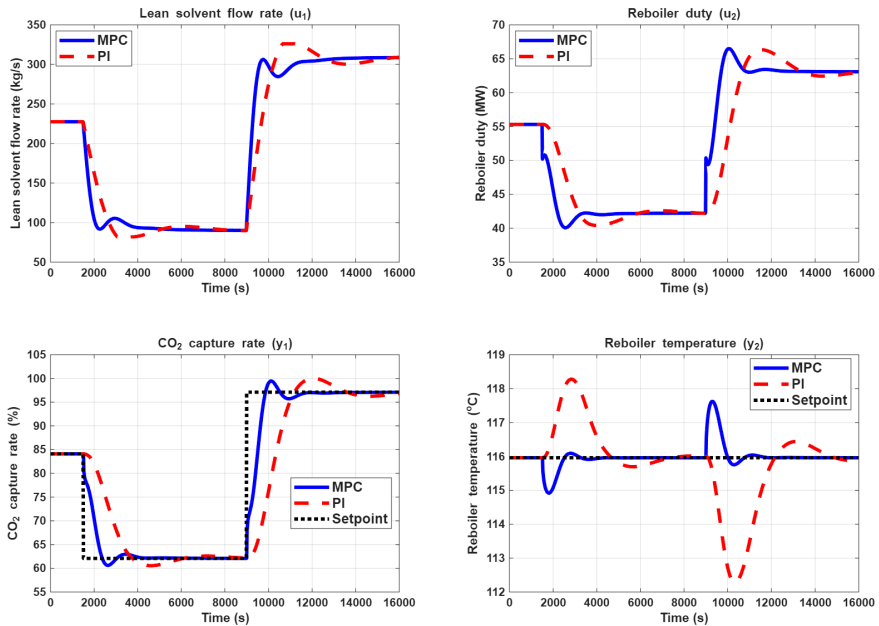


Figure 5.2: Comparison of MPC and PI controllers in Case 1.

Table 5.1: Comparison of controller performance metrics in Case 1.

Step change	Con-trol-lers	Capture rate			Reboiler temperature			
		RT (s)	OS (%)	ST (s)	IAE	MD ( $^{\circ}\text{C}$ )	RTd (s)	IAE
Step decrease	MPC	719.65	6.7485	2358	9820.3	1.0459	2538	745.78
	PI	1368.9	6.9844	6084	28864	2.3163	7254	4124.4
Step increase	MPC	719.62	6.7516	2358	15618	1.6638	2538	1186.3
	PI	1360.5	8.3503	6228	46697	3.6855	6984	6700

Table 5.2 presents the process performance metrics for Case 1 with transient time windows of [1500s 5500s] and [9000s 14000s]. The difference between two controllers varies with the setpoint direction. During step

decrease of CO<sub>2</sub> capture rate setpoint [1500s 5500s], using PI captures 5.7% more CO<sub>2</sub> and uses 4.2% more energy, resulting in a 1.5% lower average specific duty. This occurs because the slower response of PI maintains higher CO<sub>2</sub> capture rates and reboiler heat duty longer before stabilising. During step increase of CO<sub>2</sub> capture rate setpoint [9000s 14000s], using MPC captures 5.2% more CO<sub>2</sub> and uses 3.8% more energy, resulting in a 1.3% lower average specific duty, due to MPC reaching the higher setpoint sooner. However, in flexible operations, the decrease in CO<sub>2</sub> capture rate typically occurs during high electricity price periods. Under such conditions, even though using PI captures more CO<sub>2</sub>, it is not cost-effective due to higher energy use.

Table 5.2: Comparison of process performance metrics in Case 1.

Time window	Controllers	Total CO <sub>2</sub> capture amount (tonne)	Average specific duty (MJ/kg)	Total thermal energy (GJ)
Step decrease [1500, 5500]	MPC	25.23	6.741	170.10
	PI	26.74	6.639	177.55
Step increase [9000, 14000]	MPC	46.53	6.686	311.12
	PI	44.24	6.774	299.68

### 5.2.2 Case 2: FG flow rate disturbance rejection

Case 2 evaluates disturbance rejection performance when the capture rate setpoint is held constant at 84% while the FG flow rate varies. As shown in Figure 5.3, the flow rate gradually decreases from 82.9 kg/s to 56.6 kg/s (at t=1500 s) at a rate of 0.0175 kg/s per second and then increases to 95.6 kg/s (at t=9000 s) at a rate of 0.026 kg/s per second, simulating typical CHP load variations. The CO<sub>2</sub> concentration is held constant at 11.9 vol%.

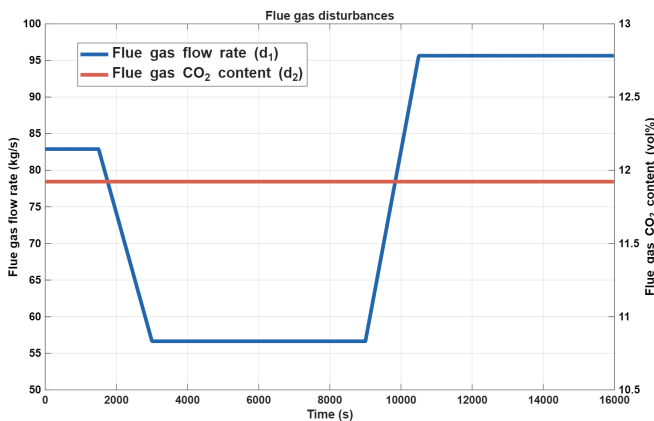


Figure 5.3: Flue gas disturbance in Case 2.

Figure 5.4 illustrates the system responses to FG flow rate disturbances. Both controllers maintain the CO<sub>2</sub> capture rate near the 84% setpoint and the reboiler temperature near the 116°C setpoint after initial transients. In response to the decrease/increase of FG flow rate, CO<sub>2</sub> capture rate first increases/decreases, deviating from the setpoint, and then decreases/increases back to its setpoint. Using MPC exhibits significantly smaller deviations and faster recovery than using PI. The difference is particularly evident in the reboiler temperature responses: using MPC maintains the temperature very close to the setpoint, while using PI shows noticeable temperature swings. To maintain constant setpoints, the MVs are decreased/increased in response to the decrease/increase of FG flow rate. Compared to MPC, PI control produces more aggressive adjustments with larger transient variations. In addition, PI initiates adjustment of reboiler duty later than MPC.

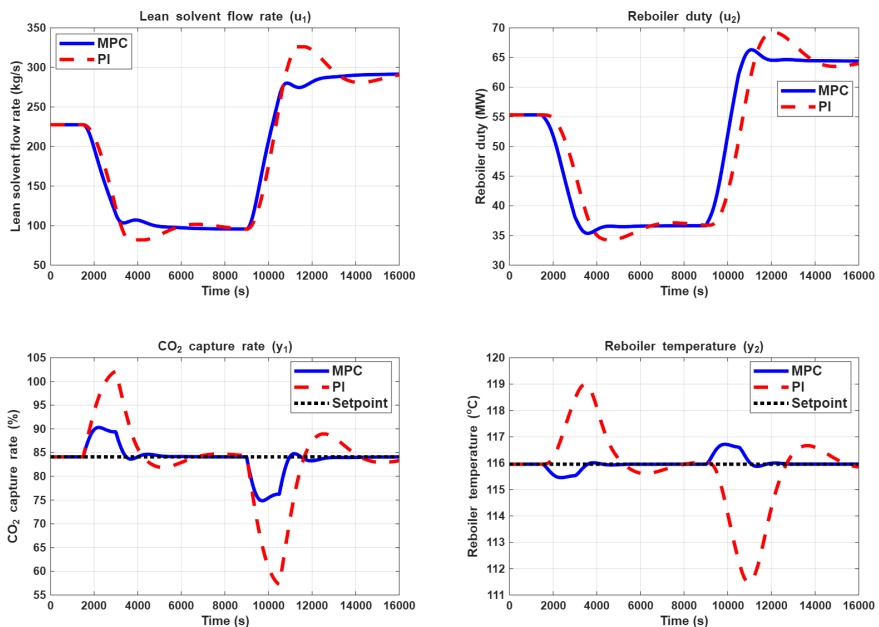


Figure 5.4: Comparison of MPC and PI controllers in Case 2.

Table 5.3 presents the quantitative controller performance metrics for Case 2. MPC demonstrates substantially superior disturbance rejection performance for both CVs. Taking the ramp decrease period as an example, MPC achieves approximately 66% lower maximum deviation, 48% faster recovery, and 70% lower IAE for CO<sub>2</sub> capture rate. For reboiler temperature, the improvements are even more pronounced: 83% lower maximum deviation, 51% faster recovery, and 87% lower IAE. MPC's superior performance stems from its measured disturbance feed-forward capability. By detecting FG flow rate changes in advance, MPC proactively adjusts both lean solvent

flow rate and reboiler duty before the disturbances significantly affect the CVs. In contrast, PI control can only react after deviations occur, resulting in larger errors and longer recovery times.

Table 5.3: Comparison of controller performance metrics in Case 2.

Ramp change	Controllers	Capture rate			Reboiler temperature		
		MD (%)	RTd (s)	IAE	MD (°C)	RTd (s)	IAE
Ramp decrease	MPC	<b>6.2076</b>	<b>3708</b>	<b>9222.3</b>	<b>0.50819</b>	<b>3654</b>	<b>738.19</b>
	PI	18.04	7182	31041	3.0225	7470	5766
Ramp increase	MPC	<b>9.2201</b>	<b>3726</b>	<b>13691</b>	<b>0.75493</b>	<b>3672</b>	<b>1096.2</b>
	PI	26.897	6984	48545	4.4931	6984	9077.9

Table 5.4 presents the quantitative process performance metrics for Case 2 with transient time windows of [1500s 5500s] and [9000s 14000s]. The difference between the two controllers varies with the disturbance direction. During ramp decrease of FG flow rate [1500s 5500s], using PI captures 4.4% more CO<sub>2</sub> and uses 4.3% more energy, resulting in a slightly lower average specific duty. This occurs because using PI exhibits a larger upward deviation from the setpoint, maintaining higher instantaneous capture rates during transition, which results in more cumulative CO<sub>2</sub> captured and higher energy use. During ramp increase of FG flow rate [9000s 14000s], using MPC captures 4.6% more CO<sub>2</sub> and uses 2.8% more energy, resulting in a 1.8% lower average specific duty. This occurs because using PI exhibits a larger downward deviation from the setpoint, with lower instantaneous capture rates during transition, resulting in less cumulative CO<sub>2</sub> captured and lower energy use.

Table 5.4: Comparison of process performance metrics in Case 2.

Time window	Controllers	Total CO <sub>2</sub> capture amount (tonne)	Average specific duty (MJ/kg)	Total thermal energy (GJ)
Ramp decrease [1500, 5500]	MPC	25.23	6.407	161.66
	PI	26.40	6.397	168.87
Ramp increase [9000, 14000]	MPC	43.60	6.818	297.31
	PI	41.67	6.944	289.36

### 5.2.3 Case 3: Disturbance rejection of FG flow rate and CO<sub>2</sub> concentration

Case 3 evaluates disturbance rejection performance under simultaneous disturbances of both FG flow rate and CO<sub>2</sub> concentration. As shown in Figure 5.5, the flow rate ramp decreases from 82.9 kg/s to 67.9 kg/s at t=1500 s at a rate of 0.01 kg/s per second and then the ramp increases to 88.9 kg/s at t=9000 s at a rate of 0.014 kg/s per second. CO<sub>2</sub> concentration step decreases from 12 vol% to 10 vol% at t=1500 s, and step increases to 15 vol% at t=9000 s. Throughout the operation, the capture rate setpoint is held constant at 84%. Such coupled disturbances commonly occur in bio-CHP plants due to boiler load changes combined with biomass fuel variability.

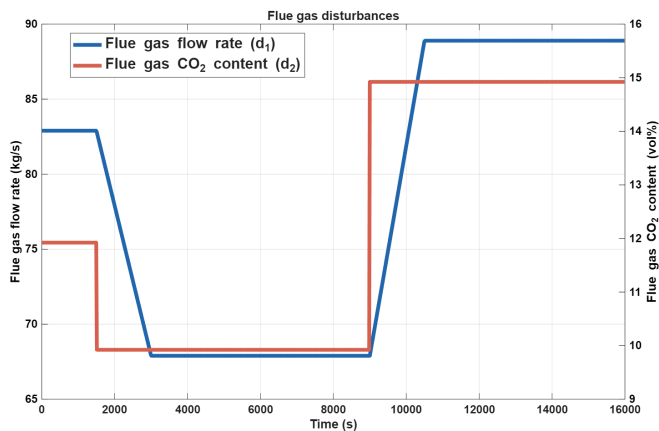


Figure 5.5: Flue gas disturbance in Case 3.

Figure 5.6 illustrates the system responses under simultaneous disturbances. Consistent with the patterns observed in Case 2, using MPC exhibits smaller deviations and faster recovery for both CVs. For the MVs, using MPC produces earlier and less aggressive adjustments than PI. Compared to Case 2, larger variation ranges are observed in the CVs due to the simultaneous disturbances. The capture rate varies between approximately 50% and 100%, and the reboiler temperature between 111°C and 119°C. This results in wider adjustment ranges of the MVs to compensate for the combined effects.

Table 5.5 presents the quantitative controller performance metrics for Case 3. As in Case 2, MPC demonstrates superior disturbance rejection performance than PI. In summary, MPC achieves approximately 9–19% lower maximum deviation, 55–56% faster recovery, and 72–74% lower IAE for CO<sub>2</sub> capture rate. For reboiler temperature, the improvements are even more pronounced: 64–69% lower maximum deviation, 59–63% faster recovery time, and 87–88% lower IAE. These results demonstrate that MPC's

coordinated control strategy remains effective even under more complex simultaneous disturbances.

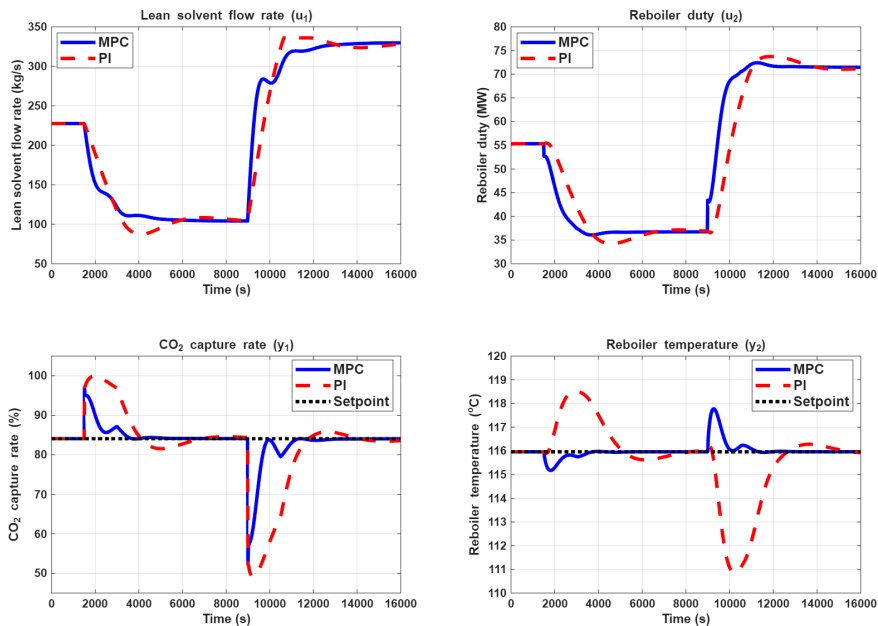


Figure 5.6: Comparison of MPC and PI controllers in Case 3.

Table 5.5: Comparison of controller performance metrics in Case 3.

Change	Controllers	Capture rate			Reboiler temperature		
		MD (%)	RTd (s)	IAE	MD (°C)	RTd (s)	IAE
Decrease	MPC	12.885	3276	8544.6	0.78613	2556	691.73
	PI	15.879	7380	33030	2.5389	6300	5790.9
Increase	MPC	31.871	2070	15687	1.8154	2196	1274.6
	PI	34.866	4590	56055	5.0999	5940	9690

Table 5.6 presents the quantitative process performance metrics for Case 3 with transient time windows of [1500s 5500s] and [9000s 14000s]. The same patterns were observed as in Case 2. PI captures 4.9% more CO<sub>2</sub> and uses 4.7% more energy, with slightly lower average specific duty during the disturbance decrease period; MPC captures 8.7% more CO<sub>2</sub> and uses 5.2% more energy, with a 3.2% lower average specific duty during the disturbance increase period. This is because the slower recovery of PI results in extended periods away from the setpoint, where PI maintains higher and lower capture

rates for an extended period during the decrease and increase period, respectively. The differences in Case 3 are somewhat larger than those in Case 2, reflecting the increased complexity of simultaneous disturbances.

Table 5.6: Comparison of process performance metrics in Case 3.

Time window	Controllers	Total CO <sub>2</sub> capture amount (tonne)	Average specific duty (MJ/kg)	Total thermal energy (GJ)
Decrease [1500, 5500]	MPC	24.09	6.484	156.21
	PI	25.32	6.474	163.93
Increase [9000, 14000]	MPC	51.92	6.569	341.08
	PI	47.76	6.789	324.26

#### 5.2.4 Summary of MPC controller performance improvements

Table 5.7 summarises the MPC improvements over PI control across all three cases. Overall, MPC consistently outperforms PI control across all cases and metrics.

For setpoint tracking of CO<sub>2</sub> capture rates, MPC achieves an approximately 3–19% reduction in overshoot, a 61–62% reduction in settling time, and a 66–67% reduction in IAE for CO<sub>2</sub> capture rate. For reboiler temperature, MPC achieves an approximately 55% reduction in maximum deviation, a 64–65% reduction in recovery time, and an 82–83% reduction in IAE.

For FG disturbance rejection, MPC achieves an approximately 9–66% reduction in maximum deviation, a 47–56% reduction in recovery time, and a 70–74% reduction in IAE for CO<sub>2</sub> capture rate. For reboiler temperature, MPC achieves an approximately 64–83% reduction in maximum deviation, a 47–63% reduction in recovery time, and an 87–88% reduction in IAE.

Table 5.7: Summary of MPC controller performance improvement over PI.

Case	Controller performance	CO <sub>2</sub> capture rate (MPC vs PI reduction, %)	Reboiler temperature (MPC vs PI reduction, %)
Case 1 (Setpoint tracking of CO <sub>2</sub> capture rates)	RT	47%	—
	OS	3–19%	—
	ST	61–62%	—
	IAE	66–67%	82–83%
	MD	—	55%
	RTd	—	64–65%
	MD	66%	83%
Case 2	RTd	47–48%	47–51%
	IAE	70–72%	87–88%
	MD	9–19%	64–69%
Case 3	RTd	56%	59–63%
	IAE	72–74%	87–88%
Cases 2–3 (Disturbance rejection of flue gas)	MD	9–66%	64–83%
	RTd	47–56%	47–63%
	IAE	70–74%	87–88%

# 6 Potential assessment of CO<sub>2</sub> capture in Swedish CHP plants

*This chapter addresses RQ3, covering plant-level results (Section 6.1) and national-scale assessment (Section 6.2).*

## 6.1 Plant-level potential of CO<sub>2</sub> capture in the reference CHP plant

### 6.1.1 CO<sub>2</sub> capture potential

According to Table 6.1 (refer also to Table 4 in Paper VI), the lower boundary of captured CO<sub>2</sub>, which is achieved when operating CO<sub>2</sub> capture in OM2, is only 99.2 kt/yr, corresponding to a capture rate of 20.3%. It cannot cover the generated fossil CO<sub>2</sub>, which is 220.3 kt/yr, and therefore results in a positive emission of 121.1 kt/yr. In order to capture more CO<sub>2</sub>, electricity has to be sacrificed. Operating CO<sub>2</sub> capture in OM1 can lead to reaching the upper boundary of captured CO<sub>2</sub>, which is 401.0 kt/yr. Evidently, this is more than the generated fossil CO<sub>2</sub> and can thus result in a negative emission of 180.5 kt/yr. It is worth noting that the avoided CO<sub>2</sub> emission is always less than the captured CO<sub>2</sub>. This is because more fuel is consumed in order to capture more CO<sub>2</sub>, and this can lead to additional CO<sub>2</sub> emissions, which nonetheless should not be emitted when CO<sub>2</sub> capture is not included. In addition, comparing the two modes, operating CO<sub>2</sub> capture in OM1 can capture 301.8 kt/yr more CO<sub>2</sub>, but reduce the electricity generation by 61.3%.

Table 6.1: CO<sub>2</sub> capture potential and the influence on example CHP.

Parameters	Reference case <sup>#</sup>	OM1	OM2
Fuel consumption ( $F$ ) (kt/yr)	394.5	420.0	419.9
Net electricity generation ( $EI$ ) (GWh/yr)	281.6	109.0	282.0
Generated CO <sub>2</sub> ( $G_{CO_2}$ ) (kt/yr)	460.0	490.0	489.6
Captured CO <sub>2</sub> ( $C_{CO_2}$ ) (kt/yr)	/	401.0	99.2
Capture rate ( $R_{CO_2}$ ) (%)	/	81.8	20.3
Net CO <sub>2</sub> emission ( $NetE$ ) (kt/yr)	/	-180.5	121.1
Avoided CO <sub>2</sub> emission ( $A_{CO_2}$ ) (kt/yr)	/	387.5	85.8

<sup>#</sup> It refers to the CHP plant without CO<sub>2</sub> capture and compression.

### 6.1.2 CO<sub>2</sub> capture cost

The associated cost is given in Table 6.2 (refer also to Table 5 in Paper VI). It is the same CO<sub>2</sub> capture unit, although it operates in different modes. Therefore, it is the same CAPEX, with the detailed equipment costs in Appendix C (Table C.1) in Paper I. The fixed OPEX is also the same when operating CO<sub>2</sub> capture in different modes. The major difference comes from the variable OPEX, which is 95.6% higher in OM1 than in OM2. One reason for the big difference is the sacrifice of electricity. When CO<sub>2</sub> capture is operated in OM1, the electricity generation is reduced, which leads to a huge loss in the benefit from selling electricity. Such a loss is considered as OPEX of CO<sub>2</sub> capture. In addition, the cost of chemical consumption is also higher in OM1 than in OM2 since more CO<sub>2</sub> is captured in OM1 than in OM2. The estimated OPEX in OM1 is 8.7 M\$/yr higher than in OM2, which further results in a 152% higher LCC. However, due to more captured CO<sub>2</sub>, the LCCA in OM1 is 44% lower than in OM2.

Table 6.2: Costs related to CO<sub>2</sub> capture in the example CHP plant.

<b>Cost (M\$)</b>	<b>OM1</b>	<b>OM2</b>
Total direct cost (TDC)	17.0	17.0
Total indirect cost (TOC)	3.4	3.4
Bare erected cost (BEC)	20.4	20.4
Engineering and contractor (EC)	5.51	5.51
Engineering procurement and construction (EPC)	25.91	25.91
Process contingency (PC)	5.1	5.1
Project contingency (PJC)	6.2	6.2
Total plant cost (TPC)	37.2	37.2
Owner's cost (OC)	5.6	5.6
CAPEX	42.8	42.8
Fixed OPEX (M\$/yr)	1.3	1.3
Variable OPEX (M\$/yr)	9.1	0.4
Total OPEX (M\$/yr)	10.4	1.7
Life-cycle cost (LCC)	153.7	60.9
Levelised cost of CO <sub>2</sub> avoided (LCCA) (\$/tCO <sub>2</sub> )	37.2	66.5

The breakdown of LCCA, including CAPEX and OPEX, is shown in Figure 6.1 (refer also to Figure 7 in Paper VI). It is clear that OPEX accounts for a significant portion of OM1 LCCA (around 72%), as a large amount of electricity needs to be sacrificed. CAPEX accounts for a substantial portion of OM2 LCCA (around 70%), as a small amount of CO<sub>2</sub> is captured.

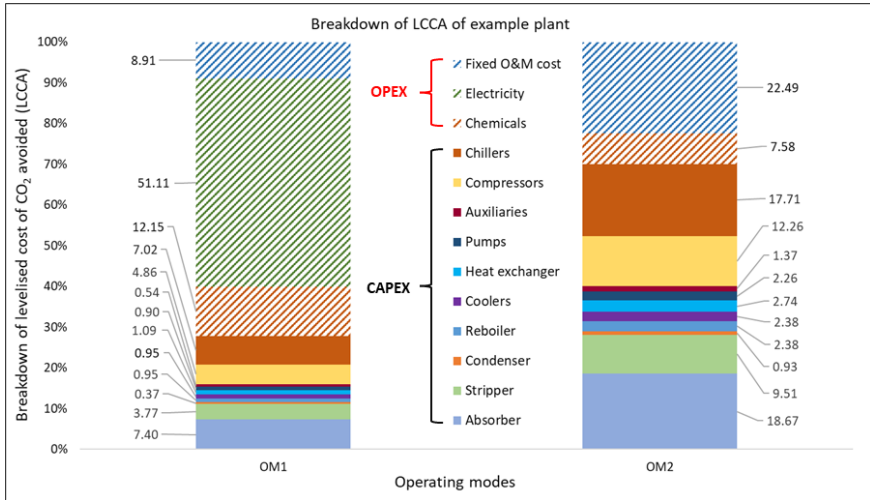


Figure 6.1: Breakdown of LCCA of example plant.

## 6.2 Nationwide potential of CO<sub>2</sub> capture in all Swedish CHP plants

The potential of CO<sub>2</sub> capture and the associated capture cost are analysed for all CHP plants in Sweden. Through aggregation of these results, the nationwide CO<sub>2</sub> capture potential and costs are assessed.

### 6.2.1 Model validation

The MEA-CA CO<sub>2</sub> capture model has been already validated during the development of first principles-based models, Dw/oC and DwC, in Section 3.2.1.1. More details can also be found in Appendix B.

To validate the w-CHP plant model, simulated results are compared with measured data under different heat demands, and the key parameters, including electricity generation and heat recovered from extracted steam, bypass steam, and FG, are selected for model validation. In general, good agreements can be observed. The MAPEs are 3.1%, 2.9%, 4.0%, and 6.2% for those selected parameters. Detailed validation results can be found in Appendix C.

The validations of the ML models show that the MAPEs are 1.3%, 8.7%, and 0.9% for the prediction of the amount of generated CO<sub>2</sub>, the net electricity generation, and the amount of captured CO<sub>2</sub>, respectively, for OM1, and 0.8% and 0.9% for the prediction of the amount of generated CO<sub>2</sub> and the amount of captured CO<sub>2</sub>, respectively, for OM2. For the prediction of

hourly heat demands, the MAPE is 5.1%. The detailed validation results can be found in Appendix D.

### 6.2.2 CO<sub>2</sub> capture potential

The nationwide potential of CO<sub>2</sub> capture is summarised in Table 6.3 (refer also to Table 6 in Paper VI). According to the Official Report of the Government of Sweden, to achieve the Swedish climate goal, at least 10.7 MtCO<sub>2</sub>/yr of negative emission is needed by 2045, in which the contribution of BECCS is expected to be 3–10 MtCO<sub>2</sub>/yr (Statens offentliga utredningar, 2020). If CO<sub>2</sub> capture is integrated in all CHP plants and operated in OM1, a negative emission of 8.7 MtCO<sub>2</sub>/yr could be achieved, which can go far towards addressing the proposed target of BECCS. However, when CO<sub>2</sub> capture is operated in OM2, it results in a positive emission of 4.3 Mt/yr. This suggests that other supplementary technologies would be needed to meet the Swedish climate goal. Nevertheless, it can still reduce emissions by 6.3 Mt/yr.

Table 6.3: Nationwide potential of CO<sub>2</sub> capture in all CHP plants in Sweden.

<b>Aggregated results</b>	<b>OM1</b>	<b>OM2</b>
Net CO <sub>2</sub> emission ( <i>NetE</i> ) (Mt/yr)	-8.7	4.3
Avoided CO <sub>2</sub> emission ( <i>AcO<sub>2</sub></i> ) (Mt/yr)	19.4	6.3
Captured CO <sub>2</sub> ( <i>Cco<sub>2</sub></i> ) (Mt/yr)	20.4	6.9
Net electricity generation ( <i>El</i> ) (TWh/yr)	8.3	16.1
Capture rate ( <i>Rco<sub>2</sub></i> ) (%)	79.1	27.5

It has been assumed that fuel with the same biogenic fraction is used in all CHP plants. It is clear that the biogenic fraction can significantly influence net CO<sub>2</sub> emissions and further impact policymaking. To understand such an influence, a sensitivity analysis is conducted, and the result is illustrated in Figure 6.2 (refer also to Figure 8 in Paper VI). It is natural that with the decrease of biogenic fraction, negative emission could change to positive emission. To reach the BECCS target of 3 MtCO<sub>2</sub>/yr, the minimum biogenic fraction should be 32.8% and 84.3% when CHP plants are operated in OM1 and OM2, respectively, while to reach the BECCS target of 10 MtCO<sub>2</sub>/yr, the minimum biogenic fraction should be 59.9% when CHP plants are operated in OM1. However, even when the biogenic fraction is 100%, operating CO<sub>2</sub> capture in OM2 can only achieve a negative emission of 7 MtCO<sub>2</sub>/yr.

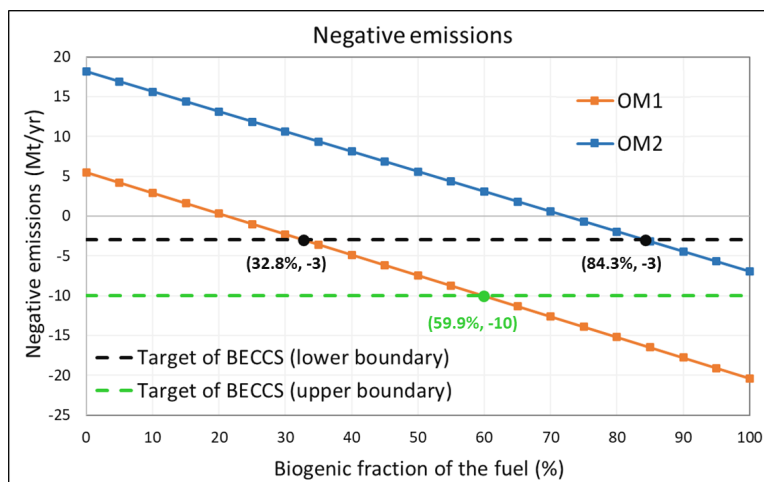


Figure 6.2: The influence of biogenic fraction of the waste on net CO<sub>2</sub> emission.

However, it is important to note that operating CO<sub>2</sub> capture in OM1 can significantly reduce electricity, which is 7.8 TWh/yr, compared to the reference case without CO<sub>2</sub> capture (16.1 TWh/yr). To compensate for the decreased electricity, more electricity needs to be generated from other sources. Based on the average carbon intensity of Sweden in 2022, which is 45 gCO<sub>2</sub>e/kWh, it is estimated that such extra electricity generation can lead to a positive emission of 0.35 Mt/yr (Our World in Data, 2023). This is negligible compared to the negative emission in OM1, which is 8.7 Mt/yr.

### 6.2.3 CO<sub>2</sub> capture cost

The associated cost for integrating CO<sub>2</sub> capture in CHP plants is given in Table 6.4 (refer also to Table 7 in Paper VI). Overall, it is estimated that the national average LCCA is about 36.9 \$/tCO<sub>2</sub> and 52.0 \$/tCO<sub>2</sub> when CO<sub>2</sub> capture is operated in OM1 and OM2, respectively. Compared to other NETs, integrating CO<sub>2</sub> capture in CHP plants may not compete with the enhanced weathering (5–10 \$/tCO<sub>2</sub>), but is clearly more cost-effective than the direct air capture (100–600 \$/tCO<sub>2</sub>) (Haszeldine et al., 2018). Moreover, compared to OM2, operating CO<sub>2</sub> capture in OM1 is more competitive. The cost also provides insights to policymakers. For example, based on the average price of the European Union Emissions Trading System (EU ETS) in 2023, which is 92.50 \$/tCO<sub>2</sub>, it implies that if the negative emission from BECCS can be traded in EU ETS, subsidies may not be necessary (Statista, 2024).

Table 6.4: Costs related to CO<sub>2</sub> capture in all CHP plants in Sweden.

Aggregated results	OM1	OM2
Levelised cost of CO <sub>2</sub> avoided (LCCA) (\$/tCO <sub>2</sub> )	36.9	52.0
Total life cycle cost (LCC) (M\$)	7657.8	3502.1
Total CAPEX (M\$)	2407.5	2407.5
Total OPEX (M\$/yr)	491.8	102.5
Fixed OPEX	72.2	72.2
Electricity cost	330.8	0
Chemical cost	88.8	30.3

Unlike LCCA, the total LCC in OM1 is double the LCC in OM2, which mainly results from the OPEX due to the reduction of electricity generation. The influence of the capacity of CHP plants on the LCCA and LCC is also studied, as shown in Figure 6.3 (refer also to Figure 9 in Paper VI). Due to economies of scale, it is clear that the larger capacity results in higher LCC but lower LCCA.

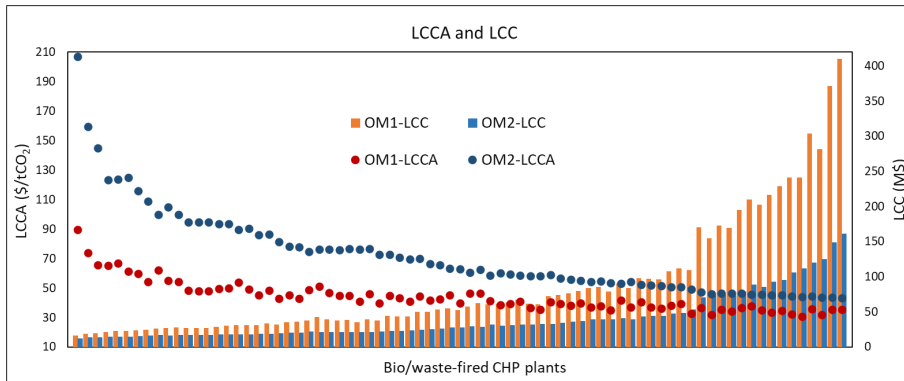


Figure 6.3: LCCA and LCC from each CHP plant.

The breakdown of the national average LCCA is shown in Figure 6.4 (refer also to Figure 10 in Paper VI). It is similar to the example plant in that OPEX accounts for a significant portion in OM1 and CAPEX accounts for a significant portion in OM2.

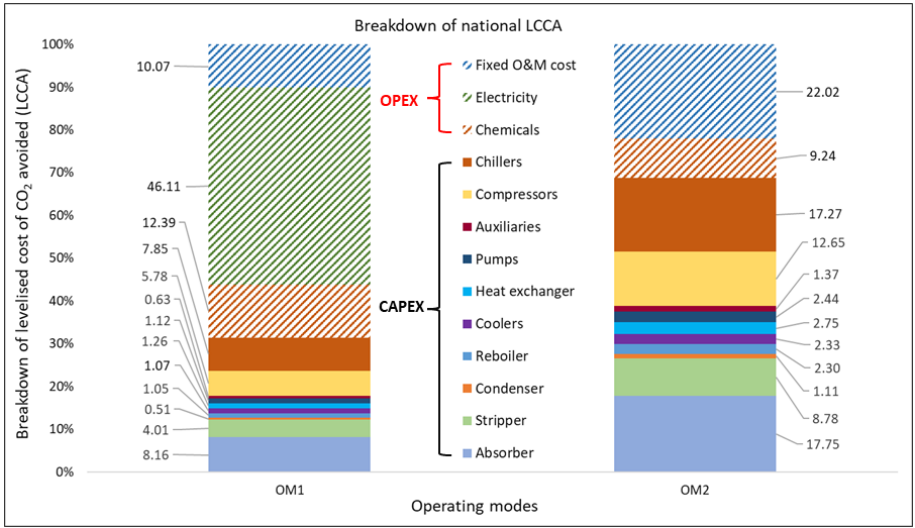


Figure 6.4: Breakdown of national LCCA.



## 7 Delimitations

*This chapter identifies the key scope boundaries and assumptions across modelling, control, and assessment.*

This dissertation is delimited to three main components – dynamic modelling, model predictive control, and potential assessment – each with specific scope boundaries that should be acknowledged when interpreting the results.

Regarding dynamic modelling, this study is delimited to validating models against simulation data and available experimental benchmarks, rather than real operational data from full-scale CO<sub>2</sub> capture plants. It is beyond the scope of this study to validate the models under real plant conditions, as pilot-scale and full-scale operational data from BECCS installations remain scarce – a common limitation in the field of dynamic modelling for CO<sub>2</sub> capture in CHP plants.

Building upon the modelling foundation, the scope of the MPC evaluation is delimited to a simulation environment. While simulation provides a controlled setting for systematic performance evaluation, it is beyond the scope of this study to account for noise measurement, actuator limitations, process disturbances, and operational constraints encountered in real plants. Furthermore, the MPC is delimited to a linear ARX model identified near the 85% nominal operating point. Nonlinear operating regions and gain-scheduled formulations are also outside the scope of this study, and prediction accuracy may therefore degrade at operating points far from the linearisation point.

Extending to the potential assessment, the scope is delimited to the capture stage of the BECCS value chain. The costs and emissions associated with CO<sub>2</sub> transport and storage are outside the scope of this study, meaning that the reported costs represent capture-only estimates, excluding CO<sub>2</sub> transport and storage. At the plant level, this work is further delimited to the assumption that no supplementary units are included in the DH system, and the capture system capacity is determined based on maximum available heat and FG flow rate without further optimisation. The absorber and stripper column sizes, obtained through a simplified scaling method, were not independently verified. At the national scale, the assessment is delimited to assuming uniform technical performance across all Swedish CHP plants based

on the example plant. This does not account for the diversity of plant configurations, technologies, fuels, and operating conditions across Sweden, particularly given the significant influence of biogenic fraction on net CO<sub>2</sub> emissions demonstrated in this study.

## 8 Conclusions

*This chapter summarises the main conclusions with respect to RQ1–RQ3.*

Integrating BECCS into biomass-fired CHP plants offers crucial potential for achieving negative emissions. However, the dynamic operation of CO<sub>2</sub> capture introduces significant challenges related to modelling, control, and system-level assessment. This dissertation addresses these challenges through dynamic modelling, model predictive control, and potential assessment. The three research questions and the main conclusions are presented below.

**RQ1** *How should the dynamic modelling approaches be selected for different applications of CO<sub>2</sub> capture in biomass-fired CHP plants?*

Understanding dynamic behaviour is essential for various applications of CO<sub>2</sub> capture, and the choice of modelling approach should be guided by specific application requirements. Through systematic comparison of first principles-based approaches, clear differences were identified in both dynamic and accumulated results, with differences in captured CO<sub>2</sub> of up to 22% (based on direct comparison between DwC and Dw/oC). The key conclusion is that Dw/oC is recommended for understanding system dynamics and safety boundary analysis, DwC is recommended for control system design and hourly dynamic optimisation, and IST is recommended for estimating long-term CO<sub>2</sub> capture potential. Regarding ML-based approaches, all models achieve satisfactory accuracy, with most MAPEs below 5%, confirming their feasibility as computationally efficient alternatives to first principles models. However, no single ML model consistently outperforms the others across all applications, confirming that model selection must be tailored to the specific application and target output variables. Where multiple approaches are applicable, the selection should be guided by the trade-off between model fidelity and computational cost, with simpler models being appropriate when accuracy differences are marginal.

**RQ2** *How does model predictive control perform for CO<sub>2</sub> capture under the dynamic operating conditions of biomass-fired CHP plants?*

With reliable dynamic models established, MPC was developed and evaluated for managing the operational fluctuations characteristic of biomass-fired CHP plants. MPC consistently demonstrated superior controller performance over conventional PI control, achieving a 3–66% reduction in overshoot and maximum deviation, a 47–62% reduction in settling and recovery time, and a 66–74% reduction in integrated absolute errors for CO<sub>2</sub> capture rate. Beyond controller performance metrics, MPC also delivers long-term operational benefits, including extended equipment lifetime and reduced solvent degradation through smoother control actions. Regarding process performance, differences in cumulative CO<sub>2</sub> capture amount between MPC and PI range from 4.4% to 8.7%, and controller selection should therefore consider not only capture amount but also energy efficiency and the economic context. These results demonstrate that MPC provides a robust control solution for coordinating the dynamic operation of CO<sub>2</sub> capture under realistic CHP conditions.

**RQ3** *What are the potentials for negative emissions and associated costs when implementing BECCS in biomass-fired CHP plants, from plant level to national scale?*

With robust models and control strategies established, the negative emission potential was assessed from plant level to national scale under two operating modes reflecting Sweden's prioritised heat supply. At the plant level, the theoretical CO<sub>2</sub> capture potential was found to be in the range of 99–401 kt/yr, corresponding to an overall capture ratio of 20–82%. The negative emission achieved under OM1 was 181 kt/yr, while no negative emission was achieved under OM2 due to the fossil fraction in the feedstock. Scaling to the national level, operating under OM1 with an average biogenic fraction of 55% can achieve 8.7 MtCO<sub>2</sub>/yr negative emissions, adequately covering Sweden's expected BECCS target. The levelised cost of CO<sub>2</sub> avoided was estimated at 36.9 \$/tCO<sub>2</sub> and 52.0 \$/tCO<sub>2</sub> for OM1 and OM2, respectively. The biogenic fraction of fuel was found to have a critical influence on negative emission potential, with minimum fractions of 32.8% and 84.3% required under OM1 and OM2, respectively, to achieve Sweden's 3 MtCO<sub>2</sub>/yr interim target. These findings demonstrate that Sweden's BECCS climate targets are technically and economically achievable, and that the choice of operating mode fundamentally determines the boundary of negative emission potential, providing policymakers with quantified scenarios for strategic decision-making.

## 9 Future work

*This chapter outlines future research directions identified from the findings and limitations of this dissertation.*

The work presented in this dissertation addresses dynamic modelling, model predictive control, and potential assessment for CO<sub>2</sub> capture in biomass-fired CHP plants. While the results provide valuable insights, several limitations and open questions point to promising directions for future research. Regarding dynamic modelling, the first principles models developed in this work are based on a specific MEA-CA process. Future work could extend these models to other capture technologies, such as hot potassium carbonate, which is being adopted in large-scale BECCS projects such as Stockholm Exergi's Värtan plant. Furthermore, the ML models were trained based on simulation data. Validating and retraining these models with operational data from real CHP plants would enhance their reliability and practical applicability. The integration of physics-informed ML approaches, which combine the interpretability of first principles models with the computational efficiency of data-driven methods, also represents a promising research direction.

On the control side, the MPC strategy developed in Paper IV focuses on the CO<sub>2</sub> capture unit in isolation. In practice, the capture process is tightly coupled with the CHP plant through steam extraction, heat supply obligations, and electricity generation. Future work should therefore extend the MPC or economic MPC (EMPC) framework from the CO<sub>2</sub> capture unit alone to the integrated CHP capture system, jointly optimising heat and power generation, steam extraction, and capture rate. Such an integrated control approach would better reflect the real operational constraints and enable more effective coordination between the CHP plant and the CO<sub>2</sub> capture process under dynamic conditions.

The potential assessment in Papers V and VI was conducted based on technical and economic analysis under current market conditions. However, the economic viability of BECCS is strongly influenced by evolving policy instruments. Future research should integrate carbon credit trading mechanisms into operational optimisation, considering the monetisation of

negative emissions through carbon markets and dynamic carbon pricing. This would allow operators to maximise both the environmental and economic benefits of BECCS by adapting capture strategies to real-time market signals, thereby providing a more comprehensive decision-support framework for BECCS investment and operation.

Finally, this dissertation focuses on the Swedish context, where biomass-fired CHP plants play a significant role in DH networks. Extending the assessment framework to other Nordic and European countries with similar CHP infrastructure would provide broader insights into the scalability and transferability of the proposed approaches for BECCS deployment.

# Appendix

## A: Validation of the steady-state model in IST

The validation of the steady-state model is based on the Tarong pilot plant in Queensland, Australia, in which a PCC plant was constructed with a designed CO<sub>2</sub> capture rate of 85% (around 100 kg/h) using an MEA solution based on the coal-fired power station (900 kg/h typical FG flow rate). Different trials have been conducted and their detailed conditions can be found in Li et al. (2015), which are helpful for model development and validation.

Table A1 shows the test conditions, including both the input and the output parameters. The maximum deviations are 4.1%, 2.6%, 2.9%, 0.3%, and 0.4% for the CO<sub>2</sub> absorption rate, reboiler temperature, reboiler duty, CO<sub>2</sub> product purity, and CO<sub>2</sub> capture rate, respectively.

Table A1: Comparison between pilot plant trials and steady-state model results (Li et al., 2015).

Test conditions	Test 1		Test 2		Test 3		Test 4		Test 5	
<b>Input parameters</b>										
Lean temp, °C	31.7		33.9		31.4		31.3		35.5	
Lean flow rate, L/min	31.7		26.9		32.0		27.0		31.3	
Lean MEA conc., wt. %	25.1		31.6		24		27.9		25.5	
Lean CO <sub>2</sub> loading, mol/mol	0.279		0.314		0.294		0.284		0.280	
Inlet flue gas flow rate, kg/h	489.6		482.8		491.1		488.6		489.4	
Stripper top pressure, kPa	181.9		189.2		180.4		177.5		189.9	
<b>Results comparison</b>										
	Exp.	Sim.	Exp.	Sim.	Exp.	Sim.	Exp.	Sim.	Exp.	Sim.
CO <sub>2</sub> absorption rate, kg/h	73.5	71.32	74.2	72.99	74.2	71.1	72.3	70.7	74.4	73.64

Reboiler temperature, °C	116.9	118.5	117.2	120.3	116.4	117.9	117.0	118.1	117.6	119.7
Specific reboiler duty, MJ/kg CO <sub>2</sub>	4.48	4.61	4.33	4.37	4.45	4.41	4.35	4.41	4.50	4.43
CO <sub>2</sub> product purity, vol%	97.7	97.74	97.6	97.27	97.7	97.76	97.8	97.96	97.7	97.73
CO <sub>2</sub> capture rate, %	82.89	82.57	76.20	75.95	82.28	82.35	82.63	82.79	83.95	83.99

## B: Validation of the dynamic model in Dw/oC and DwC

The dynamic model is first used to do steady-state simulations without changing the input parameters. The results are compared with the steady-state results from Harun (2012). As shown in Table B1, the results obtained using the dynamic model are in good agreement with the steady-state results.

Table B1: Comparison of the results of the dynamic model and the steady-state model at base case conditions.

	Lean stream	MEA	Stack gas stream		Rich MEA stream		CO <sub>2</sub> outlet from stripper	
	Sim. <sup>1</sup>	Ref. <sup>2</sup>	Sim.	Ref.	Sim.	Ref.	Sim.	Ref.
Temperature (K)	314	314	319.8	333.25	332.4	327.09	350.90	352.61
Total molar flow rate (mol/sec)	31.95	30.36	3.58	3.86	32.38	30.51	0.9050	0.914
Mole fraction								
CO <sub>2</sub>	0.0305	0.0307	0.0083	0.0055	0.0509	0.0529	0.7251	0.7292
H <sub>2</sub> O	0.8646	0.8605	0.0944	0.1652	0.8456	0.8377	0.2736	0.2622
MEA	0.1049	0.1098	0	0.0001	0.1053	0.1092	0	0.0001
N <sub>2</sub>	0	0	0.8972	0.8292	0	0.0002	0.0013	0.0085

<sup>1</sup> Sim. = dynamic model results. <sup>2</sup> Ref. = steady-state results from Harun (2012).

In addition to the steady-state validation, the dynamic model is also validated with the transient data (Harun, 2012). With the input of change of FG flow rate shown in Figure B1, Figure B2 shows the validation, including the temperature profile in the absorber, CO<sub>2</sub> removal rate in the absorber and energy penalty. For the absorber (Figure B2 (a)), the maximum temperature deviation is 5.9 K and the average deviation is 2.4 K. For the stripper (Figure B2 (b-c)), the CO<sub>2</sub> removal rate decreases with the increase in FG flow rate

because the solvent is not increased to absorb more CO<sub>2</sub>. The maximum deviation on CO<sub>2</sub> removal rate is 1.6%. The energy penalty from Harun et al. (2012) is calculated based on the amount of removed CO<sub>2</sub> in the absorber. The maximum deviation of the energy penalty is 1.6%.

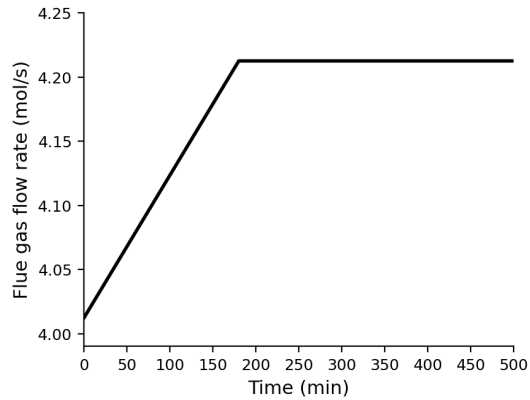
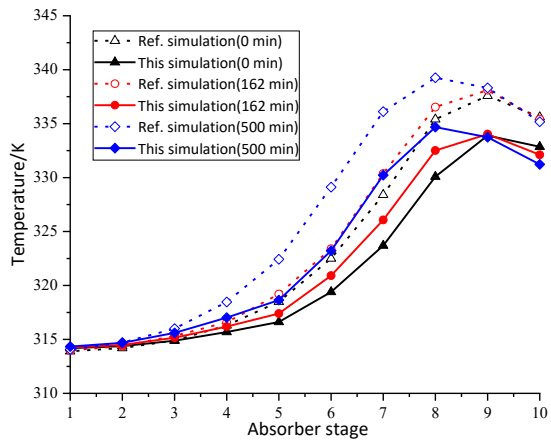


Figure B1: Changes in FG flow rate (Harun et al., 2012).



(a) Temperature profile in the absorber

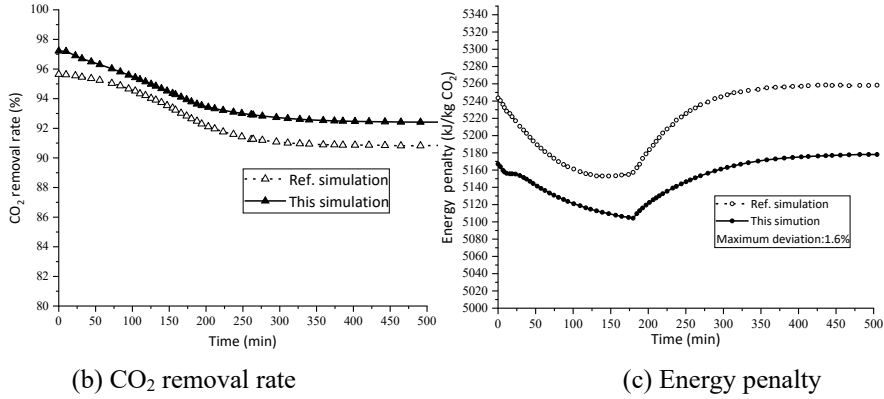
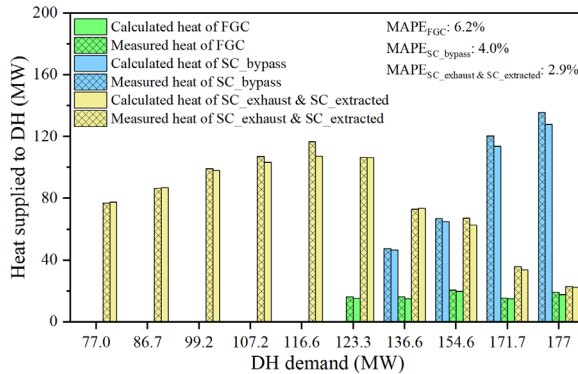


Figure B2: Validation of the Dw/oC.

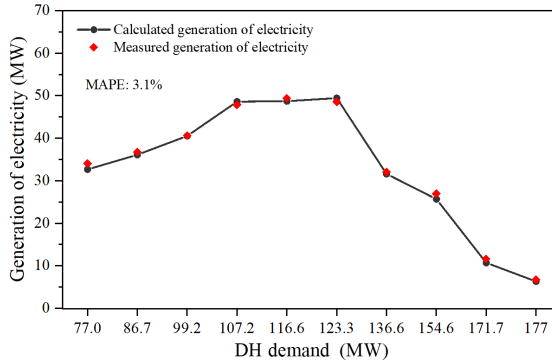
## C: Validation of the waste-fired CHP plant model

A model is developed in Aspen Plus to simulate the w-CHP plant (Li, Wang, et al., 2019). The model consists of three modules: the boiler module, which simulates the combustion and FG cleaning processes; the steam turbine cycle module, which simulates the electricity generation, steam extraction, and steam condensation; and the district heating (DH) supply module, which simulates heat generation for the DH network.

To validate the w-CHP plant model, simulated results are compared with measured data under different heat demands, as shown in Figure C2. The selected parameters include electricity generation, and the heat recovered from the extracted steam condenser (SC\_exhaust & SC\_extracted), the bypass steam condenser (SC\_bypass), and the flue gas condenser (FGC).



(a) Heat recovered from extracted steam, bypass steam, and flue gas



(b) Electricity generation

Figure C2: Validation of the waste-fired CHP plant model.

## D: Validation of machine learning models

### D1: Heat demand model

An ML model based on the back-propagation neural network (BPNN) is established to predict the heat demand (ML\_demand). The ambient temperature and wind speed are input features. The real data of the example plant are used, in which the heat demand equals the known heat supply, and the weather data are taken from SMHI. Data covering one week from each of the four seasons are used. 75% of the data is used for model training, and the other 25% for model validation. Figure D1 illustrates the validation result of the ML\_demand model, which has an MAPE of 5.1%.

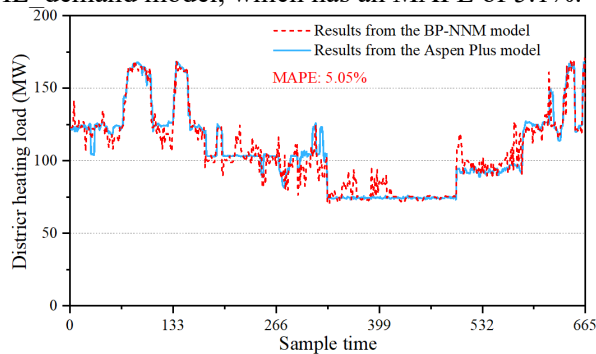


Figure D1: Validation of the ML\_demand model.

## D2: CHP model

The BPNN is also used to develop a model to simulate the operation of the CHP plant (ML\_CHP). The heat demand is an input feature, and the amount of captured CO<sub>2</sub>, the net electricity generation, and the amount of generated CO<sub>2</sub> are taken as the output. To train and validate the ML model, simulated results of the developed first principles models are used, including the data covering one week from each of the four seasons.

Two ML\_CHP models are developed corresponding to OM1 and OM2, and the validation is illustrated in Figures D2 and D3. The MAPEs are 1.3%, 0.9% and 8.7% for the amount of generated CO<sub>2</sub>, the amount of captured CO<sub>2</sub>, and the net electricity generation, respectively, for OM1, and 0.8% and 0.9% for the amount of generated CO<sub>2</sub> and the amount of captured CO<sub>2</sub>, respectively, for OM2.

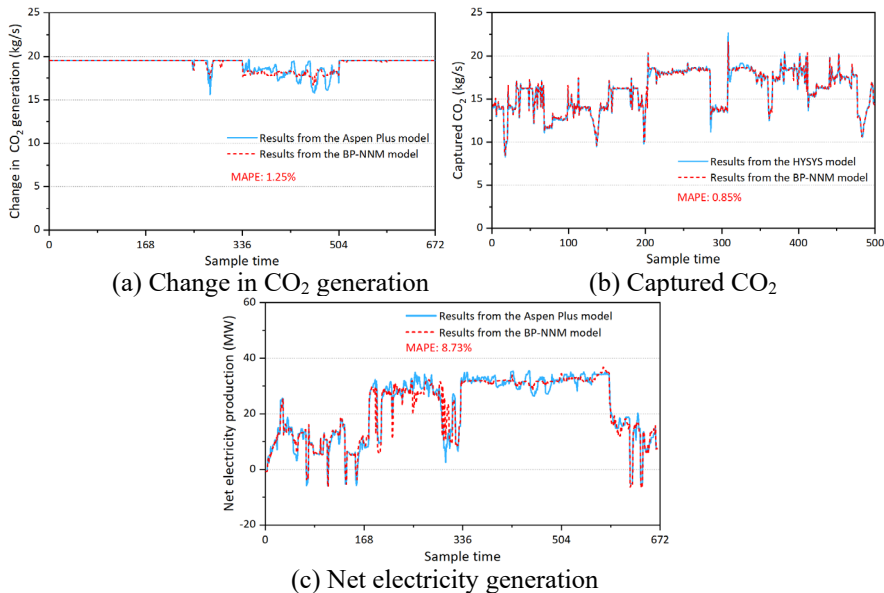


Figure D2: Validation of the ML\_CHP model in OM1.

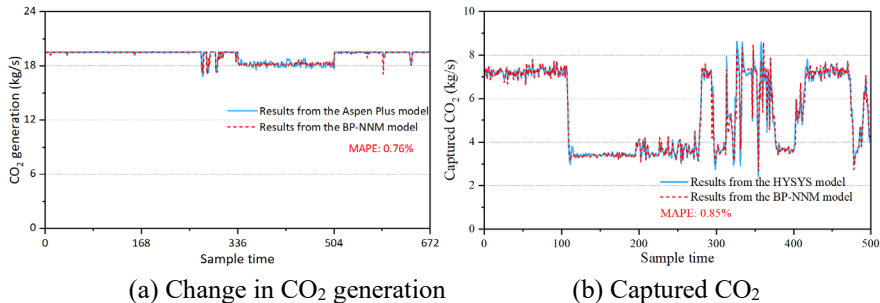


Figure D3: Validation of the ML\_CHP model in OM2.

## References

- Abdul Manaf, N., Cousins, A., Feron, P., & Abbas, A. (2016). Dynamic modelling, identification and preliminary control analysis of an amine-based post-combustion CO<sub>2</sub> capture pilot plant. *Journal of Cleaner Production*, *113*, 635–653. <https://doi.org/10.1016/j.jclepro.2015.11.054>
- Ahlmén, M., & Hellsberg, J. (2020). *Combined heat and power plants integrated with carbon capture – Process and system level potential* [Master's thesis, Chalmers University of Technology]. <https://hdl.handle.net/20.500.12380/300818>
- Åkesson, J., Laird, C. D., Lavedan, G., Prölb, K., Tummescheit, H., Velut, S., & Zhu, Y. (2012). Nonlinear model predictive control of a CO<sub>2</sub> post-combustion absorption unit. *Chemical Engineering & Technology*, *35*(3), 445–454. <https://doi.org/10.1002/ceat.201100480>
- Akram, M., Ali, U., Best, T., Blakey, S., Finney, K. N., & Pourkashanian, M. (2016). Performance evaluation of PACT Pilot-plant for CO<sub>2</sub> capture from gas turbines with exhaust gas recycle. *International Journal of Greenhouse Gas Control*, *47*, 137–150. <https://doi.org/10.1016/j.ijggc.2016.01.047>
- Anca-Couce, A., Hochenauer, C., & Scharler, R. (2021). Bioenergy technologies, uses, market and future trends with Austria as a case study. *Renewable and Sustainable Energy Reviews*, *135*. <https://doi.org/10.1016/j.rser.2020.110237>
- Beiron, J., Göransson, L., Normann, F., & Johnsson, F. (2022). Flexibility provision by combined heat and power plants – An evaluation of benefits from a plant and system perspective. *Energy Conversion and Management: X*, *16*, 100318. <https://doi.org/10.1016/j.ecmx.2022.100318>
- Beiron, J., Normann, F., & Johnsson, F. (2021). A case study of the potential for CCS in Swedish combined heat and power plants. *15th International Conference on Greenhouse Gas Control Technologies*, Abu Dhabi. [https://research.chalmers.se/publication/539298/file/539298\\_Fulltext.pdf](https://research.chalmers.se/publication/539298/file/539298_Fulltext.pdf)
- Beiron, J., Normann, F., & Johnsson, F. (2022). A techno-economic assessment of CO<sub>2</sub> capture in biomass and waste-fired combined heat and power plants – A Swedish case study. *International Journal of*

- Greenhouse Gas Control*, 118.  
<https://doi.org/10.1016/j.ijggc.2022.103684>
- Bioenergy International. (2025). *Stockholm Exergi world's first large-scale BECCS to use Capsol's carbon capture tech*. <https://bioenergyinternational.com/stockholm-exergi-worlds-first-large-scale-beccs-to-use-capsols-carbon-capture-tech/>
- Bravo, J. L., J. A. Rocha, & Fair, J. R. (1985). Mass transfer in gauze packings. *Hydrocarbon Processing*, 64, 91–95. <https://pascal-francis.inist.fr/vibad/index.php?action=getRecordDetail&idt=9038962>
- Bravo, J. L., Rocha, J. A., & Fair, J. R. (1993). A comprehensive model for the performance of columns containing structured packings. *Institution of Chemical Engineers Symposium. Series 32*, 641–651.
- Bui, M., Gunawan, I., Verheyen, V., Feron, P., Meuleman, E., & Adeloju, S. (2014). Dynamic modelling and optimisation of flexible operation in post-combustion CO<sub>2</sub> capture plants—A review. *Computers & Chemical Engineering*, 61, 245–265. <https://doi.org/10.1016/j.compchemeng.2013.11.015>
- Bui, M., Tait, P., Lucquiaud, M., & Mac Dowell, N. (2018). Dynamic operation and modelling of amine-based CO<sub>2</sub> capture at pilot scale. *International Journal of Greenhouse Gas Control*, 79, 134–153. <https://doi.org/10.1016/j.ijggc.2018.08.016>
- Camacho, E. F., & Bordons, C. (2007). *Model predictive control*. Springer London. <https://doi.org/10.1007/978-0-85729-398-5>
- Carbon Brief. (2019). *Timeline: How BECCS became climate change's 'saviour' technology*. <https://www.carbonbrief.org/beccs-the-story-of-climate-changes-saviour-technology/>
- Chikukwa, A., Enaasen, N., Kvamsdal, H. M., & Hillestad, M. (2012). Dynamic modeling of post-combustion CO<sub>2</sub> capture using amines – A review. *Energy Procedia*, 23, 82–91. <https://doi.org/10.1016/j.egypro.2012.06.063>
- Christensen, P. & Dysert, L. (2005). Cost estimate classification system – as applied in engineering, procurement, and construction for the process industries. TCM Framework: 7.3 – Cost Estimating and Budgeting. AACE International Recommended Practice No. 18R-97. <https://aheinc.ca/wp-content/uploads/2018/12/AACE-Cost-Estimate-Classification-System.pdf>
- Cohen, S. M., Rochelle, G. T., & Webber, M. E. (2012). Optimizing post-combustion CO<sub>2</sub> capture in response to volatile electricity prices. *International Journal of Greenhouse Gas Control*, 8, 180–195. <https://doi.org/10.1016/j.ijggc.2012.02.011>
- Copernicus Climate Change Service. (2025). *Copernicus: 2024 is the first year to exceed 1.5°C above pre-industrial level*. Copernicus Climate Change Service (2025). <https://climate.copernicus.eu/copernicus->

2024-first-year-exceed-15degc-above-pre-industrial-level

- Cormos, A.-M., Vasile, M., & Cristea, M.-V. (2015). Flexible operation of CO<sub>2</sub> capture processes integrated with power plant using advanced control techniques. In K. V. Gernaey, J. K. Huusom, & R. Gani (Eds.), *Computer Aided Chemical Engineering* (Vol. 37, pp. 1547–1552). Elsevier. <https://doi.org/10.1016/B978-0-444-63577-8.50103-0>
- Darby, M. L., & Nikolaou, M. (2012). MPC: Current practice and challenges. *Control Engineering Practice*, 20(4), 328–342. <https://doi.org/10.1016/j.conengprac.2011.12.004>
- Devarakonda, V. S., Sun, W., Tang, X., & Tian, Y. (2025). Recent advances in reinforcement learning for chemical process control. *Processes*, 13(6). <https://doi.org/10.3390/pr13061791>
- Dong, B., Hu, C., Skvaril, J., Thorin, E., & Li, H. (2023). Selecting the approach for dynamic modelling of CO<sub>2</sub> capture in biomass/waste fired CHP plants. *International Journal of Greenhouse Gas Control*, 130. <https://doi.org/10.1016/j.ijggc.2023.104008>
- Drax Group. (2021). *What is bioenergy with carbon capture and storage (BECCS)?* <https://www.drax.com/what-we-do/bioenergy-with-carbon-capture-and-storage-beccs/>
- Enaasen, N., Zangrilli, L., Mangiaracina, A., Mejdell, T., Kvamsdal, H. M., & Hillestad, M. (2014). Validation of a dynamic model of the Brindisi pilot plant. *Energy Procedia*, 63, 1040–1054. <https://doi.org/10.1016/j.egypro.2014.11.111>
- European Academies' Science Advisory Council. (2018). *Negative emission technologies: What role in meeting Paris Agreement targets?* EA-SAC policy report 35. [https://easac.eu/fileadmin/PDF\\_s/reports\\_statements/Negative\\_Carbon/EASAC\\_Report\\_on\\_Negative\\_Emission\\_Technologies.pdf](https://easac.eu/fileadmin/PDF_s/reports_statements/Negative_Carbon/EASAC_Report_on_Negative_Emission_Technologies.pdf)
- Gaspar, J., Jørgensen, J. B., & Fosbøl, P. L. (2015). *Control of a post-combustion CO<sub>2</sub> capture plant during process start-up and load variations*. *International Federation of Automatic Control (IFAC)*, 48(8), 580–585. <https://www.sciencedirect.com/science/article/pii/S2405896315011118>
- Gerdes, K., Summers, W., & Wimer, J. (2011). *Quality guidelines for energy system studies: Cost estimation methodology for NETL assessments of power plant performance*. National Energy Technology Laboratory (NETL). <https://api.semanticscholar.org/CorpusID:134519516>
- Harun, N. (2012). *Dynamic simulation of MEA absorption process for CO<sub>2</sub> capture from power plants* [Doctoral dissertation, University of Waterloo]. <https://scispace.com/pdf/dynamic-simulation-of-mea-absorption-process-for-co2-capture-gl4c8rujvy.pdf>
- Harun, N., Nittaya, T., Douglas, P. L., Croiset, E., & Ricardez-Sandoval, L. A. (2012). Dynamic simulation of MEA absorption process for CO<sub>2</sub>

- capture from power plants. *International Journal of Greenhouse Gas Control*, 10, 295–309. <https://doi.org/10.1016/j.ijggc.2012.06.017>
- Haszeldine, R. S., Flude, S., Johnson, G., & Scott, V. (2018). Negative emissions technologies and carbon capture and storage to achieve the Paris Agreement commitments. *Philosophical Transactions of the Royal Society. A Mathematical Physical and Engineering Sciences*, 376(2119). <https://doi.org/10.1098/rsta.2016.0447>
- IEA. (2024). *Bioenergy with carbon capture and storage*. International Energy Agency (IEA). <https://www.iea.org/energy-system/carbon-capture-utilisation-and-storage/bioenergy-with-carbon-capture-and-storage>
- Ignell, V., & Johansson, E. (2021). *Local infrastructures for CCS clusters – A case study of two CHP plants in Gothenburg*. [Master's thesis, Chalmers University of Technology]. <https://odr.chalmers.se/server/api/core/bitstreams/9a0d1960-d909-4166-ba49-fdde870896e2/content>
- Integrated Environmental Control Model Team (2019). *IECM Technical Documentation: Amine-based post-combustion CO<sub>2</sub> capture*. U.S. Department of Energy. [https://www.uwyo.edu/iecm/\\_bfiles/documentation/201901\\_iecmtd\\_amine-based-co2-cap.pdf](https://www.uwyo.edu/iecm/_bfiles/documentation/201901_iecmtd_amine-based-co2-cap.pdf)
- IPCC. Masson-Delmotte, V., P. Zhai, H.-O. Pörtner, D. Roberts, J. Skea, P.R. Shukla, et al. (2018). Summary for policymakers. In V. Masson-Delmotte, P. Zhai, H.-O. Pörtner, D. Roberts, J. Skea, P.R. Shukla, A. Pirani, W. Moufouma-Okia, C. Péan, R. Pidcock, S. Connors, J.B.R. Matthews, Y. Chen, X. Zhou, M.I. Gomis, E. Lonnoy, T. Maycock, M. Tignor, & T. Waterfield (Eds.), *Global Warming of 1.5°C. An IPCC Special Report on the impacts of global warming of 1.5°C above pre-industrial levels and related global greenhouse gas emission pathways, in the context of strengthening the global response to the threat of climate change, sustainable development, and efforts to eradicate poverty* (pp. 3–24). Cambridge University Press. <https://doi.org/10.1017/9781009157940.001>
- Johansson, F., & Kjärstad, J. (2019). *Avskiljning, transport och lagring av koldioxid i Sverige – Behov av forskning och demonstration* [Capture, transport, and storage of carbon dioxide in Sweden – Need for research, and demonstration]. Chalmers University of Technology.
- Joint Task Force on Biomass and CCS. (2018). *Biomass with CO<sub>2</sub> Capture and Storage (Bio-CCS). The way forward for Europe*. European Technology Platform for Zero Emission Fossil Fuel Power Plants: European Biofuels Technology Platform (EBTP) and Zero Emissions Platform (ZEP). <https://bellona.org/publication/26034>
- Lee, H., & Romero, J. (2023). *Climate change 2023: Synthesis report. Contribution of Working Groups I, II and III to the Sixth Assessment*

*Report of the Intergovernmental Panel on Climate Change.*

- Lennart, L. (1999). *System identification: Theory for the user*. Prentice Hall PTR.
- Li, D., Song, Z., Quan, C., Xu, X., & Liu, C. (2021). Recent advances in image fusion technology in agriculture. *Computers and Electronics in Agriculture*, *191*. <https://doi.org/10.1016/j.compag.2021.106491>
- Li, F., Zhang, J., Oko, E., & Wang, M. (2015). Modelling of a post-combustion CO<sub>2</sub> capture process using neural networks. *Fuel*, *151*, 156–163. <https://doi.org/10.1016/j.fuel.2015.02.038>
- Li, F., Zhang, J., Oko, E. & Wang, M. (2016). Modelling of a post-combustion CO<sub>2</sub> capture process using extreme learning machine. *21st International Conference on Methods and Models in Automation and Robotics (MMAR)*. 29 August–1 September. Miedzydroje, Poland.
- Li, F., Zhang, J., Shang, C., Huang, D., Oko, E., & Wang, M. (2018). Modelling of a post-combustion CO<sub>2</sub> capture process using deep belief network. *Applied Thermal Engineering*, *130*, 997–1003. <https://doi.org/10.1016/j.applthermaleng.2017.11.078>
- Li, H., Dong, B., Yu, Z., Yan, J., & Zhu, K. (2019). Thermo-physical properties of CO<sub>2</sub> mixtures and their impacts on CO<sub>2</sub> capture, transport and storage: Progress since 2011. *Applied Energy*, *255*. <https://doi.org/10.1016/j.apenergy.2019.113789>
- Li, H., Wang, B., Yan, J., Salman, C. A., Thorin, E., & Schwede, S. (2019). Performance of flue gas quench and its influence on biomass fueled CHP. *Energy*, *180*, 934–945. <https://doi.org/10.1016/j.energy.2019.05.078>
- Li, K., Cousins, A., Yu, H., Feron, P., Tade, M., Luo, W., & Chen, J. (2015). Systematic study of aqueous monoethanolamine-based CO<sub>2</sub> capture process: model development and process improvement. *Energy Science & Engineering*, *4*(1), 23–39. <https://doi.org/10.1002/ese3.101>
- Li, Q., Zhang, W., Qin, Y., & An, A. (2021). Model predictive control for the process of MEA absorption of CO<sub>2</sub> based on the data identification model. *Processes*, *9*(1). <https://doi.org/10.3390/pr9010183>
- Li, X., Li, T., Liu, L., Wang, Z., Li, X., Huang, J., Huang, J., Guo, P., & Xiong, W. (2023). Operation optimization for integrated energy system based on hybrid CSP-CHP considering power-to-gas technology and carbon capture system. *Journal of Cleaner Production*, *391*. <https://doi.org/10.1016/j.jclepro.2023.136119>
- Liang, X., Li, Y., Wu, X., Shen, J., & Lee, K. Y. (2018). Nonlinearity analysis and multi-model modeling of an MEA-based post-combustion CO<sub>2</sub> capture process for advanced control design. *Applied Sciences*, *8*(7). <https://doi.org/10.3390/app8071053>
- Lin, Y. J., Pan, T. H., Wong, D. S.-H., Jang, S.-S., Chi, Y. W., & Yeh, C. H. (2011). Plantwide control of CO<sub>2</sub> capture by absorption and stripping using monoethanolamine solution. *Industrial & Engineering*

- Chemistry Research*, 50, 1338–1345.  
<https://doi.org/10.1021/ie100771x>
- Linnenberg, S., Darde, V., Oexmann, J., Kather, A., van Well, W. J. M., & Thomsen, K. (2012). Evaluating the impact of an ammonia-based post-combustion CO<sub>2</sub> capture process on a steam power plant with different cooling water temperatures. *International Journal of Greenhouse Gas Control*, 10, 1–14.  
<https://doi.org/10.1016/j.ijggc.2012.05.003>
- Magnanelli, E., Mosby, J., & Becidan, M. (2021). Scenarios for carbon capture integration in a waste-to-energy plant. *Energy*, 227.  
<https://doi.org/10.1016/j.energy.2021.120407>
- Martinez Castilla, G., Biermann, M., Montañés, R. M., Normann, F., & Johnsson, F. (2019). Integrating carbon capture into an industrial combined-heat-and-power plant: Performance with hourly and seasonal load changes. *International Journal of Greenhouse Gas Control*, 82, 192–203. <https://doi.org/10.1016/j.ijggc.2019.01.015>
- Mehleri, E. D., Dowell, N. M., & Thornhill, N. F. (2015). Model predictive control of post-combustion CO<sub>2</sub> capture process integrated with a power plant. In K. V. Gernaey, J. K. Huusom, & R. Gani (Eds.), *12th International Symposium on Process Systems Engineering and 25th European Symposium on Computer Aided Process Engineering* (pp. 161–166). Elsevier. <https://doi.org/10.1016/b978-0-444-63578-5.50022-0>
- Mejdell, T., Kvamsdal, H. M., Hauger, S. O., Gjertsen, F., Tobiesen, F. A., & Hillestad, M. (2022). Demonstration of non-linear model predictive control for optimal flexible operation of a CO<sub>2</sub> capture plant. *International Journal of Greenhouse Gas Control*, 117.  
<https://doi.org/10.1016/j.ijggc.2022.103645>
- Montañés, R., Flø, N., & Nord, L. (2017). Dynamic process model validation and control of the amine plant at CO<sub>2</sub> Technology Centre Mongstad. *Energies*, 10(10). <https://doi.org/10.3390/en10101527>
- Nittaya, T., Douglas, P. L., Croiset, E., & Ricardez-Sandoval, L. A. (2014). Dynamic modelling and control of MEA absorption processes for CO<sub>2</sub> capture from power plants. *Fuel*, 116, 672–691.  
<https://doi.org/10.1016/j.fuel.2013.08.031>
- Notz, R., Mangalapally, H. P., & Hasse, H. (2012). Post combustion CO<sub>2</sub> capture by reactive absorption: Pilot plant description and results of systematic studies with MEA. *International Journal of Greenhouse Gas Control*, 6, 84–112. <https://doi.org/10.1016/j.ijggc.2011.11.004>
- NRDC. (2021). *Paris Climate Agreement: Everything You Need to Know*. Natural Resources Defence Council (NRDC). <https://www.nrdc.org/stories/paris-climate-agreement-everything-you-need-know#sec-what-is>
- Öberg, S. (2017). *Design of partial CO<sub>2</sub> capture from waste fired CHP*

- plants* [Master's thesis, Chalmers University of Technology]. <https://hdl.handle.net/20.500.12380/250871>
- Øi, L. E. (2007). *Aspen HYSYS simulation of CO<sub>2</sub> removal by amine absorption from a gas-based power plant*. SIMS2007 Conference, Gothenburg. <https://ep.liu.se/ecp/027/008/ecp072708.pdf>
- Olesen, D. H., Huusom, J. K., & Jørgensen, J. B. (2013). *A tuning procedure for ARX-based MPC of multivariate processes*. 2013 American Control Conference (ACC) (pp.1721–1726). <https://doi.org/10.1109/ACC.2013.6580084>
- Otitoju, O., Oko, E., & Wang, M. (2020). A new method for scale-up of solvent-based post-combustion carbon capture process with packed columns. *International Journal of Greenhouse Gas Control*, 93. <https://doi.org/10.1016/j.ijggc.2019.102900>
- Our World in Data. (2023). *Carbon intensity of electricity generation, 2000 to 2022. Carbon intensity is measured in grams of carbon dioxide-equivalents emitted per kilowatt-hour of electricity generated*. <https://ourworldindata.org/grapher/carbon-intensity-electricity?tab=chart&country=~SWE>
- Pan, S., Shi, X., Dong, B., Skvaril, J., Zhang, H., Liang, Y., & Li, H. (2024). Multivariate time series prediction for CO<sub>2</sub> concentration and flowrate of flue gas from biomass-fired power plants. *Fuel*, 359, 130344. <https://doi.org/10.1016/j.fuel.2023.130344>
- Perez, A., & Yang, Y. (2022). Offset-free ARX-based adaptive model predictive control applied to a nonlinear process. *ISA Transactions*, 123, 251–262. <https://doi.org/10.1016/j.isatra.2021.05.030>
- Pröll, T., & Zerobin, F. (2019). Biomass-based negative emission technology options with combined heat and power generation. *Mitigation and Adaptation Strategies for Global Change*, 24(7), 1307–1324. <https://doi.org/10.1007/s11027-019-9841-4>
- Qin, S. J., & Badgwell, T. A. (2003). A survey of industrial model predictive control technology. *Control Engineering Practice*, 11(7), 733–764. [https://doi.org/10.1016/S0967-0661\(02\)00186-7](https://doi.org/10.1016/S0967-0661(02)00186-7)
- Rau, G. H., & Greene, C. H. (2015). Emissions reduction is not enough. *Science*, 349(6255), 1459–1459. <https://doi.org/doi:10.1126/science.349.6255.1459-b>
- Rohini, G., Ragumadhavan, R., Bhavani, G., V.Venkatesan, Josephson, P. J., & Alaskar, K. (2022). Setpoint Tracking and Disturbance Rejection in Automobile using Predictive Controller. In *2022 3rd International Conference on Smart Electronics and Communication (ICOSEC)* (pp. 1–6). IEEE. <https://doi.org/10.1109/ICOSEC54921.2022.9951942>
- Sahraei, H., & Ricardez-Sandoval, L. A. (2014). Controllability and optimal scheduling of a CO<sub>2</sub> capture plant using model predictive control. *International Journal of Greenhouse Gas Control*, 30, 58–71.

- <https://doi.org/10.1016/j.ijggc.2014.08.017>
- Sha, P., Zheng, C., Wu, X., & Shen, J. (2025). Physics informed integral neural network for dynamic modelling of solvent-based post-combustion CO<sub>2</sub> capture process. *Applied Energy*, 377. <https://doi.org/10.1016/j.apenergy.2024.124344>
- Shahbaz, M., AlNouss, A., Ghiat, I., McKay, G., Mackey, H., Elkhalfifa, S., & Al-Ansari, T. (2021). A comprehensive review of biomass based thermochemical conversion technologies integrated with CO<sub>2</sub> capture and utilisation within BECCS networks. *Resources, Conservation and Recycling*, 173, 105734. <https://doi.org/10.1016/j.resconrec.2021.105734>
- Statens offentliga utredningar. (2020). *Vägen till en klimatpositiv framtid* (Betänkande av Klimatpolitiska vägvalsutredningen) [The path to a climate-positive future (Report of the climate policy path choice inquiry)]. Government Office of Sweden.
- Statista. (2024). *Forecast average carbon permit prices under the European Union Emissions Trading System (EU-ETS) from 2023 to 2025, by trading system (in euros per metric ton of CO<sub>2</sub>)*. <https://www.statista.com/statistics/1401657/forecast-average-carbon-price-eu-emissions-trading-system/#:~:text=European%20Union%20Emissions%20Trading%20System,first%20time%20in%20February%202023>
- Swedish Meteorological and Hydrological Institute (SMHI). (2019). *Swedish Meteorological and Hydrological Institute - Data - Temperatur*. Swedish Meteorological and Hydrological Institute <https://www.smhi.se/data/meteorologi/temperatur>
- Tan, Y., Nookuea, W., Li, H., Thorin, E., & Yan, J. (2016). Property impacts on carbon capture and storage (CCS) processes: A review. *Energy Conversion and Management*, 118, 204–222. <https://doi.org/10.1016/j.enconman.2016.03.079>
- Tang, Z., & Wu, X. (2023). Distributed predictive control guided by intelligent reboiler steam feedforward for the coordinated operation of power plant-carbon capture system. *Energy*, 267, 126568. <https://doi.org/10.1016/j.energy.2022.126568>
- Thorin, E., Sandberg, J., & Yan, J. (2015). Combined heat and power. In J. Yan (Ed.), *Handbook of Clean Energy Systems* (pp. 1–11). <https://doi.org/10.1002/9781118991978.hces021>
- UNFCCC. (2016). *Paris Agreement. United Nations Framework Convention on Climate Change*. United Nations Framework on Climate Change (UNFCCC). [https://unfccc.int/sites/default/files/resource/parisagreement\\_publication.pdf](https://unfccc.int/sites/default/files/resource/parisagreement_publication.pdf)
- United Nations Environment Programme. (2024). *Emissions Gap Report 2024: No more hot air ... please! With a massive gap between rhetoric and reality, countries draft new climate commitments*. Nairobi.

- <https://www.unep.org/emissions-gap-report-2024>
- Wang, C., Li, X., & Hailong Li, a. (2022). Role of input features in developing data-driven models for building thermal demand forecast. *Energy and Buildings*, 277. <https://doi.org/10.1016/j.enbuild.2022.112593>
- Wang, J., Zheng, Y., He, S., Yan, J., Zeng, X., Li, S., Tian, Z., Lei, L., Chen, Y., & Deng, S. (2024). Can bioenergy with carbon capture and storage deliver negative emissions? A critical review of life cycle assessment. *Journal of Cleaner Production*, 434. <https://doi.org/10.1016/j.jclepro.2023.139839>
- Wang, S., Dong, B., Gustafsson, K., Ma, C., Sun, Q., & Li, H. (2023). Assessing the CO<sub>2</sub> capture potential for waste-fired CHP plants. *Journal of Cleaner Production*, 428. <https://doi.org/10.1016/j.jclepro.2023.139379>
- World Meteorological Organization. (2025). *WMO confirms 2024 as warmest year on record at about 1.55°C above pre-industrial level*. <https://wmo.int/news/media-centre/wmo-confirms-2024-warmest-year-record-about-155degc-above-pre-industrial-level>
- Wu, L. (2022). *Equivalence of SS-based MPC and ARX-based MPC*. arXiv. <https://doi.org/10.48550/arXiv.2209.00107>
- Wu, X., Shen, J., Li, Y., Wang, M., Lawal, A., & Lee, K. Y. (2018). Nonlinear dynamic analysis and control design of a solvent-based post-combustion CO<sub>2</sub> capture process. *Computers & Chemical Engineering*, 115, 397–406. <https://doi.org/10.1016/j.compchemeng.2018.04.028>
- Wu, X., Shen, J., Li, Y., Wang, M., Lawal, A., & Lee, K. Y. (2019). Dynamic behavior investigations and disturbance rejection predictive control of solvent-based post-combustion CO<sub>2</sub> capture process. *Fuel*, 242, 624–637. <https://doi.org/10.1016/j.fuel.2019.01.075>
- Wu, X., Wang, M., Liao, P., Shen, J., & Li, Y. (2020). Solvent-based post-combustion CO<sub>2</sub> capture for power plants: A critical review and perspective on dynamic modelling, system identification, process control and flexible operation. *Applied Energy*, 257, 113941. <https://doi.org/10.1016/j.apenergy.2019.113941>
- Zanco, S. E., Pérez-Calvo, J.-F., Gasós, A., Cordiano, B., Becattini, V., & Mazzotti, M. (2021). Postcombustion CO<sub>2</sub> capture: A comparative techno-economic assessment of three technologies using a solvent, an adsorbent, and a membrane. *ACS Engineering Au*, 1(1), 50–72. <https://doi.org/10.1021/acsengineeringau.1c00002>
- Zhang, W., Chen, J., Luo, X., & Wang, M. (2017). Modelling and process analysis of post-combustion carbon capture with the blend of 2-amino-2-methyl-1-propanol and piperazine. *International Journal of Greenhouse Gas Control*, 63, 37–46. <https://doi.org/10.1016/j.ijggc.2017.04.018>

- Zhang, Z., Zhu, M., Liu, S., & Wu, X. (2022). Dynamic modeling and coupling characteristics analysis of biomass power plant integrated with carbon capture process. *Energy Conversion and Management*, 273, 116431. <https://doi.org/10.1016/j.enconman.2022.116431>
- Zhao, B., Liu, F., Cui, Z., Liu, C., Yue, H., Tang, S., Liu, Y., Lu, H., & Liang, B. (2017). Enhancing the energetic efficiency of MDEA/PZ-based CO<sub>2</sub> capture technology for a 650 MW power plant: Process improvement. *Applied Energy*, 185, 362–375. <https://doi.org/10.1016/j.apenergy.2016.11.009>
- Zhou, H., Zhang, S., Peng, J., Zhang, S., Li, J., Xiong, H., & Zhang, W. (2021). Informer: Beyond Efficient Transformer for Long Sequence Time-Series Forecasting. *Thirty-Fifth AAAI Conference on Artificial Intelligence* (AAAI-21). <https://doi.org/10.48550/arXiv.2012.07436>.
- Zhou, S. J., Rabindran, A. V. R., & Gupta, R. (2022). *Ionic liquid catalyzed MEA solvent for post-combustion CO<sub>2</sub> capture testing using the PSTU at NCCC*. Technical Report. Susteon. [https://www.national-carboncapturecenter.com/wp-content/uploads/2023/04/Susteon-Final-Report-NCCC-Campaign\\_opt.pdf](https://www.national-carboncapturecenter.com/wp-content/uploads/2023/04/Susteon-Final-Report-NCCC-Campaign_opt.pdf)